

1804~2004
Kazan University

Russian Ministry for Science and Education
NIOKR Fund of Tatarstan Academy of Science
Kazan State University
Zavoiskii Physical-Technical Institute
Research Educational Center at Kazan State University

**ACTUAL PROBLEMS
OF MAGNETIC RESONANCE
AND ITS APPLICATION**

**VIII International
Youth Scientific School**



**“NEW ASPECTS
OF MAGNETIC RESONANCE
APPLICATION”**

**PROGRAM
PROCEEDINGS**

**Kazan
15-19 August 2004**

1944
EPR discovery

NEW ASPECTS OF MAGNETIC RESONANCE APPLICATION.

Proceedings of the VIII International Youth Scientific School “Actual problems of magnetic resonance and its application”, 15—19 August 2004, Kazan.

Edited by professor M.S. Tagirov (Kazan State University).

The reports of young scientists submitted on VIII International Youth Scientific School “Actual problems of magnetic resonance and its application” carry out by Kazan State University and Zavoiskii Physical-Technical Institute in frameworks of Research Educational Center KSU (REC-007) are included in the present collection.

Compilers: I.G. Motygullin, M.S. Tagirov.

ISBN 5-94605-015-X

The administration of School

professor M.S. Tagirov (KSU, Kazan) — rector
professor V.A. Zhikharev (KFTI RAS, Kazan) — vice-rector
V.K. Voronkova (KFTI RAS, Kazan) — scientific secretary
I.P. Volodina (KSU, Kazan) — secretary

The program committee

The chairman

professor V.A. Atsarkin (IREE, Moscow)

Committee members

professor A.V. Aganov (KSU, Kazan)
professor B.I. Kochelaev (KSU, Kazan)
professor I.V. Ovchinnikov (KFTI RAS, Kazan)
professor K.M. Salikhov (KFTI RAS, Kazan)

The organizing committee of School'2004

M.S. Tagirov, V.A. Zhikharev,
I.P. Volodina, I.G. Motygullin,
A.N. Yudin, D.I. Abubakirov

PROGRAM

15 August

PLENARY SESSION P15 (Lecture Hall 210)	
$9^{00}-9^{20}$	OPENING CEREMONY
$9^{20}-10^{00}$	K.A. Müller “Jahn-Teller vibronic ground states and superconductivity”
$10^{00}-10^{40}$	T. Egami “Phonon-induced electronic bound state and its role in high temperature superconductivity”
$10^{40}-11^{10}$	COFFEE BREAK
$11^{10}-11^{50}$	A. Shengelaya “Microscopic phase separation and two type of quasiparticles in lightly doped $\text{La}_{2-x}\text{Sr}_x\text{CuO}_4$ observed by Electron Paramagnetic Resonance”
$11^{50}-12^{20}$	T. Imai “NMR investigation of $\text{NaCoO}_{2-y}\text{H}_2\text{O}$ ”
$12^{20}-12^{50}$	A. Janossy “Electron spin resonance in high temperature superconductors and related materials”
$13^{00}-14^{30}$	LUNCH
$14^{30}-16^{00}$	“NanoRes-2004” and “EPR₆₀” Section Sessions (Lecture Halls 210 and 212)
$16^{00}-16^{30}$	COFFEE BREAK
$16^{30}-18^{00}$	“NanoRes-2004” and “EPR₆₀” Section Sessions (Lecture Halls 210 and 212)
$18^{30}-22^{00}$	WELCOME PARTY

16 August

SCIENTIFIC FORUM (University Culture and Sport Hall)	
$10^{00}-12^{45}$	M. Kh. Salakhov, Rector of KSU “200 years of Kazan Univeristy” B. I. Kochelaev “60 years of EPR in Kazan” Zavoyskii’ Award Ceremony and Zavoyskii’ Award for Young Scientists Ceremony
$13^{00}-14^{30}$	LUNCH
PLENARY SESSION P16 (Lecture Hall 210)	
$14^{30}-15^{00}$	D. Pavuna “Direct Photoemission Studies on High- T_c Films: Doping, Strain, T_c and Dynamic Energy Landscapes”
$15^{00}-15^{30}$	A. Bussmann-Holder “Electron-lattice interactions as origin of two components in high T_c cuprates”
$15^{30}-16^{00}$	H Alloul
$16^{00}-16^{30}$	COFFEE BREAK
$16^{30}-18^{00}$	“NanoRes-2004” and “EPR₆₀” Section Sessions (Lecture Halls 210 and 212)
$18^{00}-19^{30}$	DINNER
$19^{30}-22^{00}$	YOUNG SCIENTISTS SCHOOL'2004 POSTER SESSION

PROGRAM

17 August

PLENARY SESSION P17 (Lecture Hall 210)	
9 ⁰⁰ -9 ⁴⁰	K. Baberschke "From local moment ESR in superconductors to nanoscale ferromagnets"
9 ⁴⁰ -10 ¹⁰	V.A. Atsarkin "Spin relaxation and internal motion in manganites: the critical and magnetic-dilution effects"
10 ¹⁰ -10 ⁴⁰	G.B. Teitelbaum "The pseudogap regime and dynamical phase separation in high-Tc cuprates"
10 ⁴⁰ -11 ¹⁰	COFFEE BREAK
11 ¹⁰ -11 ⁵⁰	K. Kono "Plasmon resonance of the 2D Wigner solid to study surface excitations of liquid He"
11 ⁵⁰ -12 ²⁰	B. Heinrich "Spin Transport and Dynamics in Magnetic Nanostructures"
12 ²⁰ -12 ⁵⁰	I.A. Garifullin "Modification of the ferromagnetic state under the influence of superconductivity in epitaxial V/Pd _{1-x} Fe _x bilayers "
13 ⁰⁰ -14 ³⁰	LUNCH
14 ³⁰ -16 ⁰⁰	"NanoRes-2004" and "EPR₆₀" Section Sessions (Lecture Halls 210 and 212)
16 ⁰⁰ -16 ³⁰	COFFEE BREAK
16 ³⁰ -18 ⁰⁰	"NanoRes-2004" and "EPR₆₀" Section Sessions (Lecture Halls 210 and 212)
19 ⁰⁰ -21 ⁰⁰	"NanoRes-2004" POSTER SESSION

18 August

PLENARY SESSION P18 (Lecture Hall 210)	
9 ⁰⁰ -9 ⁴⁰	H. Keller "Unconventional isotope effects in cuprate high-temperature superconductors"
9 ⁴⁰ -10 ²⁰	Z.H. Shen "Extracting the bosonic spectral function in cuprate superconductors"
10 ²⁰ -10 ⁵⁰	COFFEE BREAK
10 ⁵⁰ -11 ³⁰	D. Mihailovic "Evidence for a universal length scale of dynamic charge inhomogeneity in cuprate superconductors"
11 ³⁰ -12 ⁰⁰	V.V. Dmitriev "Nonlinear NMR in superfluid 3He confined with low density aerogel "
12 ⁰⁰ -12 ³⁰	H. Suzuki "X-ray diffraction study of correlated electron system at low temperatures"
12 ³⁰ -14 ⁰⁰	LUNCH
14 ⁰⁰ -22 ⁰⁰	TRIP on VOLGA-RIVER, BANQUET (Special payment)

PROGRAM

19 August

PLENARY SESSION P19-1	
TUTORIAL FOR YOUNG SCIENTISTS (Lecture Hall 210)	
9 ⁰⁰ -9 ³⁰	G. Eska “ <i>ac</i> Josephson effect in superfluid 3He”
9 ³⁰ -10 ⁰⁰	K. Kumagai “NMR studies of molecular nanomagnets”
10 ⁰⁰ -10 ³⁰	F. Dzheparov “Spin dynamics in disordered media”
10 ³⁰ -11 ⁰⁰	COFFEE BREAK
PLENARY SESSION P19-2 (Lecture Hall 210)	
11 ⁰⁰ -11 ³⁰	B.I. Kochelaev “Nanoscale properties of strongly correlated systems probed by the EPR”
11 ³⁰ -12 ⁰⁰	H. Godfrin “Nuclear magnetism of two-dimensional solid ³ He”
12 ⁰⁰ -12 ³⁰	D.A. Tayurskii “Mesoscopic effects in quantum liquids”
13 ⁰⁰ -14 ³⁰	LUNCH
14 ³⁰ -16 ⁰⁰	“NanoRes-2004” and “EPR₆₀” Section Sessions (Lecture Halls 210 and 212)
16 ⁰⁰ -16 ³⁰	COFFEE BREAK
16 ³⁰ -17 ³⁰	“NanoRes-2004” and “EPR₆₀” Section Sessions (Lecture Halls 210 and 212)
17 ³⁰ -18 ⁰⁰	CLOSING

TUTORIAL

AC JOSEPHSON EFFECT IN SUPERFLUID ^3He

G. Eska

Bayreuth University, Germany

TUTORIAL

NMR STUDIES OF MOLECULAR NANO-MAGNETS

K. Kumagai¹⁾, Y. Furukawa¹⁾, S. Kawakami¹⁾, Y. Hatanaka¹⁾, F. Borsa^{2,3)}

¹⁾Division of Physics, Graduate School of Science, Hokkaido University, Sapporo, Japan,

²⁾Dipartimento di Fisica “A.Volta” e Unita’ INFN di Pavia, Via Bassi 6, I27100 Pavia. Italy,

³⁾Department of Physics and Astronomy and Ames Laboratory, Iowa State University, USA.

e-mail: kumagai@phys.sci.hokudai.ac.jp

Recently, much attention has been paid to molecular nanomagnets with 3d transition metal (TM) elements such as $[\text{Mn}_{12}\text{O}_{12}(\text{CH}_3\text{COO})_{16}(\text{H}_2\text{O})_4]2\text{CH}_3\text{COOH}\cdot 4\text{H}_2\text{O}$ (for short, Mn12), $[\text{Fe}_8(\text{N}_3\text{C}_6\text{H}_{15})_6\text{O}_2(\text{OH})_{12}][\text{Br}_8\cdot 9\text{H}_2\text{O}]$ (Fe8) etc., because novel quantum spin tunneling phenomena appear at low temperature. The ground state of those molecules forms a high total spin state, (for instance, $S=10$ for Mn12 and for Fe8) due to strong antiferromagnetic exchange coupling among the TM spins. The ground state of high spin state is split by crystal field effects, giving super paramagnetic behavior combined with quantum phenomena. In order to shed light on the particular spin states of the molecular nanomagnets from a microscopic point of view, we have carried out NMR measurements for various nuclei of Mn, Fe, H and D with applying magnetic field parallel and also perpendicular to the magnetic easy axis in a wide temperature range. [1-6]

We have measured proton spin-lattice relaxation rates (T_1^{-1}) as functions of the external magnetic field in Mn12 and Fe8. When the external magnetic field is applied along the easy-axis (parallel field), spin-lattice relaxation rates, $1/T_1$ decreases monotonically with increasing field. The external field dependence of $1/T_1$ is well explained by a model in terms of thermal fluctuations of the magnetization due to spin-phonon interaction at high temperature range above 1.5K. [6] On the other hand, when the magnetic field is applied perpendicular to the easy-axis (transverse field), we have observed a peak of $1/T_1$, which can not be explained by the model in terms of spin-phonon interaction. We will report details of the peculiar temperature- and external magnetic field-dependences of the spin dynamics in Fe8, and will discuss the origin of the peak of $1/T_1$ in connection with tunneling dynamics under application of the transverse field.

It should be emphasized that the nuclear spin fluctuations can play an important role for their ground state dynamics though hyperfine coupling as pointed out by recent experimental and theoretical studies. [5, 6] We have performed NMR studies for the Fe8 compounds with enriched isotope of ^{57}Fe at low temperature down to 40mK. $1/T_1$ of ^{57}Fe and ^1H is

TUTORIAL

temperature-independent below 400mK. Together with extended results of ^1H -and ^{57}Fe -NMR in ^{57}Fe -enriched Fe8 cluster, we will discuss the isotope substitution effects on spin dynamics in the Fe8 clusters

References

- [1] Y. Furukawa, K. Aizawa, K. Kumagai *et al.*, Phys. Rev. **B 69**, 014405 (2004).
- [2] Y. Furukawa, S. Kawakami, K. Kumagai *et al.*, Phys. Rev. **B 68**, 180405 (2003).
- [3] Y. Furukawa, K. Watanabe, K. Kumagai *et al.*, Phys. Rev. **B 67**, 064426 (2003).
- [4] Y. Furukawa, K. Aizawa, K. Kumagai *et al.*, Mol. Cryst. Liq. Cryst. **379**, 191 (2002).
- [5] Y. Furukawa, K. Watanabe, K. Kumagai *et al.*, Phys. Rev. **B64**, 104401 (2001).
- [6] Y. Furukawa, K. Kumagai *et al.*, Phys. Rev. **B 64**, 094439 (2001).
- [7] W. Wernsdorfer *et al.*, Phys. Rev. Lett. **84**, 2695 (2000).
- [8] D.A. Garanin *et al.*, Phys. Rev. **B 61**, 12204 (2000).

TUTORIAL

SPIN DYNAMICS IN DISORDERED MEDIA

F.S. Dzheparov

Institute for Theoretical and Experimental Physics, Moscow, Russia 117218

e-mail: dzheparov@itep.ru

Three fundamental problems of spin evolution in presence of static disorder of spins spatial positions are considered: 1) delocalization of nuclear polarization within impurity spin system, 2) nuclear relaxation via paramagnetic impurities, and 3) free induction decay for disordered paramagnetic substance. Main results for these problems are:

- 1) a method for calculation of both diffusion tensor and polarization $P_{00}(t)$ of initially polarized nucleus is developed [1,2], starting from the kinetic equation, describing the process [3]; new (relative to [3,4]) analytical formula for $P_{00}(t)$ is derived; new experimental results for $P_{00}(t)$ for model spin system ^8Li - ^6Li in single crystals LiF at different concentration of impurity nuclei ^6Li are obtained by beta-NMR spectroscopy on beta-active nuclei ^8Li [5], giving important correction to previous results [4]; numerical studies for the model system are carried out;
- 2) a mean-field theory is constructed for description of nuclear relaxation via paramagnetic impurities for arbitrary spatial dimension d of the substance [6]; it is shown, that preceding treatments of the process were based on formal rearrangement of first terms of the expansion of nuclear polarization in powers of impurities concentration into cumulant expansion for $3d$ -systems, while new theory gives natural argumentation to obtain physically reasonable results in main approximation for any d ;
- 3) a theory of free induction decay (FID) for homogeneously broadened electronic paramagnetic system with arbitrary spatial dimension d is developed basing on expansion of FID in powers of concentration [7], comparison with experimental results for two-dimensional samples [8] is fulfilled.

References

- [1] F.S. Dzheparov, D.V. Lvov, V.E. Shestopal. *JETP*, **87**, 1179 (1998).
- [2] F.S. Dzheparov, D.V. Lvov, V.E. Shestopal. *Preprint ITEP N46*, Moscow 1999.
- [3] F.S. Dzheparov. *Sov. Phys. JETP*, **72**, 546 (1991).
- [4] F.S. Dzheparov, A.D. Gul'ko, P. Heitjans et al. *Physica B*, **297**, 288 (2001).
- [5] A.D.Gulko et al. *Report on this conference*.

TUTORIAL

- [6] F.S. Dzheparov, J.-F. Jacquinot, S.V. Stepanov. *Physics of Atomic Nuclei*, **65**, 2052 (2002).
- [7] F.S. Dzheparov, I.V. Kaganov. *JETP Lett.* **75**, 259 (2002).
- [8] V.A. Atsarkin, G.A. Vasneva, V.V. Demidov et al. *JETP Lett.* **72**, 369 (2000).

**MAGNETIC SUSCEPTIBILITY OF VAN VLECK PARAMAGNET THULIUM
ETHYLSULFATE AT HIGH MAGNETIC FIELDS**

D.I. Abubakirov¹⁾, M.S. Tagirov¹⁾, D.A. Tayurskii¹⁾, H.Suzuki²⁾

¹⁾Department of Physics, Kazan State University, 420008, Kremlevskaya 18, Kazan, Russia

²⁾Department of Physics, Faculty of Science, Kanazawa University, 920-1192 Kanazawa, Japan

e-mail: denis.abubakirov@ksu.ru

Van Vleck (VV) or polarization paramagnetism represents the kind of paramagnetism different from the conventional orientational paramagnetism. The magnetic susceptibility of VV paramagnets becomes temperature independent at low temperatures. The reason of such a behavior is that the electronic ground state of VV ion in electric crystal field either a singlet or a non-magnetic doublet. VV paramagnetism most often occurs in crystals containing non-Kramers rare-earth ions, i.e. rare-earth ions with an even number of electrons in the unfilled $4f$ -shell. An applied external magnetic field causes the elastic deformation of the electronic shell giving rise to an induced magnetic moment. The existence of nonzero nuclear spins makes VV paramagnets very interesting for studying electron–nuclear magnetism. The magnetic field induced at nucleus of VV ions is many times greater than applied magnetic field and causes many unusual features in the NMR of VV ions. The increase of applied magnetic field up to values where the Zeeman energy of VV ion becomes comparable with Stark splittings leads to the appearing new effects in electron–nuclear magnetism [1]. In this work the magnetic properties of well-known thulium ethylsulfate $\text{Tm}(\text{C}_2\text{H}_5\text{SO}_4)_3 \cdot 9\text{H}_2\text{O}$ (TmES) single crystal are studied by means of SQUID magnetometry at magnetic fields up to 5.5 T in a wide temperature region.

The ultra–high frequency NMR of $^{169}\text{Tm}^{3+}$ was observed at perpendicular orientation of magnetic field and axis c of the crystal where the VV susceptibility possesses a maximum [2, 3]. The highest magnetic field used in the experiment was 3 T at 700 MHz. The observed field dependence of the NMR frequency is essential non-linear and starts to differ from theoretically calculated [2, 3] at magnetic fields higher than 1.5 T. The assumption that hyperfine interaction parameters become magnetic field dependent at sufficiently high magnetic fields yields a rather good agreement with experimental data. The nature of such a behavior is the strong distortion of the $4f$ -electron shell at high magnetic fields [4].

To verify the proposed model the magnetic moment of Tm^{3+} ions in TmES has been investigated at magnetic fields up to 5.5 T in the present work. The measured field

dependences of magnetization of the TmES single crystal by means of SQUID–magnetometer in perpendicular orientation ($\mathbf{H}_0 \perp c$) at $T=4.2\text{K}$ is shown in fig.1, 2. As a specimen, sphere-shaped TmES single crystal was taken to eliminate the demagnetizing factor. The diameter was 3.4 mm and mass 39 mg. The results of magnetic moment measurements of parallel orientation ($\mathbf{H}_0 \parallel c$) are depicted in the fig.3, 4.

As it turned out, the magnetization of the crystal in plane normal to symmetry axis c is 2 orders higher than in direction parallel to this axis. At high magnetic field due to rotating moment the specimen orientates on it's own to satisfy the condition $\mathbf{H}_0 \perp c$. To prevent the rotation of the sample while measuring in orientation $\mathbf{H}_0 \parallel c$, it was fixed by low–temperature epoxy resin Stycast 1266A. The diamagnetic contribution of Stycast 1266A was less than 10 % to overall specimen magnetization.

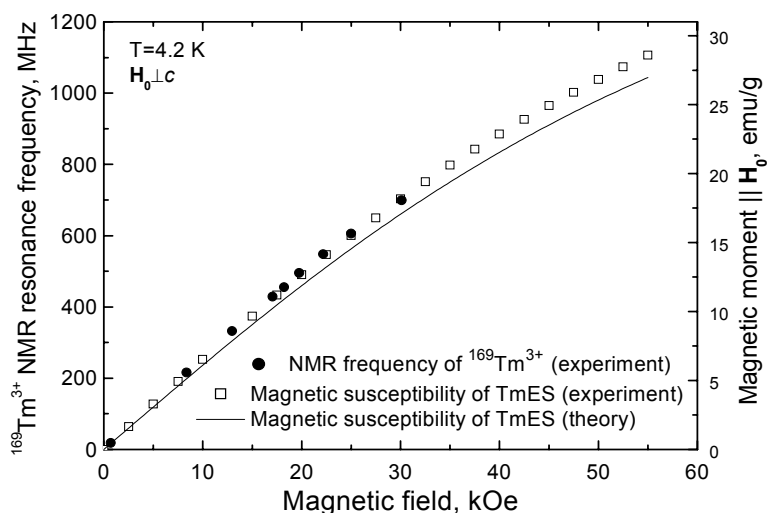


Fig. 1. Field dependence of magnetic susceptibility of TmES single crystal and field dependence of Tm^{3+} NMR frequency.

On fig.1 one can see the comparison of field dependences of Tm^{3+} NMR frequency and magnetization of TmES single crystal. As can be seen the magnetic field dependence of magnetization coincides with one of NMR frequency. As calculations showed, practically only the Tm^{3+} ions contribute into overall crystal magnetization. Hyperfine magnetic field on ^{169}Tm nucleus is proportional to magnetic moment of electronic shell. In this particular case the hyperfine field on nucleus is nearly 70 times higher than external field H_0 ; therefore the overall magnetic field on ^{169}Tm nuclei is approximately proportional to magnetic moment of Tm^{3+} electronic shell. This effect is illustrated on fig.1.

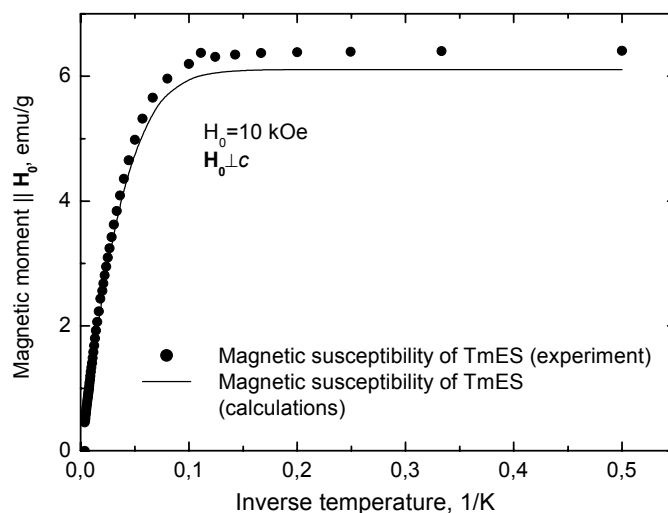


Fig. 2. Temperature dependence of magnetic susceptibility of TmES single crystal.

On fig. 2 one can see the range of so-called Van Vleck susceptibility (from 0 K to 10 K), where only the lowest sublevel of Tm^{3+} ion is occupied and magnetization of TmES crystal is non-dependent on temperature.

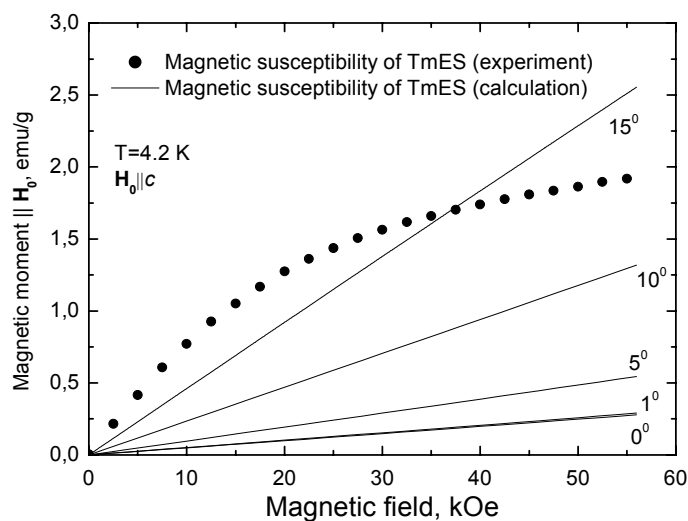


Fig. 3. Field dependence of magnetic susceptibility of TmES single crystal. For solid lines (calculations) the angles between axis c and H_0 are indicated at each curve.

On fig.3, 4 there are the dependences for magnetization in orientation $H_0 \parallel c$. The deviation of orientation from could be of order of 5 degree. To find the orientation in experiment the calculations were conducted for several slight deviations of orientation. Despite of this assumption, the calculated dependences don't coincide with experimental ones nor qualitative nor quantitative. The only good agreement is on fig.4 in range of anomalous

magnetization behavior, where it increases while temperature increases. Such a behavior is due to occupation of excited Stark levels, having higher magnetic moments.

We explain the major discrepancy between experimental data and calculations for orientation $\mathbf{H}_0 \parallel c$ by appearing the other sources of magnetism of ordinary nature in the sample after placement it in epoxy resin. Most probably, it was the Thulium sulfate, the paramagnet which was the product of chemical reaction.

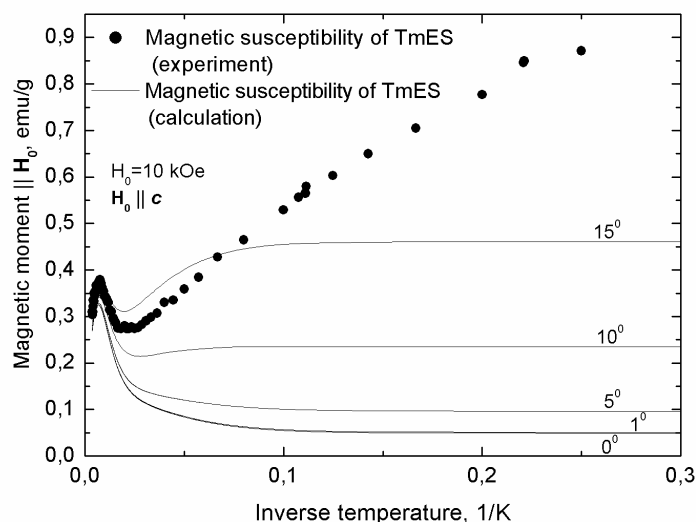


Fig. 4. Temperature dependence of magnetic susceptibility of TmES single crystal. For solid lines (calculations) the angles between axis c and \mathbf{H}_0 are indicated at each curve.

Acknowledgements

This work was supported by the KSU scientific and educational center (REC-007), the program “Universities of Russia” through grant # 01.01.011 and by RFBR foundation (grant # 02–04–16800).

References

- [1] M. S. Tagirov and D. A. Tayurskii, *Low Temp. Phys.*, **28**, 147 (2002).
- [2] D. I. Abubakirov, V.V.Naletov, M.S.Tagirov, D.A.Tayurskii, A.N.Yudin, *JETP Lett.*, **76**, 633 (2002).
- [3] D. I. Abubakirov, V.V.Naletov, M.S.Tagirov et.al. – *Physica B.*, **346–347**, 231 (2004).
- [4] D.Tayurskii and H.Suzuki. – *J. Phys.: Cond. Matt.*, **15**, S2231 (2003).

OD ESR DETECTION OF THE RADICAL IONS OF CYCLIC NITRONES IN LIQUID SOLUTIONS

M.M. Barlukova^{1,2)}, N.P. Gritsan^{1,2)}, V.A. Bagryansky^{1,2)}, V.F. Starichenko³⁾,

I.A. Grigor'ev^{2,3)}, Yu.N. Molin¹⁾

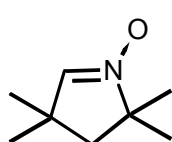
¹⁾Institute of Chemical Kinetics and Combustion, Novosibirsk, 630090, Russia

²⁾Novosibirsk State University, Novosibirsk, 630090, Russia

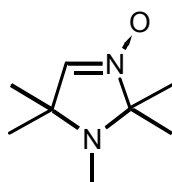
³⁾N.N. Vorozhtsov Novosibirsk Institute of Organic Chemistry, Novosibirsk, 630090, Russia

e-mail: barlukova@ns.kinetics.nsc.ru

Cyclic nitrones (N-oxides of the non-aromatic heterocyclic compounds) are widely utilized as spin traps and precursors of stable nitroxide radicals. In both applications a very



TMPO



PMIO

important role is played by ion radicals of cyclic nitrones. In the spin trapping technique which is based on the ability of nitrone group to add the short-lived free radicals to form stable nitroxide radicals, one should take into account the contribution of the radical ion channels of nitroxide radical formation. In the synthesis of nitroxide radicals a reaction of nucleophilic addition to the cyclic nitrone radical cations is used to obtain nitroxide radicals with a nucleophilic substituent in the α -position relative to the radical center. For these reasons, cyclic nitrone ion radicals are very interesting objects for study.

In this work, the radical ions of the cyclic nitrone spin traps, 3,3,5,5-tetramethyl-1-pyrroline 1-oxide (TMPO) and 1,2,2,5,5-pentamethyl-3-imidazoline 3-oxide (PMIO) formed under radiolysis of liquid squalane solutions were characterized for the first time by the method of optically detected ESR. The hfc constants and g -values of TMPO and PMIO radical anions, as well as PMIO radical cation were determined. The hfc constants and the energetic characteristics of radical anions and cations were obtained by DFT and *ab initio* molecular orbital calculations. The experimental data and the results of calculations indicate that in both the TMPO and PMIO radical anions the unpaired electron is localized mainly on the nitrone group, whereas in the PMIO radical cation, it is localized on the tertiary nitrogen atom and interacts with protons of methyl group. The experimental values of hfc constants are $a(\text{N})=1.22\pm 0.03$ mT, $a(\alpha\text{-H})=0.51\pm 0.05$ mT for TMPO radical anion; $a(\text{N})=1.33\pm 0.03$ mT, $a(\alpha\text{-H})=0.92\pm 0.04$ mT for PMIO radical anion and $a(\text{N})=1.9\pm 0.02$ mT, $a(3\text{H})=2.9\pm 0.02$ mT for PMIO radical cation.

POSTER SESSION PS2

The g -values are 2.0038 ± 0.0002 for TMPO radical anion, 2.0037 ± 0.0001 for PMIO radical anion and 2.0043 ± 0.0001 for PMIO radical cation.

The work was supported by the Russian Foundation for Basic Research (Grant No 02-03-32224a), the program “Leading Science Schools” (Grant No 84.2003.3) and INTAS (Grant No 00-0093).

STUDY OF 1,2,3-TRIFLUOROBENZENE RADICAL ANION BY OD ESR SPECTROSCOPY

M.M. Barlukova^{1,2)}, I.V. Beregovaya³⁾, V.P. Vysotsky^{2,3)}, L.N. Shchegoleva³⁾,
V.A. Bagryansky^{1,2)}, Yu.N. Molin¹⁾

¹⁾Institute of Chemical Kinetics and Combustion, Novosibirsk, 630090, Russia

²⁾Novosibirsk State University, Novosibirsk, 630090, Russia

³⁾N.N. Vorozhtsov Novosibirsk Institute of Organic Chemistry, Novosibirsk, 630090, Russia

e-mail: barlukova@ns.kinetics.nsc.ru

Polyfluorobenzene radical anions are characterized by out-of-plane Jahn-Teller distortions. Quantum chemical

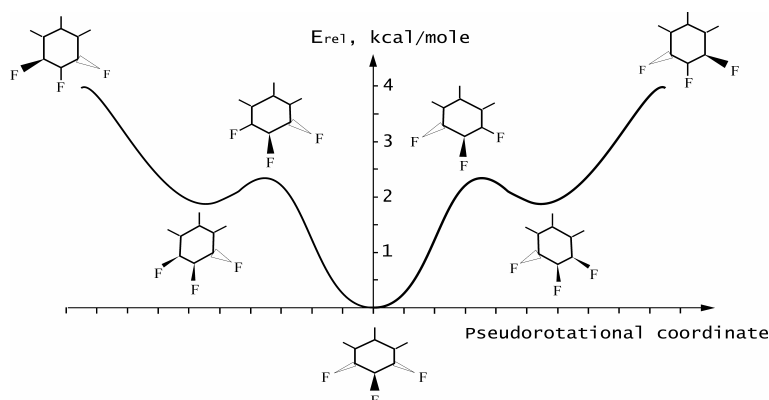


Fig. 1. Fragment of the pseudorotational surface of 1,2,3-trifluorobenzene radical anion.

calculations indicate their potential energy surfaces (PES's) to be pseudorotational surfaces with a number of local minima [1]. PES of 1,2,3-trifluorobenzene radical anion includes minima of two energetically nonequivalent types, the energy barriers between them being sufficiently low ($\sim kT$) (Fig.1). It can be supposed that dynamic transitions between these states would reveal themselves in experimental ESR spectra.

In this work, the ESR spectrum of 1,2,3-trifluorobenzene radical anion formed under radiolysis of in liquid squalane solution

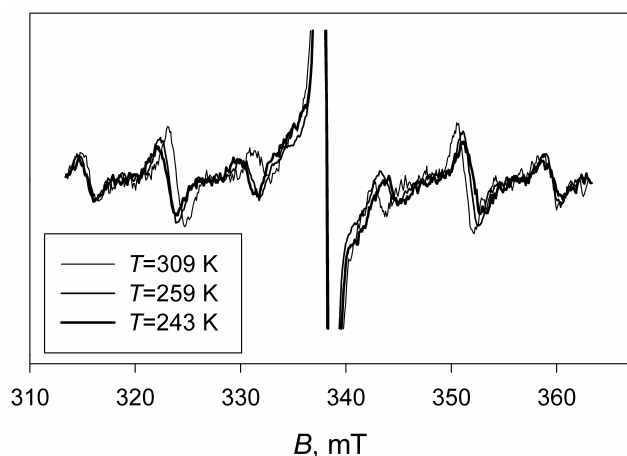


Fig. 2. OD ESR spectra of X-irradiated squalane solution of 10^{-2} M 1,2,3-trifluorobenzene and 1.5×10^{-3} M *para*-terphenyl- d_{14} at different temperatures.

was detected for the first time by the method of optically detected ESR. The temperature dependence of the spectrum in the range from $T=243$ K to $T=325$ K was measured. The spectrum consists of six lines (doublet of triplets), the distances between them being temperature-dependent due to fast exchange between the conformations

POSTER SESSION PS3

(Fig. 2). Observed values of hfc constants change in the range from $a(\text{F})=28.98$ mT and $a(2\text{F})= 7.60$ mT at $T= 243$ K to $a(\text{F})=27.71$ mT and $a(2\text{F})= 8.06$ mT at $T= 325$ K. Temperature dependence of the ESR spectrum is in good agreement with the results of quantum chemical calculations of the PES shape.

The work was supported by the Russian Foundation for Basic Research (Grants No 02-03-32224a, No 04-03-32459).

References

- [1] Beregovaya I.V., Shchegoleva L.N.: *Int. J. Quant. Chem.* **88**, 481 (2002)

SIDE CHAIN DYNAMICS OF SOLID GLOBULAR PROTEINS. COMPARATIVE STUDY BY ¹H-NMR RELAXATION AND FTIR SPECTROSCOPY

A.V. Belskaya, D.A. Fayzullin, V.D. Fedotov

Institute of Biochemistry and Biophysics, KSC RAS, Kazan.

e-mail: belsky@mail.knc.ru

Comparative analysis of nonselective ¹H-NMR relaxation at 27 MHz and FTIR data for solid human serum albumin (HSA), bovine serum albumin (BSA), lysozyme and binase reveals some protein specific features. Motions of at least two kinds have been evidenced to present in solid protein samples. The low amplitude «fast» motion manifests itself as a relaxation transition in the temperature near 160K with correlation time $\tau \sim 10^{-11}$ c. Its parameters are nearly the same for all the proteins studied and slightly depend on humidity. This motion is referred to as low amplitude high frequency restricted rotation of the methyl groups around the axis of symmetry. The large amplitude «slow» motion ($\tau \sim 10^{-5}$ - 10^{-6} c) defines magnetic relaxation in a temperature range 230-450K, being strongly depended on sample hydration and peculiar protein properties. Unlike in other proteins studied, high-temperature transition in HSA completes at comparatively mild temperatures that allows one to determine parameters more precisely. Progressive sample hydration from 0 up to 0.35 g/g leads to increasing amplitude by 1.5 – 2 times and shortening correlation time by the order of magnitude. Comparison of relaxation data and vibrational spectra of hydrocarbon side chains of proteins reveals a close correlation to be existed between slow motion parameters and band positions of CH₂- as well as CH₃-groups. Hence, unlike methylene fragments that perform only slow motion, the methyl groups participate both in fast local and slow-time large amplitude motions along with the rest of side chain. Mobility of dry proteins inversely correlates with packing density of side chain calculated from PDB-files. At the same time the mobility gain at increasing humidity is strictly proportional to solvent accessible specific surface area. Obtained results permit to draw more definite conclusions about factors governing the internal protein dynamics.

The work is supported by RFBR grant № 02-04-48907.

**IRREVERSIBILITY LINE OF THE BI-2212 THIN FILMS AS REVEALED BY
NONRESONANT MICROWAVE ABSORPTION**

A.N. Bukharaev¹⁾, Yu.I. Talanov²⁾

¹⁾Kazan State University, 420008, Kremlevskaya str. 18, Kazan, Russia.

²⁾Zavoiskii Physical-Technical Institute, 420029, Sibirskii tract 10/7, Kazan, Russia.

e-mail: talanov@kfti.knc.ru

Introduction

The pinning energy and/or the surface barrier potential govern such an important parameter of superconductors as the critical current density. They determine also the position of an irreversibility line (IL) on the phase plane “magnetic field – temperature” (H - T). IL is the boundary between the area, in which the nondissipative current flow is possible, and the area with the dissipative current only. The efficiency of the vortex interaction with pinning centers can change considerably as the thickness of a superconductor placed in the perpendicular magnetic field decreases. In this case the pinning force of columnar defects may weaken due to the decrease of the interaction length. On the other hand, the ratio of the point defect size to the total length of the vortex line increases as the thickness of a superconducting film decreases. In the limit of the thickness comparable with the interaction length the unusual state can occur, in which the pinning force of point centers is comparable with that of columnar defects. At present the thin-film technology is widely used in the preparation of superconducting samples and devices. Thus the investigation of pinning effects in thin films of superconductors is important for obtaining materials with required properties.

We study films of the high-temperature superconductor $\text{Bi}_2\text{Sr}_2\text{CaCu}_2\text{O}_8$ (Bi-2212) with a thickness d comparable with the field penetration depth ($d = 200\text{nm} \approx \lambda_{ab}(0)$) and that four times greater than $\lambda_{ab}(0)$. To obtain the IL points we measure the hysteretic nonresonant microwave absorption (MWA). This method is sensitive enough to study very thin films. It allows us to vary the temperature T and applied magnetic field H_a in wide limits (T from 10K to T_c and H_a from 0 to 10 000 Oe). Moreover, the measurement technique permits us to separate contributions of bulk pinning and surface pinning by the shape of the loop [1], so it makes it possible to study the influence of the film thickness on the surface barrier.

Experimental

The $\text{Bi}_2\text{Sr}_2\text{CaCu}_2\text{O}_8$ films were prepared on a LaAlO_3 substrate with sputtering technique (the details of the preparation method can be found in Ref.[2]). The films #1 and #2 have the rectangular shape of $3 \times 5 \text{ mm}^2$ size and 800 nm and 200 nm in thickness, respectively. The films #3 with the thickness $d = 200 \text{ nm}$ is partitioned into 40 equal circles of 0.5 mm diameter with the help of photolithography technique. The films have the superconducting transition temperature T_c near 85 K.

We studied irreversible properties of films by measuring the hysteresis of the nonresonant microwave absorption. The detailed description of this method one can find in Refs.[2,3]. The X-band ($\nu = 9.4 \text{ GHz}$) spectrometer of electron spin resonance (ESR) BER-418s (Bruker) was used to measure the microwave absorption. A sample was placed into the spectrometer cavity inside the helium gas flow cryostat. Its orientation was as follows: the DC field H_a was applied perpendicularly to the film plane (parallel to the c -axis), and the microwave field H_1 was in the film plane. The field H_a was modulated with the frequency of 100 kHz and the amplitude from 0.1 to 10 Oe.

To record the MWA hysteresis loop H_a was swept with the velocity of 40 Oe/s from 0 to the field of disappearance of the hysteresis (it ranges from $\sim 100 \text{ Oe}$ to $10\,000 \text{ Oe}$ versus temperature) and back. The ESR signals of the paramagnetic impurity in the substrate were recorded along with the MWA hysteresis loop and used to avoid the instrumental error of detected hysteresis. The IL points $H_{ir}(T)$ were obtained by registering the field at which the MWA hysteresis collapsed.

Results and discussions

Examples of the MWA hysteresis loops are presented in Fig.1. They are obtained for the film #2 at $T=62 \text{ K}$ and two values of the field modulation amplitude: $H_m=0.4 \text{ Oe}$ and $H_m=8 \text{ Oe}$. It was established in work [1] that the shape of the MWA hysteresis loop and its dependence on the modulation amplitude were governed by the type of pinning: bulk or surface. According to [1] the shape of the loop obtained with $H_m=0.4 \text{ Oe}$ is largely determined by bulk pinning. The small addition of the “surface” loop occurs only in low fields ($<1000 \text{ Oe}$). The irreversibility due to bulk pinning disappears in the field marked by arrow 1. This field is called the irreversibility field and equals 4100 Oe. The second loop is obtained with the modulation $H_m=8 \text{ Oe}$. The high modulation amplitude suppresses the “bulk pinning” loop and amplifies the contribution of surface pinning. As a result, the loop has the

purely surface shape. The irreversibility field due to the surface barrier is shown by arrow 2 and equals about 5000 Oe.

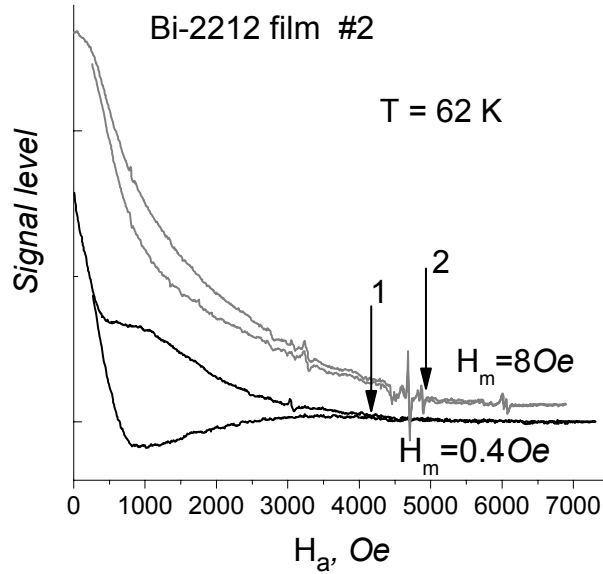


Fig.1

In Fig.2 the IL points of three studied samples are plotted versus the reduced temperature T/T_c : squares, the thickest film ($d=800$ nm); diamonds, the solid thin film ($d=200$ nm); circles, the patterned thin film ($d=200$ nm). All points are obtained with the modulation $H_m=0.4$ Oe except for the open squares which are measured at $H_m=8$ Oe. At high temperatures close to the critical temperature T_c the surface pinning is observed. The relevant IL points are shown by crossed squares.

In Fig.2 the ILs of two single crystals of different thicknesses are shown along with our data obtained for thin films. The dashed line is plotted for the thick crystal of Bi-2212 ($d \approx 50 \mu\text{m}$) from Ref.[4], and the dotted line is for the thin crystal ($d = 3 \mu\text{m}$) from Ref.[5]. One can see that IL shifts towards the high temperature as the thickness of a superconductor decreases. Only the thinnest films with $d = 0.2 \mu\text{m}$ do not obey this rule. The shift of IL to higher temperatures is probably due to the strengthening of the pinning centers as mentioned above. But such strengthening is limited to the thickness $d = 0.2 \mu\text{m}$. It is reasonable to assume that if the thickness of a superconductor is comparable with or less than the field penetration depth λ_{ab} the suppression of bulk pinning occurs. The analogous effect is observed for the surface pinning on the lateral surface. Increasing the lateral surface by means of patterning a film from a big rectangle to 40 small circles does not result in the expected increase of the surface contribution to the MWA loop and to the irreversibility field.

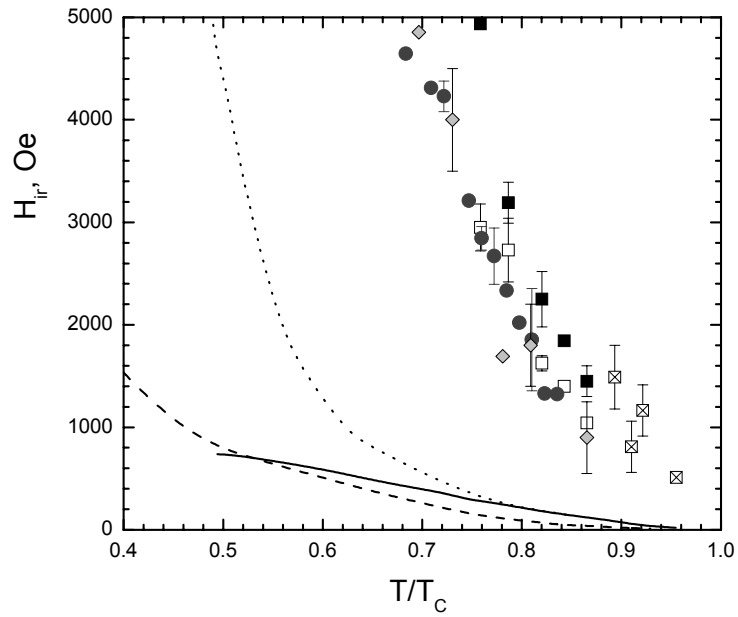


Fig.2.

Thus we have established that the decrease of the superconductor thickness down to λ or less causes the decrease of the bulk pinning and the lowering of the lateral surface barrier.

The work is supported by the Russian Foundation for Basic Research (grant no. 03-02-96230) and the NIOKR Fund of the Academy of Sciences of Tatarstan (grant no. 06-6.2-234).

References

- [1] T. Shaposhnikova, Yu. Vashakidze, Yu. Talanov, *Physica C* **385** 383 (2003).
- [2] P. Wagner, F. Hillmer, U. Frey, H. Adrian, *Physica C* **215** 123 (1993).
- [3] T. Shaposhnikova, Yu. Vashakidze, R. Khasanov, Yu. Talanov, *Physica C* **300** 239 (1998).
- [4] A. Schilling, R. Jin, J.D. Guo, H. R. Ott, *Phys.Rev.Lett.* **71** 1899 (1993).
- [5] S. Sas, F. Portier, K. Vad, *et al.*, *Phys.Rev.B* **61** 9113 (2000).

**THE INFLUENCE OF DIAMAGNETIC SALTS ON THE STATE OF
PARAMAGNETIC AQUA-ION Gd(3+) BY EPR-SPECTROSCOPY DATA**

V.Yu. Buzko, I.V. Sukhno, S.V. Dubrovin, I.V. Kornienko

Chemistry Department, Kuban State University, Krasnodar, 350040, Russia

e-mail: Sukhno@chem.kubsu.ru; <http://public.kubsu.ru/sukhno>

Now there is no simple theory to predict the magnetic-resonance parameters for systems, in which the paramagnetic REE ions and diamagnetic salts present simultaneously.

It was investigated the state of paramagnetic Gd(3+) ion in aqueous diamagnetic salt solutions (KCl, KBr, MgCl₂, CaCl₂) by EPR-spectroscopy method (Radiopan SE/X 2543, 9.30 GHz, the standard deviation for width of EPR lines $\pm 0.15-0.20$ mT, for g-factor values ± 0.0005). It was used the CPESPP program to calculate the stability constants, limit widths of EPR lines ΔH (mT/mol) and species distribution of complexes.

It was found the increase of width of EPR line for Gd(3+) ion in aqueous KCl and KBr solutions. We believe that this is consequence of formation of GdCl²⁺, GdCl₂⁺ and GdBr²⁺, GdBr₂⁺ complexes with shorter electronic relaxation times T_S than for Gd(3+) aqua-ion. We think this is also consequence of accumulation of such complexes at increase of KCl and KBr salt concentration. The potassium salts were used because they do not influence on structure of liquid water and correlation times τ_R , τ_V of paramagnetic Gd(3+) aqua-ion. The results of mathematical modeling testify that limit width of EPR line for GdCl²⁺ and GdBr²⁺ complexes is more narrow than one for Gd(3+) aqua-ion in a aqueous Gd(NO₃)₃ solutions. Although the limit widths of EPR lines for GdCl₂⁺ and GdBr₂⁺ complexes are wider. This fact is explained by considerable decrease of distortion life time τ_V of paramagnetic complex at replacement of one of water molecule in coordination sphere of Gd(3+) aqua-ion on a halide-ion. The decrease of distortion life time τ_V of paramagnetic complex is explained by anisotropy of brownian rotation of aqua-ion. It should be noted that the correlation time τ_R increases slightly. The larger size of hydrated bromide-ion in comparison with a chloride-ion coordinated with paramagnetic Gd(3+) aqua-ion is cause of greater anisotropy of τ_R values and more narrow limit width of EPR lines for GdBr²⁺ species than for GdCl²⁺ species and Gd(3+) aqua-ion. The greater values of limit widths of EPR lines for GdCl₂⁺ species and GdBr₂⁺ species (smaller T_S values as well) in comparison with Gd(3+) aqua-ion can be explained by considerable increase of correlation time τ_R values for di-haloid complexes.

POSTER SESSION PS6

It is found that the greatly hydrated Mg(2+) and Ca(2+) cations decrease the width of EPR line for Gd(3+) aqua-ion by exchange mechanism. At that the life times of water molecules $\tau_B(\text{H}_2\text{O})$ in coordination sphere of paramagnetic ion increase. The exchange mechanism does not correlate with electronic interactions, which are caused by splitting in a zero field, therefore

$$\Delta H \sim 1/T_S = 1/T_{2e} + 1/\tau_B(\text{H}_2\text{O}),$$

where T_{2e} – the electronic spin-spin relaxation time.

Thus the increase of life time of water molecules $\tau_B(\text{H}_2\text{O})$ in coordination sphere of paramagnetic Gd(3+) aqua-ion leads to the decrease of correlation time τ_V values because the statistical probability of distortions for the period of life time of paramagnetic complex increase. So the EPR line of paramagnetic Gd(3+) aqua-ion narrows.

This work was supported by Russian Foundation For Basic Research (grant 03-03-32296).

INVESTIGATION OF Mn^{2+} IONS INTERACTION WITH HUMIC SUBSTANCES

P.V. Chaplieva¹⁾, I.V. Borovykh²⁾, O.E. Trubetskaya³⁾, I.I. Proskuryakov¹⁾, O.A. Trubetskoj¹⁾

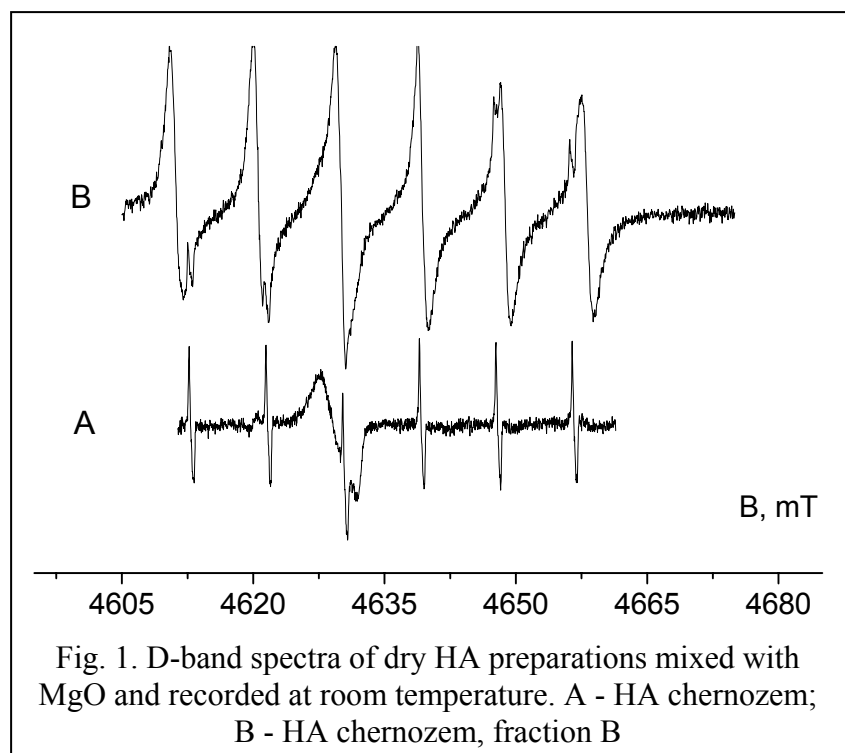
¹⁾Institute of Basic Biological Problems RAS, Pushchino, 142290, Russia

²⁾Department of Biophysics, Huygens Laboratory, 2300 RA Leiden, The Netherlands

³⁾Branch of the Shemyakin Institute of Bioorganic Chemistry RAS, Pushchino, 142290, Russia

E-mail: polina@issp.serpukhov.su

Humic acids arise from soil organic matter as a result of humification processes when biological substances are converted into amorphous group of dark-colored material known as soil humic matter. Humic substances are generally accepted as a matter that has considerable influence on soil fertility. Currently their ability of binding heavy metal ions was brought under discussion. In [1] an isolation of several humic acids (HA) fractions differing in physico-chemical properties has been reported. In the present work we report on varying ability of the HA fractions to interact with Mn^{2+} ions, as studied with EPR. Humic substances were extracted from different soils and their fractions prepared according to [1]. As the source of Mn^{2+} , its moiety in MgO powder was used, which was mixed with the dry samples at room temperature. The studies have shown that in non-fractionated HA the shape of the Mn^{2+} spectrum was the same as in pure MgO. Mixing with HA fractions, however, resulted in strong changes of the spectrum. Most visible these changes are in the D-band spectra (Fig. 1), pronounced as the linewidth increase and change of the hyperfine interaction (Fig. 1B). The



singlet line overlapped with the third Mn^{2+} component in Fig. 1A belongs to free-radical species present in most of the HA preparations. We interpret the observed spectra as resulting from buildup of Mn^{2+} interaction with chemically active groups present in HA fractions, but absent in non-treated

POSTER SESSION PS7

HA. The results will be discussed from the point of view of possible applications to heavy metal detoxication processes.

Acknowledgement

The authors express their thanks for the financial support to INTAS (project 01-0186) and RFBR (grant 04-05-64687).

References

[1] O.A.Trubetskoj, O.E.Trubetskaya, T.E.Khomutova: *Soil. Biol. Biochem.* **24**, 893 (1992).

TEMPERATURE DEPENDENCE OF THE ION COORDINATION IN WATER SOLUTION AND THE PROBLEM OF THERMOREGULATION OF WARM-BLOODED ANIMALS

A.V. Donets, V.I. Chizhik

Saint-Petersburg State University, 198504, Ulyanovskaya st., 1, Petrodvorets, St.Petersburg, Russia.

e-mail: aldonets@mail.ru

Method

Investigations of the microstructure of aqueous electrolyte solutions are of great interest due to their important role in various physical, chemical, technological, and biological processes. The method [1] developed in the Department of Quantum Magnetic Phenomena makes it possible to determine important parameters of the microstructure of electrolyte solutions (coordination numbers of ions and reorientation times of solvent molecules in different substructures). The method is based on an analysis of the concentration and temperature dependence of magnetic relaxation rates of solvent nuclei.

Under the assumption of the complete dissociation of solute, the structure of solution can be described as the superposition of three substructures: hydration shells of anions, hydration shells of cations, and a zone of pure water. If the exchange of nuclei between all these substructures is fast, the spin-lattice relaxation rate is given by the expression:

$$\frac{1}{T_1} = \frac{1}{T_{10}} + \sum_{i=1}^{N-1} \frac{mn_i \alpha^{\pm}}{M} \left[\frac{1}{T_{1i}} - \frac{1}{T_{10}} \right] \quad (1)$$

where m is the molality of the solution; T_{1i} and T_{10} are the relaxation times of the nuclei in the i -th substructure of the solution and in the pure solvent, respectively; n_i is the number of water molecules in the i -th substructure; M is the number of moles in 1000 g of the solvent (for water, $M=55.5 \text{ mol kg}^{-1}$); α^{\pm} is the number of positive and negative ions in the solute molecule; N is the number of substructures in the solution.

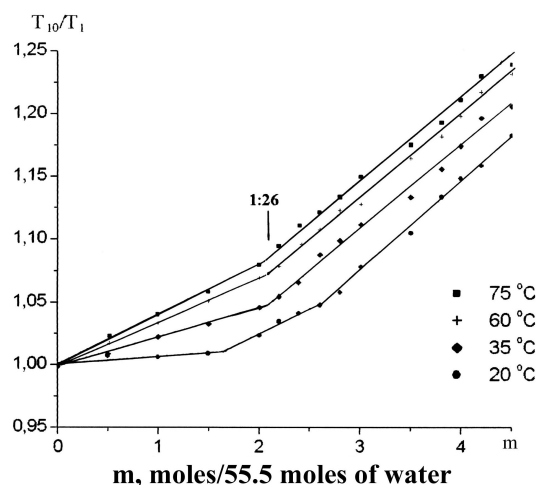


Fig 1. Concentration dependence of the deuteron spin-lattice rates in the solution $\text{NaNO}_3\text{-D}_2\text{O}$ at different temperatures.

Expression (1) predicts the linear concentration dependence of $(1/T_{1i})$, but experimentally distinct deviations from linearity have been observed (Fig.1). The deviation can be explained by the change of substructures in the solution or by the disappearance of some of them (for example, the structure of pure water, then the most weak layers of hydration shells). It was shown that the second reason is valid.

It is well known that in the case of fast movement the relaxation rate is described by the formula:

$$\frac{1}{T_{1i}} = A * \tau_i \quad (2)$$

where A is the constant; τ_i is the reorientation time of the molecules of solvent in the i -th substructure.

Results

An analysis of the results leads to the formulation some rules for the formation of the ion hydration shells [1]. It has been shown that monatomic ions are surrounded by high symmetrical shells. The microstructure near cations is supposed to be trigonal. For example, the hydration shells of the Na^+ ion are characterized by 6 water molecules in the first layer and 12 in the second one. Lonely electron pairs of the water molecule in the first layer are blocked by the cation and that molecules can have only two hydrogen bonds with water molecules in the second layer.

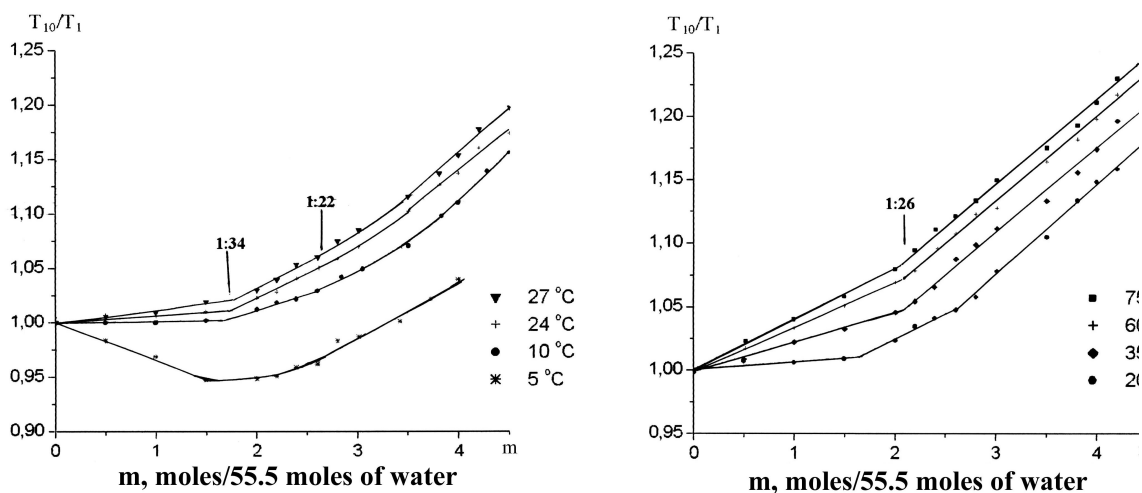


Fig 2. Concentration dependence of the deuteron spin-lattice rates in the NaBr solutions in D_2O at different temperatures.

The monatomic anions Cl^- , Br^- and I^- create the tetrahedral structure (4 water molecules in the first layer). The hydration shells of the anions fit the water structure (at the temperature below 30°C).

It was experimentally shown, that the majority of ions keep their coordination number with concentration and temperature change. But it has been found that some ions change the microstructure of their hydration shells in the diapason of $30\text{-}40^\circ\text{C}$ (see, Fig.2). At the temperatures below 30°C the bend of experimental curves, at the concentration $m = 1.6$, corresponds to the full filling of the ion hydration shells. The hydration shell of the Br^- ion consists of 4 water molecules. When the temperature is below 30°C , the energy of hydrogen bonds is sufficient to maintain the regular tetrahedral structure of water. However, when the temperature exceeds 30°C , the bend is shifted to the higher concentration $m = 2.1$. The energy of thermal motion increases and becomes comparable with the energy of hydration bounds between the water molecules. As a result, the tetrahedral molecular structure is destroyed. The ions are capable to form independent hydration shells. At higher temperature ($>35^\circ\text{C}$) hydration shell of the Br^- anion consists of 8 water molecules (this conclusion can be derived from the data represented in Fig.2). The formation of the secondary shells is also possible. The similar effect is registered for the Cl^- anion.

Hypothesis

The ions play an important role in different biochemical and physiological processes. It was shown, that ions Na^+ , K^+ , Cl^- , Ca^{2+} , Mg^{2+} strong by influence on all kinds of metabolism and transport of substances through cellular membranes (owing to the nonequilibrium concentration of ions). Recently the large number of works on problems of the thermoregulation of warm-blooded animals are published. However in that works only the hypothetical treatment of experimental data are described, and the theory, describing the mechanism of thermoregulation, is not present. Probable that the effect of the change of the coordination number of the Cl^- anion in the range of $30\text{-}40^\circ\text{C}$ can be responsible for the thermoregulation of warm-blooded animals. Our hypothesis is:

The temperature growth up to 30°C and more results in the decrease of the amount of undisturbed water structure and the energy-release reactions flow more difficult. In contrary after the decrease of the temperature below 30°C the quantity of the free water increases and the energy-release reactions become more effective.

Acknowledgments

This work was supported by the Russian Foundation for Basic Research (04-03-32639) and the Government of St. Petersburg (grant M03-4.0Д-30).

References

[1] Chizhik V.I. Molec. Phys. 1997. V. 90 № 4. P. 653-659.

**EPR SPECTROSCOPY, STRUCTURES AND DYNAMICS OF COPPER(II)
COMPLEXES WITH N,O,P,S-CONTAINING LIGANDS**

R.R. Garipov, V.G. Shtyrlin, A.L. Kon'kin, Yu.I. Zyavkina, A.V. Aganov, N.G. Zabirov,
A.V. Zakharov

Kazan State University, Kazan, 420008, Russia

e-mail: Ruslan.Garipov@ksu.ru

Set of copper(II) complexes with P,S,O- and N,O-containing ligands have been investigated by EPR in crystals, liquid and frozen solutions and by quantum-chemistry methods. Using the methodology proposed [1,2] the accurate procedure for the simulation of EPR spectra in frozen solutions was developed to determine anisotropic spin-Hamiltonian parameters. The information obtained has been used for precise description of experimental isotropic EPR spectra. Based on the modification of Wilson-Kivelson theory [3], the general approach for analyzing the complete liquid solution spectra involving two copper isotopes and ligand hyperfine splitting was advanced. By this means we determined the spin-Hamiltonian and hydrodynamic parameters (rotational correlation times and effective hydrodynamic radii) of various Cu(II) complexes with N-(thio)phosphoryl-(thio)amides $RC(S)NHP(X)(OPr^i)_2$ ($R = Ph, benzo-15-crown-5; X = O, S$) and -(thio)ureas $RR'NC(S)NHP(X)(OPr^i)_2$ ($R = H, R' = Ph, cyclohexyl; R = R' = Et; RR' = morpholyl, aza-18-crown-6, 1,10-diaza-18-crown-6; X = O, S$) in organic solvents (toluene, benzene, hexane, acetone, acetonitrile). Three different coordination modes were established in these compounds: six-membered S,S- and S,O- and four-membered S,N-type chelates. The chemical exchange involving charge migration between sulfur atoms within the metal-chelate cycles was described for S,S-complexes. The S,O-coordinated complexes do not exhibit resolved superhyperfine splitting whereas S,N-coordinated compounds reveal nitrogen and phosphorus splittings observed in all temperature range (77-360 K).

The procedure elaborated was successfully applied to the simulation of complicated spectra of several simultaneously presented binary copper(II) complexes with natural tripeptides (GlyGlyGly, GlyGlyTyr, GlyGlyHis, GlyHisGly, HisGlyGly, and oxidized glutathione, GSSG) having various coordination modes and forming in aqueous solutions in a wide pH-range. As a result the unique structural, dynamic, and hydrodynamic information which is important for bioinorganic chemistry has been acquired.

The species under investigation considering possible isomer forms were put in quantum-

chemical geometry optimization procedure by the density functional theory method using large basis sets (effective-core potentials SBK and TZ2P) in program PRIRODA [4]. Under the calculation results the decision on the forms actually presented in solution was made. The calculated hyperfine structure constants of optimal structures agree well with experimental ones and the geometric parameters found confirm with our X-ray for single-crystal complexes.

The support of BRHE (REC-007) and RFBR (grant 02-03-32919) was gratefully acknowledged.

References

- [2] Froncisz W., Hyde J.S.: *J. Chem. Phys.* **73**, 3123 (1980)
- [3] Pilbrow J.R.: *Transition Ion Electron Paramagnetic Resonance*, Oxford: Clarendon Press 1990.
- [4] Wilson R., Kivelson D.: *J. Chem. Phys.* **44**, 154 (1966); **44**, 4440 (1966)
- [5] Laikov D.N.: *Chem. Phys. Lett.* **281**, 151 (1997)

PHONON ECHO OF INTERACTING TUNNELING STATES IN GLASS

E.V. Gazeeva, R.V. Saburova

Kazan State Power-Engineering University, 420066, Krasnoselskaya str., 51, Kazan, Russia.

e-mail: elena.gazeeva@list.ru

Consider an ensemble of the elastic tunneling defects with two degrees of freedom in elastic continuum of glass [1],

$$H = -\sum_i^N \left(\epsilon_i \hat{S}_i^z + \Delta_i \hat{S}_i^x + \gamma_i e_i \hat{S}_i^z \right) + H_{ph}, \quad \hat{S}_i^\alpha = c_i S_i^\alpha, \quad c_i = 0;1, \quad (1)$$

where S_i^α ($a = x, y, z$) are the Pauli matrices, ϵ_i is the initial asymmetry of the two-well potential of the defect, Δ_i tunneling parameter, γ_i potential, e_i is the deformation site i . We suppose the strong defect-phonon coupling. H_{ph} represents the harmonic part of the vibrations of the elastic continuum (acoustic vibrations are taken into account only at low temperatures); $H_{ph} = \sum_{\mathbf{k}} \hbar \omega_{\mathbf{k}} a_{\mathbf{k}}^+ a_{\mathbf{k}}$ where \mathbf{k} is the wave vector of the acoustic vibration a^+ and a are the annihilation and creation phonon operators, $\omega_{\mathbf{k}}$ is the frequency of the phonon with wave vector \mathbf{k} [2].

In this system there are elastic collective excitations like spin waves in magnetic spin glasses [3]. We found the spectrum of the coupled tunnel pseudospin-phonon excitations with unit energy quantum of the form [3]

$$\nu_{a(=1,2)}^2 = \frac{1}{2} \left(\epsilon + \omega_{ac}^2 + \bar{\nu} \right) \pm \left[\frac{1}{4} \left(\epsilon^2 + \omega_{ac}^2 + \bar{\nu} \right)^2 - \epsilon^2 \omega_{ac}^2 \right]^{1/2}, \quad (2)$$

where $\epsilon^2 = \bar{w}^2 - c \Delta \langle \sigma^x \rangle_0 J_{\mathbf{k}}$, $\bar{\nu} = 3c\gamma^2 w \langle \sigma^z \rangle_0 (m \nu_s^2)^{-1}$, ν_s is average acoustic velocity, m is ω_{ac} the acoustic phonon frequency. We see that the mode ν_2 may be soft [3]. $w_i^2 = \Delta_i^2 + \Lambda_i^2$, $\Lambda_i = \sum_j J_{ij} \langle \hat{\sigma}_j^z \rangle$, σ^a may be found from $S^z = \sigma^z \cos \varphi - \sigma^x \sin \varphi$, $\sin \varphi = \frac{\Delta}{\omega}$; $S^x = \sigma^z \cos \varphi + \sigma^x \sin \varphi$; $iS^y = \sigma^y$; J_{ij} is an elastic dipole interaction bond, $J_{ij} \sim r_{ij}^{-3}$ where r_{ij} is the distance between dipoles i and j .

Owing to dipole-dipole interaction the resonance frequency of the collective mode is different than the resonance frequency of the single tunneling defect (TLS).

On the whole the collective excitation spectrum is equidistant. The echo with dipole type transitions is impossible in the system with equidistant spectrum. Therefore we shall assume a small nonequidistantness parameter Γ . Then the collective echo with dipole type transitions is possible; this echo is in dynamics of the anharmonic oscillator 0_∞ [4]. The Hamiltonian describing the collective excitations has a form (the Hamiltonian of anharmonic oscillator [4])

$$H = h\nu_2 \left(a^+ a + \frac{1}{2} \right) + \Gamma (a^+ + a)^3 .$$

(3)

The spectrum of eigen values of anharmonic oscillator is nonequidistant: $E_n - E_{n-1} = \hbar(\nu_a - 2n\Omega)$, $h\Omega = 30\Gamma^2/h\nu_a$ and n denotes energy level.

The primary phonon echo on collective modes is excited by two short pulses of external acoustic field. Let the pulse length is $t_\gamma (\gamma = 1, 2)$, the interval between first and second pulses is τ_{12} , pulse amplitude is e_0 and the acoustic field frequency is and wave vector of acoustic wave is \mathbf{k} .

The Hamiltonian of interaction with external ac field pulse has a form

$$H_j = -\gamma e_0 \left[a \exp(i\omega t - i\mathbf{k}\mathbf{r}) + a^+ \exp(-i\omega t + i\mathbf{k}\mathbf{r}) \right], \quad (4)$$

where γ is the deformation potential.

The following conditions have been fulfilled for the echo observation: $t_\gamma < T_1, T_2, T_2^*$ and $T_2^* < \tau_{12} < T_1, T_2$ where T_1 is the longitudinal relaxation time, T_2^* and T_2 are the transverse reversible and irreversible relaxation time for TLS. The intensity of primary echo is equal to

$$I(\mathbf{k}, t) = I_0(\mathbf{k}) N^2 \theta_1^2 \theta_2^4 \tilde{\Gamma}^2 4\tau_{12}^2 \nu_a^2 \exp\left[(t - 2\tau_{12})^2 / T_2^{*2} \right] \exp(-4\tau_{12}/T_2) \lambda_s^2 S_0^{-1}, \quad (5)$$

where $\tilde{\Gamma} = 30\Gamma^2/h\nu_a$, N is the number of emitted quasiparticles. I_0 is the spontaneous emission intensity along the \mathbf{k} direction for the single energy quantum of collective excitation in unit solid angle, $I_0 = \gamma^2 \nu_a^4 (16\pi\rho\nu_s^{-5})^{-1}$, θ_γ is the square of γ pulse, $\theta_\gamma (\gamma = 1, 2) = \hbar^{-1} t_\gamma \gamma e_0$, λ_s is the acoustic wave length, S_0 is the sample transverse square. Because of different temperature dependence of collective mode resonance frequencies there is different dependence of echo intensity on temperature. At the phase transition temperature there is anomalous behaviour. When the soft mode frequency becomes approximately equal to zero, then the echo intensity has extremum value.

We note the different relaxation times for the single TLS and the collective mode quantum energy. The "collective" relaxation time is more longer than the relaxation time due to the isolated defect. Collective tunneling decreases relaxation time of the "collective" system of the interacting TLS's.

We estimate the echo intensity now. It is difficult to determine a number of N . We assume that $N \sim 10^{14} \text{ cm}^{-3}$. At $\nu_a = 7 \cdot 10^9 \text{ Hz}$, $T_1 \sim T_2 \sim T_2^* \sim 10^{-8} \text{ c}$, $e_0 = 0,5 \cdot 10^{-5}$, $\rho = 2 \text{ g/cm}^3$, $\lambda_s = 1,8 \cdot 10^{-4} \text{ m}$, $\gamma \sim 1 \text{ eV}$, $T = 1 \text{ K}$, $\Gamma = 10^{-2}$, $S_0 = 4 \cdot 10^{-9} \text{ m}^2$ the integrated intensity of echo intensity along direction $\mathbf{k} = 2\mathbf{k}_2 - \mathbf{k}_1$ will be maximum at the time moment $t = 2\tau_{12}$ and equal to $I \sim 10^{-2} \text{ erg/s}$. So echo signal is enough intensive and may be observed.

Conclusion

We consider the collective echo in glass.

1. There are different phases in considered system of the interacting elastic TLS's. These phases existence depends on defect concentration. The temperature dependence of echo signals was investigated in these different phases.

The temperature dependence of the collective echo and "single" echo are different. We may receive information about phase transition like orientational glass one at low temperature because there is anomalous T -dependence for collective echo at the phase transition temperature point.

2. In contrast to "single" TLS echo the emission frequency of the "collective" echo is different than the resonance frequency of "isolated" dipole because of the dipole-dipole interaction between elastic dipole moments of the TLS changes the resonance frequency.

3. The relaxation times of single TLS T_s and relaxation times of the collective modes τ_a are different; $\tau_a > T_s$ because the relaxation times τ_a are more long due to the collective motion of the system (collective tunneling) of the interacting dipoles.

Echo-method is a powerful method which gives the different kinds of information about tunnel characteristic of the TLS, dipole moments, relaxation times and dipole-dipole interactions between TLS's. The observation of the predicted peculiarities of echo formation in glass gives a possibility to receive an important information about the phase transition and the specific parameters in these materials.

References

- [1] G.Busiello, R.Saburova. Low-temperature orientational-glass-like phase transition in glass model. *Physica B*, 245 (1998), p. 27-33.
- [2] Tunneling systems in amorphous and crystalline solids. Editor: P.Esquinazi. Springer, Berlin, 1998, 599 p.
- [3] G.Busiello, R.Saburova. Tunneling electric dipole defects in insulating glass. *Physica B*, 263-264 (1999), p. 324-326.
- [4] U.H.Kopvillem, S.V.Prantz. Polarization echo. *Science, Moscow*, 1985, 189 p.

**MAGNETIC RESONANCE AND OPTICAL SPECTROSCOPY
OF TETRAGONAL Yb³⁺ CENTER IN CaF₂**M.L. Falin¹⁾, K.I. Gerasimov¹⁾, V.A. Latypov¹⁾, A.M. Leushin²⁾¹⁾Zavoisky Physical-Technical Institute, Kazan 420029, Russian Federation²⁾Kazan State University, Kazan 420008, Russian Federation

It is known that depending on the conditions of crystal synthesis, the Yb³⁺ in a CaF₂ single crystal forms up to 14 paramagnetic centers (PC) with different symmetry [1]. They appear depending on the conditions of the crystal growth, various mechanisms of the excess charge compensation and the treatment of samples (hydrolysis, thermal annealing). Exclusively for the cubic PC (T_c) energy levels were nearly completely established and the parameters of its crystal field (CF) were determined. However, the CF parameters determined from the experimental optical data [2, 3] differ from those determined from the hyperfine parameters obtained by Electron-Nuclear Double Resonance (ENDOR) [4]. In these papers the positions of the energy levels Γ_6 and Γ_8 in the ground multiplet $^2F_{7/2}$ also differ. Only one optical spectral line is unambiguously experimentally identified for Yb³⁺ center of tetragonal (T_{tet}), trigonal and rhombic symmetry [5, 6]. Analogous to the method developed in [4], the CF parameters for the Yb³⁺ center of tetragonal symmetry (T_{tet}) were determined on the basis of the known position of one optical line and the hyperfine parameters obtained by ENDOR [7]. To the best of our knowledge the energy level diagram obtained in [7] was not confirmed experimentally. This work presents results of the detailed investigation of the PCs formed by the Yb³⁺ ions in CaF₂ using optical and magnetic resonance spectroscopy, laser selective excitation of luminescence, concentration series, phase fluorimetry methods and thermal processing.

EPR spectra of T_c and T_{tet} were identified. Empirical diagrams of the energy levels were established and potentials of the CF were determined. Information was obtained on the CaF₂ : Yb³⁺ phonon spectra from the electron-vibrational structure of the optical spectra. The CF parameters were used to analyze the crystal lattice distortions in the vicinity of the Yb³⁺ ion and the F⁻ ion, compensating the positive excess charge in T_{tet}. Within the frames of a superposition model, it is established that four F⁻ ions from the nearest cubic surrounding, located symmetrically with respect to the fourfold axis from the side of the ion-compensator, approach the impurity ion and deviate from the PC axis. The second set of four fluorine ions also approaches the Yb³⁺ ion and the PC axis. The ion-compensator F⁻ also approaches considerably the impurity ion.

POSTER SESSION PS11

This work was supported by the Russian Foundation for Basic Research (project 02-02-16648) and ISTC 2121.

References

- [1] Anderson C.H.: Crystal With the Fluorite Structure, Ch. 5 (Ed.: W.Hayes), Oxford: Clarendon 1974; J.M.Baker, *ibid.* Ch. 6
- [2] Low W.: Phys. Lett., **26A**, 234 (1968)
- [3] Kiro D., Low W.: Magnetic Resonance p 247 (Eds.: C.K. Coogan, N.S. Ham, S.N. Stuart, J.P.Pilbrow and G.V.H.Wilson), New York: Plenum 1970
- [4] Baker J.M., Blake W.B.J., Copland J.M.: Proc. Roy. Soc. A **309**, 119 (1969)
- [5] Kirton J., McLaughlan S.D.: Phys. Rev., **155**, 279 (1967)
- [6] Kirton J., White F.M.: Phys. Rev., **178**, 543 (1969)
- [7] Baker J.M., Blake W.B.: Proc. Roy. Soc. A **316**, 63 (1970)

**STUDY OF SiO₂ GLASSES DOPED WITH Er³⁺ IONS
AND CO-DOPED WITH N AND F**

R.R.Gubaidullin, S.B.Orlinskii, R.M.Rakhmatullin

MRS Laboratory, Kazan State University, Kremlevskay 18, 420008 Kazan, Russia

e-mail: rara@ksu.ru

1. Introduction

The study of near surrounding and dynamics of rare earth ions (RE) in silica glasses are of scientific and technological importance. Silica glasses doped with rare earth ions (RE) are applied in optical fiber systems as amplifiers and lasers [1]. A poor solubility of RE in glasses leads to the formation of clusters even at small concentration of RE ($> 10^{18} \text{ cm}^3$) [2], that represents a problem for creation of effective miniature optical devices. It has been established experimentally that incorporation of some additional impurities in SiO₂ glass, for example Al₂O₃ or P₂O₅, improve essentially solubility of RE in the glass and correspondingly improve the laser efficiency [3]. It has been assumed that Al or P ions occupy positions nearby to RE forming bonds RE - O - Al/P [4]. This has been confirmed by the pulse EPR studies of SiO₂ glass doped with Nd³⁺ and co-doped with Al₂O₃ [5].

The purpose of this work was the study of influence of co-doping with N and-or F on the formation of Er³⁺ clusters in SiO₂ glass with electron spin echo (ESE) method.

2. A technique & samples

Pulsed EPR measurements were carried out at the X-band home-built spectrometer in which microwave pulses are formed by a magnetron with the output power of 5 kW.

The electron spin echo envelope modulation (ESEEM) were recorded using the two pulse sequence $2\pi/3 - 2\pi/3$, where the echo intensity is measured as a function of the time interval τ between pulses. The paramagnetic resonance spectra were recorded as a dependence of the ESE amplitude on magnetic field.

The samples were synthesized by means of plasma chemical deposition in the laboratory of fiber optics center of the Russian Academy of Science, Moscow. The composition of glasses and the concentration of impurities are presented in the Table.

Table

Composition	Notation	Dopant & co-dopant
SiO ₂ +Er+N	ErN	0.03at%Er, 0.08at%N
SiO ₂ +Er+F	ErF	0.3at%Er, 1.8at%F
SiO ₂ +Er+N+F	ENF	0.15at%Er, 0.05at%N, 0.6at%F

3. Experimental results and discussion.

3.1. SiO₂+Er+F

ESE spectra have been registered at temperatures 1.6 - 4.2K. It was observed only one line (the line width is approximately 500G) with the g-factor close to 2.

The study of T_m on magnetic field has shown that we have at least 2 types of the centers. It was found that echo amplitude decay was described by 2 exponents, and the contribution from one of them decreased with the magnetic field increase. The temperature dependence of the longest T_m has been measured. It turned out that T_m does not depend on temperature in the investigated range and it is equal approximately 0.6 mks.

Based on the obtained experimental results it is possible to assume that the observed paramagnetic centers is formed by structural defects and not connected directly to Er ions.

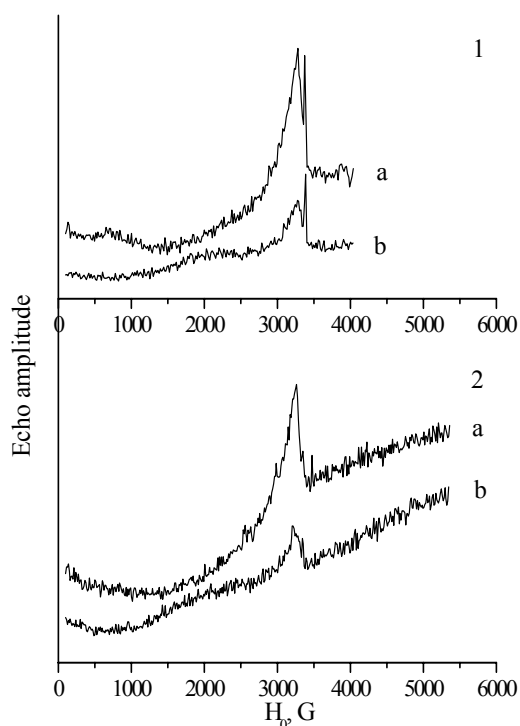


Fig.1. ESE spectra of ErN. 1 T=2.1K;
2 T=1.6K; a $2\tau = 0.57$ mks; b $2\tau = 1$ mks.

3.2. SiO₂+Er+N

The dependence of the ESE spectra on the temperature is presented in fig.1. The transformation of a spectrum with temperature was observed. In the magnetic field corresponding to the $g = 2$ two lines were recorded. One line with a width of ~ 500 G is similar to the line in the sample ErF and the second one has the width of the several Gauss. Besides, several broad lines were observed.

ESE spectra for various values of a delay τ between pulses have been measured (fig.1). It can be seen that these spectra were changed depending on τ . The

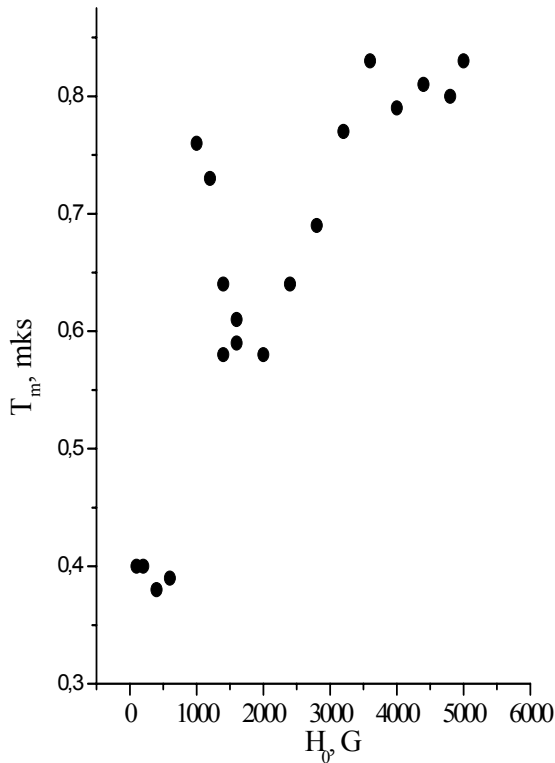


Fig.2. Phase relaxation of ErN

dependence T_m on magnetic field H_0 has been obtained, one of which is presented in fig.2. This dependence is not monotonous. In the areas where $T_m(H_0)$ has peaks ($H_0 \sim 1000\text{G}$ and $H_0 \sim 3500\text{G}$) the relaxation decay is described by 2 exponents. Hence, besides lines on $g \sim 2$, it is possible to allocate, at least, 2 types of the centers which can be identified as lines from single Er ions and Er clusters.

3.3. $\text{SiO}_2+\text{Er}+\text{N}+\text{F}$

The spectrum of this sample is similar to ErN one. The strongest differences of this sample from others are observed for modulation effects in the magnetic fields typical for single site Er^{3+} ions. The analyses of ESEEM on the magnetic field showed that the oscillation period is due to N^{14} nucleus and close to the Larmor frequency.

4. Conclusion

On the basis of obtained experimental data we supposed that there are at least four types of the paramagnetic centers in studied samples. Two of them are related to the broad and narrow lines at $g \sim 2$, probably, due to the defects of a glass arising at doping. We attribute the narrow line to the E' defect centers arising at doping by F ions and the broad line ($\sim 500\text{G}$) apparently, is due to the centers formed by charge compensation of RE ions.

The other two centers are directly

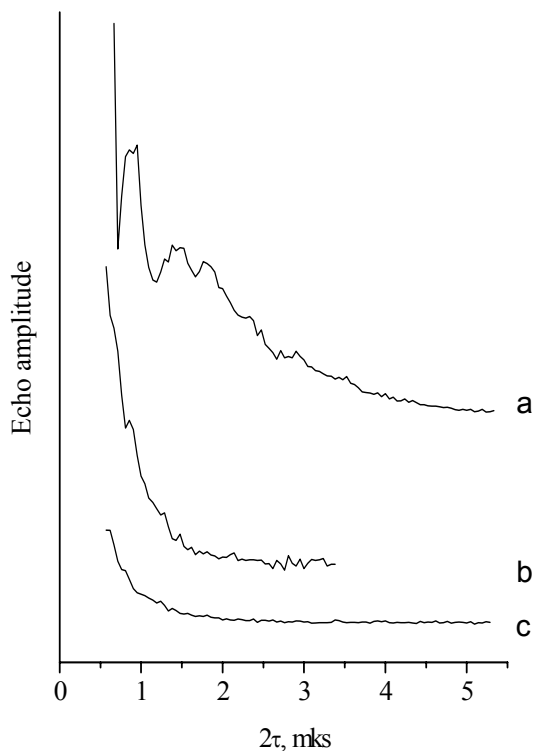


Fig3. ESEEM. a ErFN, $H_0=2900\text{G}$, $T=1.6\text{K}$; b ErN, $H_0=2900\text{G}$, $T=1.9\text{K}$; c ErF,

connected to the doping with Er^{3+} ions. We should note that in the ErF sample we could not detect confidently the lines due to Er^{3+} ions. This is probably connected with the presence in sample ErF a lot of clusters and hence, the shorter T_m that allows us to register with our spectrometer.

The most important result is the observation of a comparatively strong modulation due to N^{14} nucleus in the sample ErNF, whereas in ErF and ErN samples modulations are extremely weak (fig.3). Besides, the phase relaxation time in ErNF is longer than in ErN at less concentration of RE ions. We suppose that doping with F or N ions did not break out clusters of RE while the combined doping with N and F ions results to the reduction of clusters. The whole set of obtained results lead us to the following supposed model, the joint embedding of N and F lead to the formation of the complex: RE – F – N.

References

- [1] Makoto Shimizu, Makoto Yamada, Masaharu Horiguchi and Etsuji Sugita, IEEE Photonics Technology Letters, v.2, N 1, 1990, p. 43-45.
- [2] Man F.Yan, Proceedings of the XVIII International Congress on Glass, San Francisco, 1998.
- [3] Kazuo Arai, Hiroshi Namikawa, Ken Kumata, Tatsutoki Honda, Yoshira Ishii and Takashi Handa, J.Appl. Phys, v.59, N 10, 1986, p. 3430-3436.
- [4] S. Sen and J. F. Stebbins, J. Non-Cryst. Solids v. 188, 1995, p.54-61.
- [5] K.Arai, S. Yamasaki, J. Isoya, H. Namikawa, J. Non-Cryst. Solids, v. 196, 1996, p.216-220.

**THE PROGRAM FOR CALCULATION THE ELECTRONIC STRUCTURE
OF THE IMPURITY CENTERS IN CRYSTALS**

E.N. Irinyakov

Zavoisky Physical-Technical Institute, Kazan 420029, Russia.

e-mail: irinyakov@mail.ru

Optical and EPR spectroscopy of the rare-earth ($4f^N$) and transition metal ($3d^N$) ions, which determine the important properties of various useful crystals [1], requires knowledge of the energy levels and state vectors of an ion. The latter are characterized by the crystal field (CF) parameters.

In order to analyze the optical and EPR spectroscopy data using the CF approach, a computer program «Optical Spectra Analyzer» (OSA) has been developed. It allows calculating an energy spectrum and wave functions of the free and impurity ions with unfilled electronic d and f-shells ($d^1 - d^9$, $f^1 - f^3$, $f^1 - f^{13}$). The full energy operator consist the electrostatic repulsion of electrons, magnetic interactions ("spin-orbit", "spin-spin", "spin-other-orbit", "correlated spin-orbit"), linear and nonlinear parts of electronic excitations ("configuration" interaction) and crystal field interaction with symmetry of any of 32 point groups.

There is an opportunity of the self-consistent fit the calculated and experimental energy levels and g-factors, that considerably simplifies finding-out the CF parameters and parameters of interactions. Matrix elements of all interactions are calculated in basis $|l^n \gamma LSJM_J\rangle$ using Wigner-Racah algebra [2, 3] and the fractional parentage coefficients (FPC) [4]. OSA allows fitting experimental data using different nonlinear optimization methods (Powell method, BFGS, Simplex etc.). Also there are many useful functions included in the program: viewing values of all matrix elements, FPC, 3j-6j-9j-symbols in symbolical and numerical form and transformation of CF parameters (Wybourne and Stevens notation).

The program is written in Pascal language in Delphi, has the convenient interface and has been used in [5] for calculation of spectrum $\text{LiNbO}_3: \text{Cr}^{3+}$ and iron group spectra for elements with $3d^2$, $3d^3$, $3d^7$ and $3d^8$ configurations [6].

This work was supported by the Russian Foundation for Fundamental Research (project 02-02-16648).

References

- [1] Henderson B., Imbusch G.F., Optical Spectroscopy of Inorganic Solids, Oxford: Clarendon 1989.
- [2] Judd B.R.: Operator Techniques in Atomic Spectroscopy, New-York: McGraw-Hill 1963.
- [3] Rudzikas Z.: Theoretical Atomic Spectroscopy, Cambridge: Cambridge University. Press 1997.
- [4] Nielson C.W., Koster G.F.: Spectroscopic Coefficients for the p^N , d^N and f^N Configurations. Cambridge, Mass.: M.I.T. Press 1963.
- [5] Leushin A.M., Irinyakov E.N.: Sbornik trudov "Kogerentnaya optika i opticheskaya spektroskopiya" (in Russian), vol. V, pp. 228-234. Kazan: Regent 2001.
- [6] Irinyakov E.N., Mikhailov S.A.: Sbornik trudov "Kogerentnaya optika i opticheskaya spektroskopiya" (in Russian), vol. VI, pp. 88-101. Kazan: Regent 2002.

THE DETERMINATION OF NO IN HEART AND LIVER OF RATS BY METHOD OF EPR-SPECTROSCOPY AFTER MYOCARDIAL INFARCTION

A.I. Ismailova¹⁾, L.N. Muranova¹⁾, V.V Andrianov¹⁾, Kh.L. Gainutdinov¹⁾, O.I. Gnezdilov¹⁾, A.G. Nasyrova²⁾, R.R. Nigmatullina²⁾, A.A. Obynochny¹⁾, F.F. Rahmatullina²⁾, A.L. Zefirov²⁾

¹⁾Kazan Physical-Technical Institute of Russian Academy of Sciences, Kazan

²⁾Kazan State Medical University, Kazan

E-mail: Asja.Ismailova@rambler.ru

In last few years the intent attention attracts an nitric oxide (II) (NO), which plays a role of the signal molecule (Schuman, Madison, 1994). Specifically significant its role in the cardiovascular system, where NO regulated the vascular tonus, arterial pressure, proliferation of endothelial and smooth-muscular cells of the vascular side (Guo et al., 1995; Tronc et al., 1996). It is possible to speak about two diametrically opposite directions of NO influences (Manukhina, 2000): first - stimulated, positive, and secondly, it has the capability to toxic, damaging action. Therefore an exact determination of the contents of the radical of nitric oxide in heart is actual. The EPR measurements were conducted on samples of the tissues of heart, liver, kidney, pancreas, blood vessel and blood at the temperature of the fluid nitrogen on EPR-spectrometer ER-200E-SRC of company "Bruker". During coupling of NO with lipophylic trap - diethylditiocarbamate (DETC) there were formed the paramagnetic mononitrozyl complexes of iron (MNCl) with DETC, characterised by EPR signal with $g_{\perp} = 2,036$, $g_{||} = 2,01$ and extrathin and tryplete structure under g_{\perp} . It was observed the essential difference between EPR-signals in fields near 3000 e for left and right half of the rat heart. This was, probably, connected with the different contribution to the total observed signals from complexes of NO with Fe^{2+} and Cu^{2+} of blood and the signals from injected traps of stable radicals. Through 10-15 minutes after the production of the experimental myocardial infarction (EMI) animals were injected by trap (n=20). During the comparative analysis of EPR spectra of MNCl-DETC of the control and experimental animals it was discovered that in rats after EMI the EPR spectra of MNCl-DETC were noticeably of smaller intensity, than in control animals. Thus, the production of NO in the first hours after the experimental myocardial infarction decreases. Obviously further study of NO role in the heart functions in norm and during pathology will increase our knowledge about pathogenesis of diseases, and - to the appearance of new methods of their therapy.

Supported by RFBR, grant N 03-04-96257 and NIOKR RT 03-3.1-243.

TR EPR STUDY OF THE ELECTRON TRANSFER PROPERTIES IN PHOTOSYSTEM I WITH ANTHRAQUINONE AS SECONDARY ACCEPTOR

I. Karyagina, J. Pushkar, D. Stehlik

Free University of Berlin, Physics Department, Arnimallee 14, 14195 Berlin, Germany

e-mail: dietmar.stehlik@physik.fu-berlin.de

Light-induced electron transfer (ET) in PS I proceeds from the primary donor (a chlorophyll heterodimer) P_{700} along a chain of low potential electron acceptors: the chlorophyll monomer A_0 , the phyloquinone A_1 , and three [4Fe-4S] clusters named F_X , F_A , F_B . Multi-frequency TR EPR spectroscopy is used to investigate structural and dynamic properties of the sequential radical pair states $P_{700}^+A_1^-$ and $P_{700}^+A_1[FeS]^-$ under physiological conditions when anthraquinone (AQ) instead of native phyloquinone (PhyQ) is reconstituted into the A_1 binding site of PS I [1]. Besides harsh organic solvent extraction of the native A_1 prior to AQ substitution, another method of reconstitution is introduced, based on quinone biochemical pathway mutants. ET from AQ to FeS speeds up in accordance with a more negative AQ redox potential. Correspondingly, the preceding ET step from the first radical pair $P_{700}^+A_0^-$ to $P_{700}^+AQ^-$ is found to slow down as evaluated from the spin dynamics and correspondingly altered spin polarisation patterns of the observable consecutive radical pair states $P_{700}^+AQ^-$ and $P_{700}^+[FeS]^-$. The temperature dependence of the ET kinetics is presented. Quantitative evaluation of the A_0 to AQ ET kinetics follows a model based on a distribution of lifetimes/redox potentials of A_0 as applied before to interpret altered spin polarisation patterns and ET kinetics in PS I particles from site-directed mutants of the A_0 ligand methionin [2]. The reported first simultaneous EPR observation of two consecutive ET processes in real time opens new possibilities for quantitative interpretation of ET and spin dynamics.

References

- [1] S. Itoh, M. Iwaki, I. Ikegami; *Biochim. Biophys. Acta* 1507 (2001) 115-138
- [2] R. O. Cohen, G. Shen, J. H. Golbeck, Wu Xu, P. Chitnis, A. Valieva, Art van der Est, Y. Pushkar, D. Stehlik. *Biochem.* (2004), in press

In cooperation with John. H. Golbeck (Pennsylvania State University), Art van der Est (Brock University)

PULSED FIELD GRADIENT NMR SPECTROSCOPY IN INVESTIGATION OF ASSOCIATION OF MACROMOLECULES IN LIQUIDS

S.V. Kharlamov¹⁾, A.A. Nafikova²⁾,
A.S. Mihajlov²⁾, V.S. Reznik²⁾, Sh.K. Latypov²⁾, A.V. Aganov¹⁾

¹⁾Kazan State University, 420008, Kremlevskaja str., 18, Kazan, Russian Federation.

²⁾Institute of Organic and Physical Chemistry, Kazan Science Center of Russian Academy of Sciences, 420088, Arbuzov str., 8, Kazan, Russian Federation.

e-mail: khsergey@land.ru, nmr@iopc.knc.ru

1. Introduction

Determination of fine molecular structure of organic compounds, mechanism of molecular recognition and effects on biomolecules is a very important task. As is well known, a spatial structure and a molecular mobility determine physiological properties of compounds. And the High Resolution NMR spectroscopy is a very powerful method of investigation of material structure [1, 2], especially in liquid. This work is the step on the way to the determination of a spatial structure of macromolecular compounds, which belong to a perspective class of matters, used as drugs in therapeutics of cancer and cardiovascular

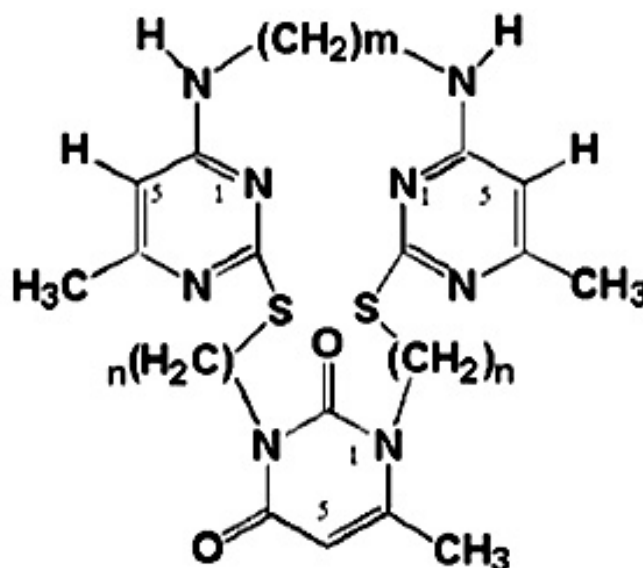


Fig. 1. Molecules of compound under investigation.

diseases (see fig. 1).

Macromolecular compounds under investigation include the pyrimidine bases (derivatives of 6-methyl uracils and other bases of this series). Specific peculiarity of these

bases is their ability to form the supramolecular selforganized assemblies, possessing new physical, chemical and pharmacological characteristics. These compounds show significant physiological activity.

The peculiarity of NMR spectra of macromolecules (see fig. 1) is the presence of spectral features of asymmetric molecular packing of the alkylpyrimidine substituents referring to the central uracil ring (the signals of fifth protons of terminal pyrimidine rings are non-equivalent).

Theoretical modelling for these molecules (spatial models of molecules were built by "Molecular mechanics" computer program) shows that minimum of steric energy corresponds to molecules, which convolute in capsule. Also it shows that the molecules of compound exhibit a tendency to forming a permolecular structure.

One- and two-dimensional relaxation NMR experiments (such as 1D-NOE-DIF, T_1 spin-lattice relaxation time analysis, ROESY) show that there are non-trivial dipole-dipole interactions between protons of different parts of molecule, the removed groups being among them. That is consequence of specific packing of molecule.

But the task is considerably complicated. The point is that studying molecules have a lot of conformations in liquid. There are no any pronounced intramolecular interactions, which are able to stabilize the conformation. Or different interactions (with close magnitudes) work simultaneously.

2. Results and discussion

Thus, in terms of the complexity of our task, it was divided into 2 subgoals: 1) analysis of the conformational features of the compound and 2) investigation of its supramolecular structure.

This work was dedicated to the 2nd part. Our previous research shows the capability of the molecules to form the strong spatially ordered supramolecular structure. It follows from specific concentration chemical shift's dependences [4]. And this is conforming to the theoretical modeling (see above). It is necessary to note that the study of molecular association is of paramount importance to understand solution structures.

We made a number of experiments by DOSY method – investigation of self-diffusion coefficients of molecules in liquid –, which is wide used for structural investigations [6]. In diffusion-ordered spectroscopy (DOSY), which was introduced only a few years ago [5], the results are displayed as 2D spectra with the NMR chemical shift on the horizontal axis and the derived diffusion coefficients on the vertical axis. Such DOSY plots are obtained by effective

data inversion of the pulsed field gradient (PFG) spin echo NMR data obtained by incrementing the gradient strength. PFG NMR is a very effective tool to study the translational motion of molecules, and is used for studying molecular associations. However, DOSY has the advantage of immediately visualizing the effects even in more complex mixtures.

The results of our investigation exactly show that there is an intermolecular association of the studying molecules in liquid. We found that the hydrodynamic radius of the molecules appreciably increases with increasing of the concentration (data not shown). We emphasize that it was taken into account the dependence of the effective hydrodynamic radius from the viscosity of the mixture [7].

4. Acknowledgements

This work was supported by the CRDF (*REC-007*).

References

- [1] C. Rossi. – *Encyclopedia of NMR*, **7**, 4237 (1995).
- [2] T. Parella. – *Magn. Reson. Chem.*, **36**, 467 – 495 (1998).
- [3] S. Kharlamov. – *Proceedings of Students Physical Seminar of Kazan State University*, **4**, 63 – 68 (2003).
- [4] S. Kharlamov. – *Proceedings of Students Physical Seminar of Kazan State University*, **4**, 17 – 22 (2003).
- [5] K.F. Morris, C.S. Johnson, *J. Am. Chem. Soc.*, **114**, 3139; **115**, 4291 (1992).
- [6] G.S. Kapur, S. Berger, E.J. Cabrita, *Tetrahedron Letters*, **41**, 7181 – 7185 (2000).
- [7] E. J. Cabrita, S. Berger, *Magn. Reson. Chem.*, **39**, 142–148, (2001).

TWO-FREQUENCY EXCITATION. NEW APPLICATIONS

D.Ya. Osokin, R.R. Khusnutdinov

Kazan Physical-Technical Institute, Russian Academy of Sciences.

The two-frequency excitation in nuclear quadrupole resonance (NQR) was suggested and investigated by V.S.Grechishkin and co-workers [1, 2] many years ago but the application of this technique remains very restricted [2]. In recent years there has been a growth interest in the use of the two-frequency technique [3, 4] again. This interest may have been excited by the recent observations of the coherent optical information storage, dark states and the possibility of application of these phenomena for quantum information processing [5, 6]. The multilevel spin systems themselves are supposed to be a perspective framework for implementation of quantum computers [8, 9].

In this respect we would like to present a simple and effective technique for solving any problem in a three-levels system by the transition in Liouville space which was used in our previous paper [10]. This transition replaces the unitary transformations in Hilbert space by simple multiplication of the Liouville supermatrices that can be carried out using symbolic computations with Mathematica, Maple, Mathcad and others.

The results of calculations are as follows. The simultaneous two-level irradiation creates an echo signal at the third transition. The serial irradiation does not. The transient signals at the irradiated transitions arise due to coherence transfer and look like echo signals if the inhomogeneous broadening at these transitions correlate. So the two-frequency excitation in ^{14}N NQR can be applied for investigations of the inhomogeneity in crystals.

References

- [1] Grechishkin V.S.: Nuclear Quadrupole Interactions in Solids (in Russian). Moscow: Nauka 1973.
- [2] Anferov V.P., Grechishkin V.S., Sinyavski N.Ya.: Nuclear Spin Resonance, New Methods (in Russian). Leningrad: Leningrad University 1990.
- [3] Mozjoukhine G.V.: Appl. Magn. Reson. 22, 31 (2002)
- [4] Sauer K.L., Suits B.N., Garroway A.N., Miller J.B.: Chem. Phys. Lett. 342, 362 (2001)
- [5] Liu C., Dutton Z., Behroozi C.H., Hau L.V.: Nature 409/25, 490 (2001)
- [6] Phillips D.F., Fleischhauer A., Mair A., Walworth R.L.: Phys. Rev. Lett. 86, 793, (2001)

POSTER SESSION PS17

- [7] Fleischhauer M., Lukin M.D.: Phys. Rev. Lett. 84, 5094 (2000)
- [8] Kessel A.R., Ermakov V.L.: Zh. Eksp. Teor. Fiz. 117, 317 (2000)
- [9] Zaretskiy D.F., Sazonov S.B.: Zh. Eksp. Teor. Fiz. 121, 521 (2002)
- [10] Osokin D.Ya., Kurbanov R.Kh., Ermakov V.L., Shagalov V.A.: Zh. Eksp. Teor. Fiz. 106, 596 (1970).

DETECTION OF FREE RADICALS FORMATION IN HAEMOLYMPH OF INSECTS BY EPR SPECTROSCOPY

D. Komarov¹⁾, I. Slepneva¹⁾, V. Glupov²⁾, V. Khramtsov¹⁾

¹⁾SB RAS, Institute of Chemical Kinetics and Combustion, 630090 Novosibirsk, Russia

²⁾SB RAS, Institute of Animal Systematics and Ecology, 630091 Novosibirsk, Russia

e-mail: komarov@kinetics.nsc.ru

Melanotic encapsulation is the main process in immune response of insects. The key enzyme of melanization, phenoloxidase (PO), converts mono- and diphenols to quinones. During this process the potentially cytotoxic quinoid intermediates are generated, which can cause the production of the reactive oxygen species (ROS) such as superoxide anion and hydroxyl radical. Due to their high reactivity these species can be involved in cytotoxic reactions in the insects.

The most important reaction of melanization is oxidation of dihydroxyphenylalanine (DOPA) by PO. In this work we have studied generation of ROS during oxidation of DOPA by purified PO and in isolated haemolymph of insects by EPR method using spin traps. No EPR signal of spin adducts was observed using nitron-based spin trap DEPMPO. Moreover the DEMPO-OOH spin adduct did not form when superoxide anion was generated by independent source in the presence of DOPA in concentration over 10 μM . We have shown that DOPA can react with superoxide anion. We have estimated the rate constant of such interaction as $k = 3.5 \cdot 10^5 \pm 0.2 \text{ M}^{-1} \text{ s}^{-1}$. So the presence of DOPA in a sample can interfere with determination of superoxide anion using nitron spin traps, particularly DEPMPO which interact with superoxide anion with rate constant $k = 0.53 \text{ M}^{-1} \text{ s}^{-1}$.

Therefore we applied other spin trap, 1-hydroxy-3-carboxy-pyrrolidine (CP-H), which can be oxidized by ROS, including quinoid-nature compounds, to stable nitroxyl radical CP. We have detected the formation of ROS in haemolymph of insects by studying kinetics of CP-H oxidation. The addition of DOPA in haemolymph significantly increased CP-H oxidation rate. Superoxide dismutase did not affect the rate of CP formation, but specific inhibitor of PO phenylthiourea completely inhibited it. These data suggest that rather DOPA-semiquinone than superoxide radical is responsible for CP-H oxidation.

O-semiquinones such as DOPA-semiquinone are very short-lived. To detect the formation of DOPA-semiquinone in haemolymph we applied spin stabilization technique of o-semiquinones by cations of divalent diamagnetic metals. We have obtained the EPR spectra

POSTER SESSION PS18

of complex DOPA-semiquinone with Mg^{2+} in haemolymph of insect. No spectra were observed in the presence of phenilthiourea. These data indicate that DOPA-semiquinone really produced in insect haemolymph during melanization and its formation is concerned with PO activity.

So we did not show that superoxide form during melanization, but the fact it readily react with DOPA suggests that it can not be involved in cytotoxic reactions against internal parasites. The formation of DOPA-semiquinone in haemolymph and its high reactivity allows us to consider it as cytotoxic molecule in the immune response of insects.

This work was partly supported by Russian Foundation of Basic Researches (00-04-49563, 02-04-48374).

FREQUENCY DEPENDENCE OF THE EPR SPECTRUM OF PENTANUCLEAR CLUSTER $[\text{Cu}_3\text{Dy}_2(\text{ClCH}_2\text{COO})_{12}(\text{H}_2\text{O})_8] \cdot 2\text{H}_2\text{O}$

L.V. Korobchenko, R.T. Galeev, E.R. Zhiteytsev

Kazan Physical –Technical Institute, Russian Academy of Sciences, Kazan, Russian Federation

e-mail: korobchenko@kfti.knc.ru

EPR studies are carried out in the X- and Q-band at $T=300$ K and 4.2 K on the polycrystalline samples of the compound $[\text{Cu}_3\text{Dy}_2(\text{ClCH}_2\text{COO})_{12}(\text{H}_2\text{O})_8] \cdot 2\text{H}_2\text{O}$. EPR researches in mixed systems of paramagnetic centers with 3d-4f interactions represent the interest in the search of new magnetic materials.

The compound is composed of the pentanuclear complexes $\text{Cu}_3\text{Dy}_2(\text{ClCH}_2\text{COO})_{12}(\text{H}_2\text{O})_8$ and water molecules in the ratio 1:2. In pentanuclear clusters the Cu(II) ions alternate with rare – earth ions of Dy(III) and cluster may be presented as a linear fragment: Cu(2)-L(2)-Dy-L(1)-Cu(1)-L(1)-Dy-L(2)-Cu(2), where L(1) and L(2) are the bridging fragments and Cu(1) and Cu(2) are the structurally nonequivalent copper complexes[1]. The distances Cu(1)-Dy, Dy-Cu(2) and bridging fragments L(1), L(2) are differ, consequently one expects the exchange and dipole interaction between Cu(1)-Dy and Dy-Cu(2) are differ too.

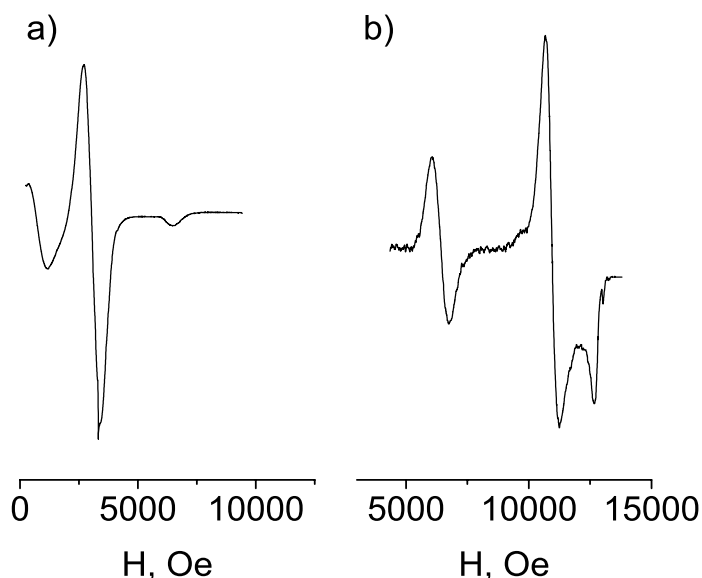


Fig.1 EPR spectra of the polycrystalline samples of the compound $[\text{Cu}_3\text{Dy}_2(\text{ClCH}_2\text{COO})_{12}(\text{H}_2\text{O})_8] \cdot 2\text{H}_2\text{O}$ at $T = 4.2$ K: a) X-band; b) Q-band.

In the spectra at room temperature in X-band and Q-band the lines due to only the copper complexes of the first type Cu(1) are observed. These spectra are typical for spin $S = \frac{1}{2}$ and may be simulated with parameters $g_z=2.32\pm 0.01$ and $g_{xy}=2.07\pm 0.005$.

At temperature 4.2 K in X-band and Q-band the complicated spectra are observed (Fig.1).

The analysis of these spectra and extraction of the information from such spectra is not a simple task.

First of all it is necessary to determine possible spin-states of this pentanuclear cluster Cu-Dy-Cu-Dy-Cu. It is well known that for rare-earth ions the spin-orbit coupling exceeds the influence of the crystalline field. The ground term ${}^6H_{15/2}$ of a trivalent dysprosium ion (f^9) is split in the low – symmetry ligand crystalline field into eight Kramers doublets [2]. At temperature $T=4.2K$ we may consider, that Dy(III) ion has effective spin $S' = 1/2$. Thus at low temperature that pentanuclear cluster represents system consisting of five the coupling paramagnetic centers with spins $S = 1/2$.

In the present work attempt of the analysis frequency dependences of such spectrum is made. Possible variants of interactions of the paramagnetic centers in the cluster were considered: 1) exchange interaction very weak and an observably spectrum may be submitted as the sum of spectra caused by three nonequivalent centers with $S = 1/2$: Cu(1), Cu(2) and Dy; 2) the approach of the strong exchange between Dy and Cu(2) ions and very weak exchange between Dy and Cu(1) ions, in this case the pentanuclear cluster may be considered as composed of two Cu(2)-Dy dimers and Cu(1)-complex; the states with $S = 0, 1$ and with $S = 1/2$ are realized (when interaction between Dy and a copper complex of the first type Cu(1) can be not taken into account); 3) exchange interactions between Dy and Cu(1) ions, Dy and Cu(2) ions are taking into account; in that case the states with $S = 1/2, 3/2, 5/2$ are realized.

For the interpretation of the experimental spectrums the numerical calculations was carried out. The analysis has shown that Dy ions interact with copper centre of the second type Cu(2) more strongly than with Cu(1). The conclusion about the antiferromagnetic character of the interaction of the Dy ions with Cu ions is made.

This work is supported by the RFBR, project № 04-02-17163.

References

- [1] V.K. Voronkova, R.T. Galeev, S. Shova, G. Novitchi, C.I. Turta, A. Caneschi, D. Gatteschi, J. Lipkowski, YU.A. Simonov .: Appl. Magn. Reson.25, 227-247 (2003)
- [2] Abragam A., Bleaney B.: Electron Paramagnetic Resonance of Transition Ions. Oxford: Clarendon Press 1970.

**INVESTIGATION OF 3D STRUCTURE OF BIOACTIVE COMPOUNDS BASED ON
PYRIMIDINE DERIVATES USING DYNAMIC NMR SPECTROSCOPY**

A.V. Kozlov¹⁾, Sh.K. Latypov²⁾, A.A. Nafikova²⁾, A.V. Aganov¹⁾, A.S. Mihajlov²⁾,
V.S. Reznik²⁾

¹⁾Kazan State University, 420008, Kazan, Kremlevskaja str. 18, Russian Federation

²⁾Institute of Organic and Physical Chemistry, Kazan Science Centre of Russian Academy of Sciences,
420088, Kazan, Arbuzov str. 8, Russian Federation

e-mail: akozlov@land.ru

The main purpose of this work is a determination of 3D structure of complex macromolecule compound with Pyrimidine bases of DNA (see fig.). This compound exhibit a very high level of bioactivity. And it is reason of interest in the compound. This bioactivity allows to suppose a possibility of using this compound as a base of super strong remedies in therapeutics of cancer and cardiovascular diseases. Recently there are no any results of experimental 3D structure investigation of this compounds in literature.

One of the most powerful techniques of investigation of complex organic compounds in liquid is the High Resolution NMR spectroscopy [1, 2].

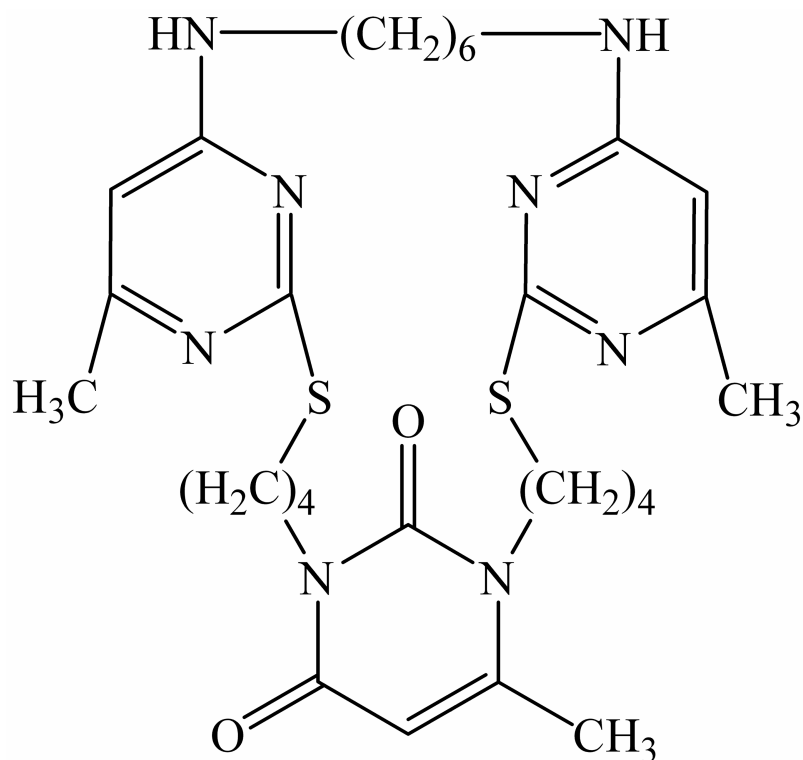


Figure. Chemical structure of compound under investigation.

Macromolecular compounds under investigation is complex and only verification of chemical structure isn't a trivial task. For overcoming this task it is necessary to use 1D and 2D heteronuclear correlating experiments besides homonuclear (^1H - ^1H) correlating experiment (COSY) and simple 1D ^1H and ^{13}C one. Because of low gyromagnetic ratio and weak abundance of ^{13}C nuclei it is necessary to employ the techniques which are based on the polarisation transfer phenomenon [3]. It is 1D INEPT, DEPT experiments and 2D HETCOR, COLOC experiments of NMR spectroscopy. Aside from we obtain a better ^{13}C nuclei detection sensitivity in heteronuclear correlating experiments using the Inverse NMR spectroscopy (HSQC, HMBC).

One of the methods of researching spatial structure of complex organic compounds in liquid is an investigation of dipole-dipole interactions between different parts of molecule. And one of the ways of the investigation of dipole-dipole interactions is a measurements of nuclear Overhauser enhancements between interacting nuclei. But according to colleague's work [4] this molecule possess a high level of mobility at room temperature and have a lot of conformations in liquid. There are no any pronounced intramolecular interactions, which are able to stabilize the conformation. Or different interactions (with close magnitudes) work simultaneously. Thus the task is considerably complicated.

The next step of our work is an investigation of dynamic properties of a given compound. Analysis of ^1H and ^{13}C spectra lines shapes dependences from variation of temperature show that chemical exchange processes exist in the molecule.

At present time we realize detailed analysis of chemical exchange processes using two dimensional EXSY method of NMR spectroscopy. In addition a measurements of nuclear Overhauser enhancement at low temperature and theoretical calculations, we suppose, allows to draw an exacter conclusions about spatial structure of investigating compounds.

This work is supported by the Civilian Research and Development Foundation and Research and Educational Center of Kazan State University REC-007 (grant for young scientist).

References

- [1] C. Rossi. – *Encyclopedia of NMR*, **7**, 4237 (1995).
- [2] T. Parella. – *Magn. Reson. Chem.*, **36**, 467 – 495 (1998).
- [3] Atta-ur-Rahman. – *One and two dimensional spectroscopy*, Elsevier 1989.
- [4] S. Kharlamov. – *Proceedings of Students Physical Seminar of Kazan State University*, **4**, 63 – 68 (2003).

MULTIFREQUENCY EPR STUDY OF METAL-LIKE DOMAINS IN POLYANILINE

V.I. Krinichnyi¹⁾, S.V. Tokarev²⁾, H-K. Roth³⁾, M. Schroedner³⁾, B. Wessling⁴⁾

¹⁾Institute of Problems of Chemical Physics, Institutski Prospect 16, Chernogolovka 142432 Russia

²⁾Kazan State University, Kremlevskaya 18, Kazan 420008 Russia

³⁾TITK Institute Rudolstadt, Physical Materials Research, Breitscheidstrasse 97, Rudolstadt
D-07407 Germany

⁴⁾Ormecon GmbH, Ferdinand-Harten-Strasse 7, Ahrensburg D-22926 Germany

The magnetic, relaxation and electronic dynamic parameters of paramagnetic centers (PC) in crystalline domains of polyaniline (PANI) being in the metallic state (“organic metal”) were studied at 3-cm (9.7 GHz) and 2-mm (140 GHz) wavebands EPR at wide temperature region. The sample studied was a polymer blend containing 36% of PANI and PMMA. Spin-spin and spin-lattice relaxation times of these PC were obtained by the steady-state saturation method. At all wavebands EPR the PC in PANI demonstrate Lorentzian single line with Dysonian contribution taking a possibility to determine an intrinsic conductivity of the metal-like domains (ca. 4000 – 7000 S/cm at room temperature) in PANI. The conductivity was shown to decrease sufficiently as the sample is evacuated and/or is deposited on a glass surface. Phase transition in PANI was registered at T=160 K. PC and air (water and/or oxygen) interact strongly below and weakly above the critical temperature that leads to an extremal temperature dependence of the polymer linewidth. The latter value depends weakly on the EPR registration frequency that is evidence of strong spin-spin interaction in the polyaniline sample studied.

**MAGNETIC RESONANCE AND OPTICAL SPECTROSCOPY OF TRIGONAL Yb^{3+}
CENTER IN CsCaF_3 SINGLE CRYSTAL**

M.L. Falin¹⁾, B.N. Kazakov²⁾, V.A. Latypov¹⁾, A.M. Leushin²⁾, A. Hofstaetter³⁾

¹⁾Zavoisky Physical-Technical Institute, Kazan 420029, Russia

²⁾Kazan State University, Kazan 420008, Russia

³⁾Physics Institute, University of Giessen, D-35392 Giessen, Germany

Crystals of the perovskite type ABF_3 ($\text{A} = \text{Cs}^+$, $\text{B} = \text{Ca}^{2+}$) are promising materials for practical applications and good model systems for the corroboration and development of the theory of electron-nuclear interaction between impurity rare-earth ions and magnetic moments of ligand ions in the nearest environment (transferred hyperfine interaction - THFI). EPR and preliminary optical investigations on CsCaF_3 crystals doped with Yb^{3+} ion revealed several types of paramagnetic Yb^{3+} centers including one in an unusual 12fold-coordinated position [1]. This paper presents further experimental results obtained by ENDOR, optical spectroscopy and theoretical studies of the THFI of Yb^{3+} in this matrix.

$\text{CsCaF}_3 : \text{Yb}^{3+}$ single crystals were grown by the Bridgman-Stockbarger method in graphite crucibles in a fluorine atmosphere adding 1.5 mol.% of YbF_3 to the melt. The concentration of Yb^{3+} resulting in the sample was approximately 0.01%. Experiments were carried out using an X-band spectrometer Bruker ESP300E at $T = 4.2$ K.

The ENDOR experiments were performed on the trigonal Yb^{3+} center. In order to establish exactly the correspondence between the resonances observed and the respective fluorine nuclei angular dependencies of the ENDOR spectra in the (001) plane were measured and from that values of the THFI parameters determined. A structural model of the center was determined.

Parameters of crystal fields are used to analysis distortions of the crystal lattice in the vicinity of Yb^{3+} . Within the limits of the superposition model it is established that three F^- ions of the nearest cubic surrounding symmetrically placed respective the third-order axis from the side of the vacancy, under formation of the trigonal center are somewhat approach the impurity ion and deviate from the C_3 -axis. The second set of three fluorine ions also approaches the Yb^{3+} but, on the contrary, comes somewhat closer the C_3 -axis.

The obtained distances are used in the theoretical evaluation of the THFI parameters, which was carried out basing on the bonding mechanisms of rare-earth ion to ligands developed in [2, 3]. In these calculations the covalency parameters for the electron transfer from the ligand to the rare-earth ion calculated *ab initio* are used for the first time [4].

POSTER SESSION PS22

This work was supported by the Russian Foundation for Fundamental Research (project 02-02-16648), NIOKR RT (project 06-6.1-246) and Deutscher Akademischer Austauschdienst.

References

- [1] Bespalov V.F., Falin M.L., Kazakov B.N., Leushin A.M., Ibragimov I.R., Safiullin G.M.: Appl. Magn. Res. **11**, 125 (1996)
- [2] Anikeenok O.A., Eremin M.V., Falin M.L., Meiklyar V.P.: J. Phys. C: Solid State Phys. **15**, 1557 (1982)
- [3] Falin M.L., Eremin M.V., Bill H., Lovy D.: Appl. Magn. Reson. **9**, 329 (1995)
- [4] Anikeenok O.A.: Phys. Sol. State **45**, 812 (2003)

CALCULATIONS OF RATE CONSTANTS OF THE BIMOLECULAR SPIN EXCHANGE BETWEEN PARAMAGNETIC PARTICLES IN A CASE OF A DIFFUSION PASSAGE OF THE INTERACTION REGION

A.E. Mambetov, K.M. Salikhov

Kazan Physical-Technical Institute, Kazan, Russia

e-mail: mambetov@kfti.knc.ru

Spin exchange between paramagnetic particles plays an important role in many occasions. It is one of the model processes of chemical physics (see, e.g., [1]). For example, this process is an elementary act of the spin polarization transfer in diluted mixed solutions of molecules in the spin polarized triplet state and stable free radicals [2].

Bimolecular spin exchange was comprehensively studied theoretically in the case of paramagnetic particles with spin $1/2$. Rate constants were calculated for two models: the sudden collision approximation and the diffusion passage of the interaction region [1, 3]. For paramagnetic particles with $S > 1/2$ the spin exchange rate constants were found theoretically only in the sudden collision approximation. In this report we present the results of our calculations of the bimolecular spin exchange rate constants when paramagnetic particles possess arbitrary spins and the colliding particles cross the interaction region in a course of mutual diffusion of the colliding particles. The general expressions are reduced to useful formulae for some particular cases.

References

- [1] Molin Yu.N., Salikhov K.M., Zamaraev K.I. Spin Exchange. Principles and Applications in Chemistry and Biology. Springer Verlag. Heidelberg Berlin (1980).
- [2] Gnezdilov O.I., Mambetov A.E., Obynochny A.A., Salikhov K.M. Time-resolved EPR study of electron spin polarization and spin exchange in mixed porphyrin -stable free radical solutions. Appl. Magn. Reson., v.25, pp.157-170 (2003).
- [3] Salikhov K.M. Diffusion approach to describe the exchange broadening of the EPR lines for diluted solutions of paramagnetic particles. Theoret. Experim. Khimiya, v. 10, pp.310-317 (1974).

**DISTRIBUTION OF MAGNETIC FIELD IN ANISOTROPIC SUPERCONDUCTORS
WITH NONREGULAR VORTEX LATTICE**

A.V. Minkin, S.L. Tsarevskii

Kazan State University, 420008, Kremlevskaya 18, Kazan, Russia.

e-mail: Alexander.Minkin@ksu.ru

EPR and NMR experiments, muon spin rotation measurements, Bitter pattern experiments, and the application of the magnetic force microscope as well as scanning Hall probe experiments give a detailed information about the magnetic field distribution $\mathbf{h}(\mathbf{r})$ of the flux lattice near the surface of superconductor. These experiments call for a simple theory allowing the calculation of $\mathbf{h}(\mathbf{r})$. One of possible way for treating of vortex line structure was suggested by Clem in a model with a fit function for the order parameter. This model works very well for a sole vortex, but for a vortex lattice this model contain some difficulties due to necessity to allow a vortex-vortex interaction. For the large Ginzburg-Landau parameter κ it can be done using the London's equation. A vortex core is described usually by the two-dimensional δ -function with a divergence at the vortex center. In particular, these equations had been used previously to calculate the magnetic field distribution in the bulk of superconductor and near its surface both inside and outside of the superconductor boundary [1].

Unfortunately, solutions of the mentioned equations have an obvious defect: the magnetic field $\mathbf{h}(\mathbf{r})$ diverges at the core centers. The removal of these divergences for a single vortex and for the vortex lattice of the infinite superconductor is quite simple, the solution has to be truncated at the vortex core of the radius $\sim \xi$ (ξ is the coherence length). However, the corresponding procedure is not evident near the surface of a finite superconductor, especially outside of the superconductor. On the other hand it is clear, that the divergences appear due to oversimplified ways of incorporating of the vortex core structure into the London's equations. We improve this procedure on the basis of the London's equations and using a standard vortex core model. As a result we derive modified London's equations, which allow to calculate the magnetic field $\mathbf{h}(\mathbf{r})$, having no singularities, at any point in and outside superconductor.

So, the modified London's equation for the magnetic field $\mathbf{h}(\mathbf{r})$ of the vortex lattice takes the following form:

$$\text{rot} \mathbf{h} + h = \sum_i \frac{1}{\kappa \zeta} \delta(|\rho - \rho_i| - \zeta) \mathbf{e}_z. \quad (1)$$

Consider a solution of equation (1) for the vortex lattice in a superconductor, occupying semispace $z \geq 0$ ($z < 0$ relates to vacuum) and $\mathbf{H} = \mathbf{H}(0, 0, H)$. For the Fourier-components \mathbf{h}_G we have:

$$\begin{aligned}
 -\frac{d^2 h_G}{dz^2} + (1 + G^2)h_G &= \frac{2\pi}{\kappa S_0} J(G\zeta) e_z, \\
 z \geq 0; \quad iG_x h_G^x + iG_y h_G^y + \frac{dh_G^z}{dz} &= 0; \\
 z < 0; \quad -G^2 \psi_G + \frac{d^2 \psi_G}{dz^2} &= 0; \quad h = -\nabla \psi,
 \end{aligned} \tag{2}$$

where ψ_G is the Fourier-component of ψ .

The solution of equation (2) takes the form (with accounting to standard boundary conditions for the magnetic field on the superconductor-vacuum boundary):

a) \mathbf{h}_G -within superconductor ($z \geq 0$):

$$\begin{aligned}
 h_G^{x,y} &= idG^{x,y} G^{-1} h_G^0 \exp(-\sqrt{1+G^2} z); \\
 h_G &= \left[1 - \frac{dG}{\sqrt{1+G^2}} \exp(-\sqrt{1+G^2} z) \right] h_G^0, \\
 \text{with } d &= \frac{\sqrt{1+G^2}}{G + \sqrt{1+G^2}};
 \end{aligned} \tag{3}$$

b) \mathbf{h}_G -outside superconductor ($z < 0$):

$$h_G^{x,y} = idG^{x,y} G^{-1} h_G^0 \exp(Gz), \quad h_G^z = dh_G^0 \exp(Gz). \tag{4}$$

At $z \rightarrow -\infty$ $h = H$, $H = h_G^z = h_{G=0}^0$ ($= \varphi_0 / S_0$, if to return to the usual units; φ_0 is the flux quantum).

At $z \rightarrow +\infty$ $h_G^z = h_G^0$, h_G^0 equal to the Fourier-components of $\mathbf{h}(\boldsymbol{\rho})$ of the infinite superconductor, if the vortex lattice is represented as a superposition of Abrikosov's vortex lines with normal core of a radius ζ . As expected, the result of solutions takes the form of the solution of the London's equations with singularities at vortex centers given in [6], if to put $J_0(\zeta G) = 1$. One can see that h_G^0 has improved asymptotic behavior in G -space, so that the Fourier set, representing h_G^0 , converges at any point of space.

That equation (1) may be easily generalizing for anisotropic superconductor. For example, if \mathbf{H} is parallel to the symmetry axis of anisotropic superconductor, it will be sufficient to perform a scale transformation along this axis.

So, for anisotropic superconductor we have:

$$m_{ij} \text{rot}_i \text{rot}_j h + h = \sum_i \frac{1}{\kappa \zeta} \delta(|\rho - \rho_i| - \zeta) e_z. \quad (5)$$

where m_{ij} – mass tenzor.

We can solve of equation (5) for anisotropic superconductor in a case when a vortex is displaced. The map of distribution of local magnetic field in regular vortex lattice is presented in fig.1. The map of distribution of local magnetic field in a case when a vortex is displaced is presented in fig.2.

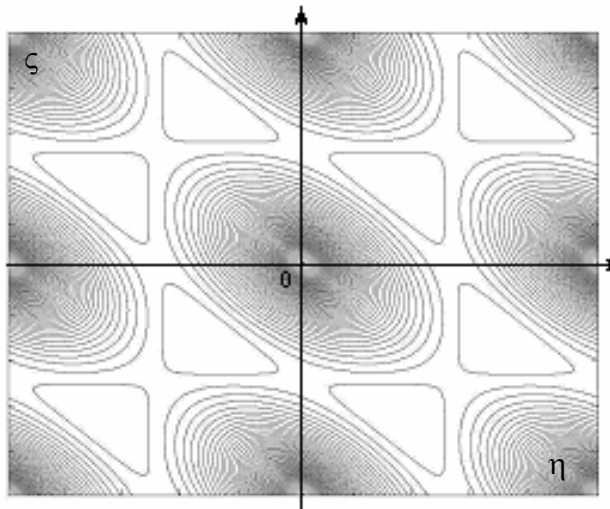


Fig. 1. The map of distribution of local magnetic field in regular vortex lattice.

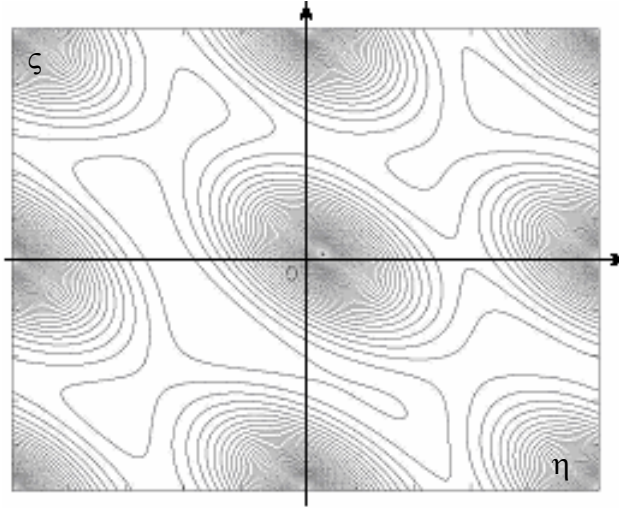


Fig. 2. The map of distribution of local magnetic field in a case when a vortex is displaced on small distance $\mathbf{a}(1/20,0)$.

Hence, we can see that displacement of the flux line lattice essentially changes the distribution of local magnetic field. The account of such changes for all space of a superconductor when each vortex is displaced on any distance \mathbf{a}_i , can give information about the real vortex lattice of a superconductor.

We can say, that all calculations were carried out in the framework of two-dimensional model of vortex. However, these equations and some other procedure of calculation let us construct the model of three-dimensional pinning.

This work was supported by a grant CRDF REC 007.

References

- [1] B.I. Kochelaev, Yu.N. Proshin, S.L. Tsarevskii, Fiz. Tverd. Tela (St. Petersburg), **38** 3220 (1996)

**THE MEASUREMENTS OF NO IN RAT TISSUES
BY METHOD OF EPR-SPECTROSCOPY AT TEMPERATURE 77 K**

L.N. Muranova¹⁾, A.I. Ismailova¹⁾, V.V. Andrianov¹⁾, Kh.L. Gainutdinov¹⁾, O.I. Gnezdilov¹⁾,
A.A. Obynochny¹⁾, A.L. Zefirov²⁾

¹⁾Kazan Physical-Technical Institute of Russian Academy of Sciences, Kazan

²⁾Kazan State Medical University, Kazan

e-mail: M.Luda@rambler.ru

There is a large amount of methods for the measurement of the of the nitric oxide (II) (NO) production in biological systems. However, the exact measurement both stationary concentrations of NO and the velocities of its generation in biological systems is a difficult problem because of low activities of NO-synthases, small times of life and low values of stationary concentrations. The spectrophotometric method and methods, based on the spin-echo coupling possess a comparatively high specificity and sensitivity to NO. Method of the spin-echo coupling is based on the reactions of the radical (in this measurement - NO) with the spin-echo trap. One of the main advantages of this method is a possibility of detection of NO complexes with molecules from biological samples. The EPR measurements were conducted on samples of heart, liver, kidney, pancreas, blood vessel and blood at the temperature of the fluid nitrogen. During the coupling of NO with lipophylic trap DETC there were formed the paramagnetic mononitrozyl complexes of iron (MNCl) with DETC, characterised by EPR signal with $g_{\perp} = 2,036$, $g_{\parallel} = 2,01$ and extrathin and tryplete structure under g_{\perp} . Besides the EPR spectra from MNCl-DETC we also observed the signals from free radicals under $g \approx 2,0$ and recalled iron-coupling proteins under $g \approx 1,94$. Most of the measurements were conducted on tissues of heart, livers and pancreas, because tissues the EPR spectra were the most intensive in these. Particularly intensive EPR signal was found in MNCl-DETC of rat livers. The EPR signal from blood vessel was nearly 10 times less intensive compared with the signal from liver. The received results is pointed to the perceptiveness of a method of EPR-spectroscopy for determination of the NO contents in biological tissues.

Supported by RFBR, grant N 03-04-96257 and NIOKR RT 03-3.1-243.

NUMERICAL CALCULATIONS OF THE ELECTRON SPIN POLARIZATION FOR SEQUENTIAL RADICAL PAIRS IN MICELLES

A.R. Mursalimov, K.M. Salikhov

Kazan Physical-Technical Institute, Kazan, Russia

e-mail: mursalimov@kfti.knc.ru

Photochemical reactions do often proceed via a sequence of radical pair or ion-radical (electron-hole) pair states. The very well-known example is charge separated states in photosynthetic reaction centers. There were carried out simulations of time-resolved EPR spectra of sequential radical pairs in reaction centers. It was shown [1] that by analyzing the shape of polarization pattern of the subsequent radical pair $P_{700}^+Q_K^-$ one can determine the lifetime of the preceding pair $P_{700}^+A_0^-$ and the exchange integral (a sign and a value) in that pair. This approach was used to find the lifetime and the exchange integral for $P_{700}^+A_0^-$ in M688L (PsaA) mutant reaction center. In reaction center co-factors do not diffuse, so that the distances between partner radicals and exchange interaction between two radicals in a pair are fixed.

Here we have analyzed the spin polarization pattern of two sequential radical pairs in micelles. In contrast to reaction center case, in micelles mutual diffusion of radicals stochastically modulate exchange interaction between partner radicals in pairs. It was supposed that exchange integral depends exponentially on the distance between radicals. We have analyzed whether for reactions in micelles the spin and molecular dynamics in the primary radical pair can be subtracted from the EPR spectrum of the secondary radical pair.

References

- [1] Salikhov K.M., Pushkar N., Golbeck H., Stehlik D. Interpretation of Multifrequency Transient-EPR spectra of the $P_{700}^+A_0Q_K^-$ state in Photosystem I Particles using a Sequential Correlated Radical Pair Model: Wild Type versus A_0 mutants. Appl. Magn. Reson. 24, 467-482 (2003).

SURFACE NMR: SENSORS DEVELOPMENT AND INVESTIGATION OF ELASTOMERS

I.A. Nikolaev, L.U. Grunin, E.A. Nikolskaya, L.V. Shvaleva, T.V. Smotrina, U.B. Grunin
Department of Physics, Mary State Technical University, 424000, Lenin sq., 3, Yoshkar-Ola, Russia
e-mail: nmr@marstu.mari.ru

1. Introduction

After exposing by thermal stress on rubber samples a spin-spin relaxation times have been measured by spin echo decay method. Dependence of amplitude of a single spin echo, measured at a fixed echo-time on the time, which is told below, have been obtained. Moreover, improved surface NMR sensor was used and comparison between results obtained by using convenient NMR system and this sensor has been conducted.

2. Results and discussion

To investigate structural-dynamic properties of elastomers [1] the following experiment has been performed. The rubber samples had being exposed to thermal treatment during fixed period, and just after that the time of spin-spin relaxation was measured by spin echo decay method using surface NMR sensor. All measurements were taken periodically during an hour after the thermal shock to observe changes of the polymer network dynamics.

Macromolecules can be in different conformations during thermal motion. Transition between conformations usually happen by internal rotation of polymer links around single bounds. It is nearly impossible for a free rotation in a real molecule of elastomer, since approaching lateral groups in the links affect on transition of attraction into repulsion force. Moreover, the slow down process of free rotation takes place also by interaction of the chain the link with surrounding links of another polymer's chains. Therefore, there exists a potential barrier that reduces internal rotation.

The dependence of spin echo amplitudes on the time passed from a thermal stress has shown the fast initial decay (Figure 1.). So we observed the clearly defined minimum due to decreasing of links mobility. We suppose that this minimum of stiffness is caused by the minimum of potential energy of molecular conformations. Probability of the rest transitions to higher levels depends on oscillatory motions of rather big atomic chains and rotational motion of functional groups, mostly lateral. These transitions, observed as the rest increase of the

spin-spin relaxation time are considered as the result of two factors: energetic (overcoming of intermolecular interaction) and entropic (increase of polymer chains flexibility).

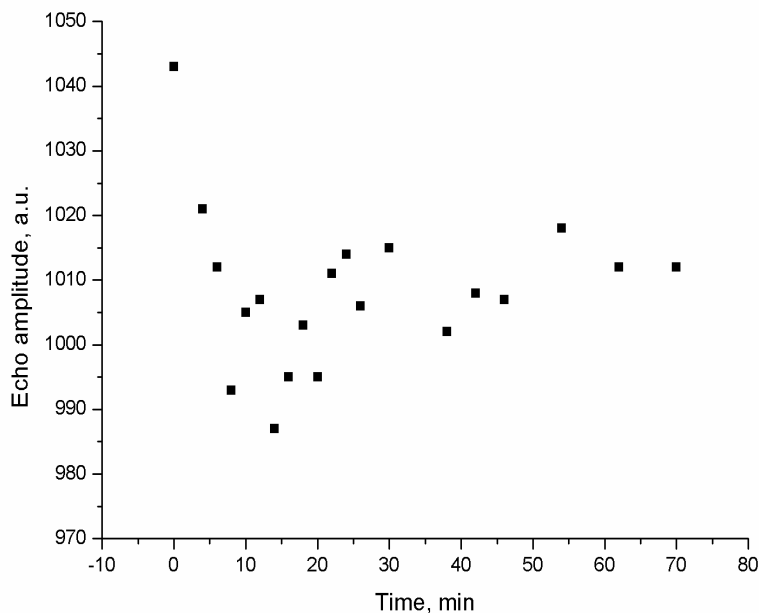


Figure 1: Dependence of amplitude of a single spin echo, measured at a fixed echo-time on the time, passed from thermal stress.

Acknowledgements

This work was partially supported by German rubber company Phoenix AG.

References

- [1] L.Grunin , M.Bruder,. Low Field NMR in Rubber Structure Investigation, *IRC'03 summaries*, 207-209 (2003).

**NEW PROGRAMS WITH THE WYSIWYG INTERFACE FOR SIMULATION
OF EPR SPECTRA NITROXIDE SPIN-LABEL**

V. Novikov, V. Timofeev

Engelhardt Institute Molecular Biology RAS, Moscow, 119991, Russia

e-mail: tim@eimb.ru

As the performance of personal computers grows and calculating methods use in considerable amount of works, the deficiency of programs for simulation of EPR spectra with the friendly interface under the most popular operational systems of Microsoft Windows family was formed. The advantage of such programs in comparison with the most calculation modules, using out-of-date operational system MS-DOS, is evident because they do not require long training of users and there is opportunity to manipulate usual for the majority of users WYSIWYG ("What You See Is What You Get") interface. Besides that Microsoft Windows allows usage of memory space limited only by the hardware.

The present program (S_imult 5.1) carries out simulation of EPR spectra using the model in which spin-label take part of two kinds of movement (fast and slow) simultaneously.

It is possible to get full identity of calculated and experimental spectra for a wide range of initial parameters if the distribution on positions of a spin-label for all possible states (depend on the nearest environment) is assumed.

Except for nitroxide radical three-component magnetic tensors values, three dynamic parameters \mathcal{S} , k (set a direction of an oscillation axis) and α (determines a corner of nitroxide oscillation) are entered. The program is integrated with the most widespread computing packages for processing the spectral data. The calculation model covers three experimental cases of sample preparation: in a solution, in a "powder" condition and in crystal state.

OBSERVATION OF NOISE-LIKE MAGNETIC RESONANCE SPECTRA OF THIN FILMS PRODUCED BY Fe⁺ IMPLANTATION INTO PMMA

N.Yu. Panarina, N.R. Khabibullina, V.Yu. Petukhov

Kazan Physical-Technical Institute, Kazan, Russia.

e-mail: petukhov@kfti.knc.ru

In recent years nanostructural magnetic materials have been the subject of intensive scientific investigation due to their promising technical application. One of the effective methods for a granular metal-containing thin films formation is ion beam synthesis (IBS). Using IBS ferromagnetic nanostructural films in polymer matrix have been produced [1]. In this work, the results of magnetic radio-spectroscopy investigation of the films ion-synthesized in polymethylmetacrylate (PMMA) are presented.

The samples of chemically modified phosphorus-containing PMMA, deposited by centrifugation on a silicon substrate, were implanted with 40 keV Fe⁺ ions at ion current density of 4 μA/cm², the dose of implantation being 1.2·10¹⁷ ion/cm². At this dose variously shaped and sized fine-dispersed particles are formed in a near-surface layer [1]. The results of transmission electron microscopy (TEM) revealed that along with fine particles of ~ 20 nm in diameter one can distinguish conglomerates of particles with sizes more than 600 nm.

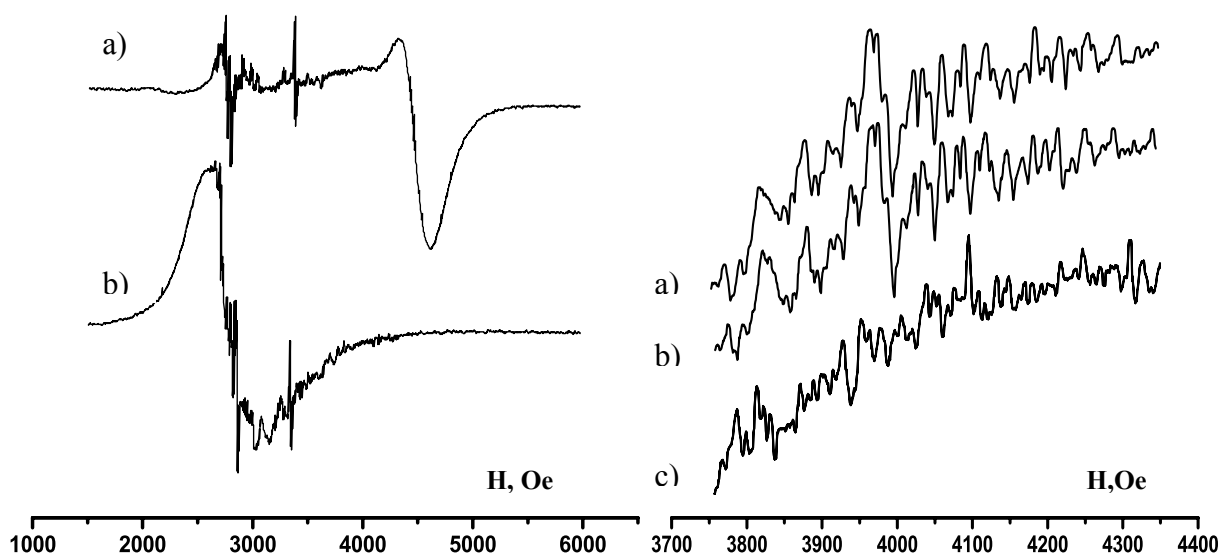


Fig.1. Noise-like spectra of PMMA implanted with Fe⁺ a) $\mathbf{H} \parallel \mathbf{n}$ b) $\mathbf{H} \perp \mathbf{n}$

Fig.2. a),b) –the parts of noise-like spectra recorded at the same sample position in the cavity; c) spectrum of the same sample turned by 5°

Magnetic properties of produced samples were investigated by using “Varian – E12” radiospectrometer with working frequency 9.5 GHz at room temperature. A complicated magnetic resonance spectrum was observed (Fig.1). The spectrum consisted of a sufficiently broad (~500 Oe) anisotropic absorption line and a set of narrow low-intensity lines. Intensive broad line showed a strong angle dependence of resonant field from sample orientation with respect to external magnetic field. The character of such dependence testifies that a thin ferromagnetic film in a near-surface layer has been formed, therefore, the observed anisotropic absorption line represents a ferromagnetic resonance one. A peculiarity of obtained spectra lies in a presence of great amount of narrow lines similar to ordinary noise. However, unlike instrumental noise, which is a low-intensity signal varying with every spectrum registration, observed noise-like lines have an amplitude several orders of magnitude higher than actual noise and are repeated in independent series of the registration (Fig.2 a,b). It must be emphasized that spectrum is repeated with high accuracy only when the position of the sample in the cavity is invariant during following number of experiments. A turn of the sample en on several degrees completely modifies noise-like spectrum (Fig.2 c).

It is well-known [2] that for FMR the position of a resonance line is described by Kittel’s formula

$$\left(\frac{\omega_{RES}}{\gamma}\right)^2 = [H_0 \cos(\theta - \theta_H) - H_{eff} \cos 2\theta][H_0 \cos(\theta - \theta_H) + H_{eff} \cos^2 \theta] \quad (1), \text{ where}$$

H_0 and ω_{RES} – resonance magnetic field and resonance frequency, respectively,

γ - gyromagnetic ratio,

H_{eff} – field of effective anisotropy,

θ and θ_H – angles between normal to the surface and direction of magnetization and external magnetic field, respectively.

For thin films, when $\theta = \theta_H$ that often takes place in sufficiently high magnetic fields one can put down the expression for different orientation of the film in external magnetic field as

$$\left(\frac{\omega_{RES}}{\gamma}\right)^2 = H_0 \cdot (H_0 + 4\pi M_S) \quad \text{for } \mathbf{H}_0 \perp \mathbf{n} \quad (2)$$

$$\left(\frac{\omega_{RES}}{\gamma}\right)^2 = H_0^2 - 4\pi M_S^2 \quad \text{for } \mathbf{H}_0 \parallel \mathbf{n} \quad (3),$$

where \mathbf{n} – normal to the film surface,

M_S – saturation magnetization of the sample.

It is evident that when $\mathbf{H} \parallel \mathbf{n}$ a resonance line shifts towards higher magnetic fields and otherwise when $\mathbf{H} \perp \mathbf{n}$ it moves to the lower magnetic fields. Similar behavior of broad intensive absorption line is observed experimentally in registered spectra. Therefore, our assumption about the formation of thin ferromagnetic film in near-surface layer is correct for the system under study. It may be concluded that formation of flat conglomerates of particles with size 600 nm or more determines the appearance of a broad ferromagnetic resonance anisotropic line. The value of saturation magnetization calculated from (2) and (3) for the sample distinguishes from the theoretical value for bulk α -Fe. This assumption becomes apparent from the experiment when the distance between the positions of broad absorption line in different orientations of the sample in magnetic field turned out to be less than in theoretical calculations. The fact signifies that after implantation either ferromagnetic solid solutions or metal oxides are formed.

TEM patterns showed that near-surface layer consists not only of conglomerates but also separate particles of ~ 50 -200 nm. Those particles possess ferromagnetic nature and can give individual resonance absorption line in spectrum that can be registered by spectrometer. In fact spectrometer sensitivity for ferromagnetic resonance is ~ 3 orders higher than for paramagnetic resonance. Rough estimate of minimal spherical iron particle size, signal from which may be registered by spectrometer, gives the value ~ 100 nm. Thus, it is possible that ion-synthesized iron particles of that size are responsible for the appearance of noise-like spectra.

The difficulty of noise-like spectra investigation is connected with relatively low intensity noise-like signal in comparison with broad intensive line. To gain a better understanding of observed phenomena a computer program for spectra smoothing with averaging interval more than width of narrow noise-like lines and following subtraction of smoothed component from original spectra has been written. This operation was applied for obtained spectra and certain features were revealed (Fig.3).

It should be mentioned that a narrow intensive absorption line in the field $H_0 \sim 3400$ Oe (line "holder" in Fig.3) is not connected with the sample under investigation but this is a signal from the sample holder. The rest of the registered lines belong to the sample. One of the important fact is that all narrow lines in both spectra are situated in the interval between the positions of broad absorption lines recorded for $\theta=0^0$ and $\theta=90^0$. It can be explained by two reasons. First, the particles responsible for narrow lines have a different shape varying from sphere-like to oblate/prolate-like forms. Second, the orientation of nanoparticles in the film is various.

Fig.3 shows that noise-like spectra in two extreme positions of the sample with respect to the magnetic field differ negligibly. This fact indicates that oblate-shaped particles variously oriented regarding the film plane are presented in the near-surface layer with equal angle distribution.

Experimentally observed high density of absorption lines in lower fields ($H \sim 2800$ Oe) in comparison with higher fields can be explained by nonlinearity of Kittel's formula (1) regarding the angle between direction of magnetization and axes of particles. It follows that when

angle θ is close to 90° distance in the magnetic field between two absorption lines from individual particles is less than when θ is near zero. Therefore, as a result of individual lines superposition the intensity of the signal in small fields arises.

In the samples of chemically modified phosphorus-containing PMMA during implantation with Fe^+ ions under certain conditions a complicated granular nanostructure is formed. The spectra of ferromagnetic resonance consists from a broad strongly anisotropic line, which is due to flat big conglomerates of particles behaving in magnetic relationship as thin ferromagnetic film, and from a set of narrow noise-like lines, which are determined by signals from relatively big (~ 50 - 100 nm) individual weakly interacted oblate-shaped particles. The shorter axes of the particles are oriented at various angles to the surface of the sample and this angle distribution is equiprobable. The magnetic characteristics of produced near-surface layers may be explained by formation of ferromagnetic phase differing from bulk α -Fe and also by presence of radiation-induced defects.

References

- [1] Petukhov V.Yu. et al.: Polymer Sci. Ser. A. **43**, 1154 (2001).
 [2] Kittel C.: Phys. Rev. **65**, 155 (1948).

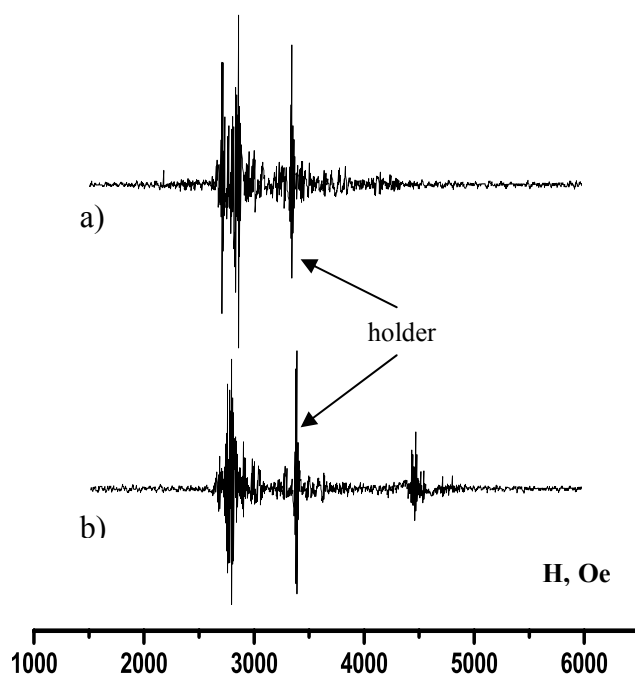


Fig.3. Noise-like magnetic resonance spectra of PMMA implanted with Fe^+ after subtraction of smoothed component a) $\mathbf{H} \perp \mathbf{n}$ b) $\mathbf{H} \parallel \mathbf{n}$

RESEARCH OF DIMENSIONAL-INDEPENDENT COMPONENTS OF A SPECTRUM OF A MAGNETO-DIMENSIONAL RESONANCE

E.A. Prokofeva, A.V. Kovalenko

Department of Radiophysics, Dnepropetrovsk National University, Nauchnaya street 13,
Dnepropetrovsk, 49050, Ukraine

e-mail: proelen@ua.fm

Using magneto-dimensional resonance (MDR), earlier [1] we investigated physical characteristics of crystals InSb. The typical kind of spectra MDR for such samples is submitted on fig. 1.

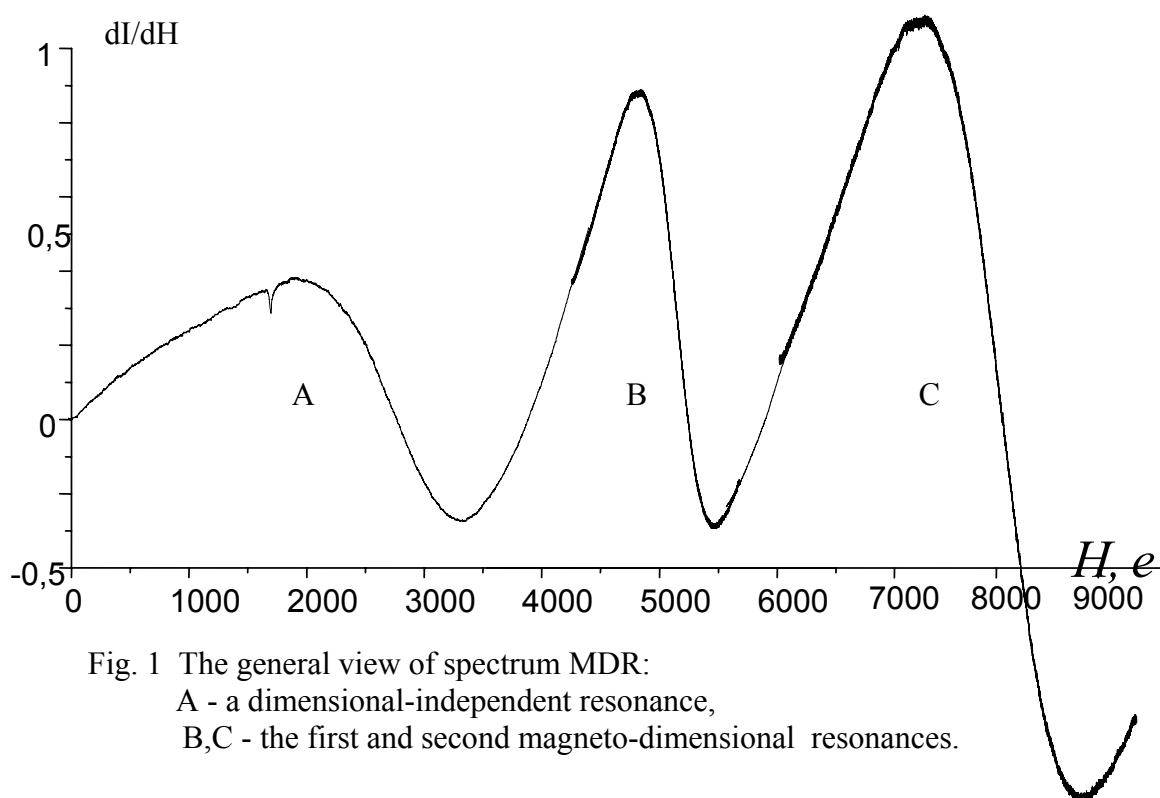


Fig. 1 The general view of spectrum MDR:
A - a dimensional-independent resonance,
B,C - the first and second magneto-dimensional resonances.

Apparently from fig. 1 resonances B and C - magneto-dimensional, they have been described earlier [2,3]. In the given work we have concentrated the attention on structure of a dimensional-independent resonance (fig. 1, A).

Our researches were carried out on compensated crystals InSb with concentration of carriers of a charge $2 \cdot 10^{13} \div 10^{17} \text{ cm}^{-3}$ by means of radiospectrometer EPR "Radiopan" in a three-centimetric range of lengths of waves.

To get rid of dimensional and plasma effects, we have formed the samples of disks with thickness $\sim 0,1 \text{ mm}$ and radius $\sim 0,5 \text{ mm}$. The crystals were located in the resonator of a

radiospectrometer in such point, where the magnetic component of superhigh-frequency field (SFF) H_1 is maximal and $H_1 \perp H$, and the electrical component of SFF E_1 is minimal and $E_1 \parallel H$.

In this case for samples InSb of the small sizes in low magnetic fields ($H = 10 \sim 3000$ e) the first derivative of a spectrum of absorption represents a symmetric single wide line $\Delta H_{max} = 1500$ e (fig. 2, line 1).

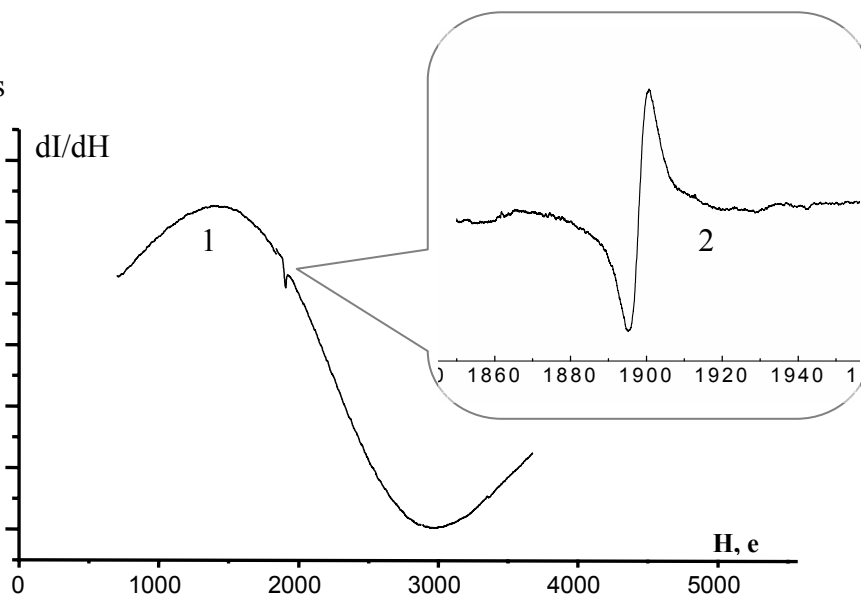


Fig. 2 The spectrum of a dimensional-independent resonance:
 1 - electronic paramagnetic resonant radiation;
 2 - electronic paramagnetic resonant absorption;

Thus if to carry out registration of such line simultaneously with a reference sample which gives narrow line EPR - absorption (DFPG, crystal $ZnS:Mn^{2+}$), EPR - the signal of absorption always is in an antiphase with a wide line.

In our disposal there were crystals $ZnS:Fe$, in which the ions of an impurity of iron (Fe^{2+}) are given a narrow line EPR - by absorption with the g-factor equal 2,032 (fig. 2, line 2). In small crystals $ZnS:Fe$ the wide line also is in antiphase with a line EPR, caused by ions of an impurity of iron (Fe^{2+}). Above told allows to make the assumption, that in small on the size crystals InSb the wide single line represents not a line of resonant absorption of SFF - capacity, as in a case EPR, and resonant radiation of SFF - capacity.

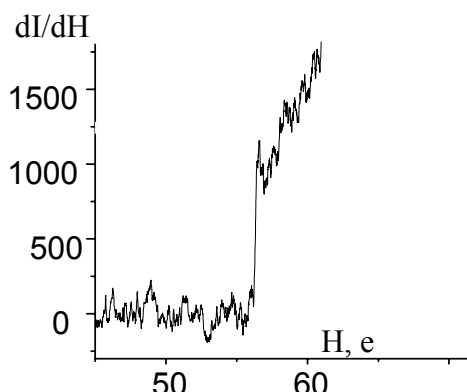


Fig.3 Spectrum of " a narrow resonant signal " with $g = 98,3$

That fact, that we dealt with radiation, proves to be true and registered current of the SFF - detector: during record of a wide line the current of the SFF - detector was increased on $20 \div 30$ %, depending on the dimension of samples.

During registration of a line EPR - absorption the current of the SFF - detector decreased. At research of spectra MDR in the field of magnetic fields about 60 e the

narrow resonant signal (fig. 3) was registered small on intensity.

Width "of a narrow resonant signal " is equal ≈ 1 e, the g-factor is equal 98,3.

The value of the g-factor does not change at change of concentration, that specifies that the electrons belong to a zone of conductivity.

The intensity of the given signal poorly depends on a level of SFF - capacity.

Considering a phase of the given signal, it is possible to make a conclusion, that it concerns to a signal of radiation.

Thus, it is possible to assert, that at a spectrum of a magneto-dimensional resonance of a resonance there is dimensional-independent of a component, which concerns to electronic paramagnetic to resonant radiation.

References

- [1] Shtambur I.V., Prokofeva E.A., Kovalenko A.V. Research of a magneto-dimensional resonance in samples InSb. // Photoelectronics.- The interdepartmental scientific collection ONU, Odessa, №11, 2002, p.6-8.
- [2] Prokofeva E.A., Kovalenko A.V., Shtambur I.V. Research of macroscopical parameters of semiconductors such as $A^3 B^5$ contactless method MDR. Dnepropetrovsk, the Bulletin to the DNU, 2002, № 9, p.179 - 183.
- [3] Application of a magneto-dimensional resonance at research of macroscopical parameters of semiconductors. // New aspects of application of a magnetic resonance. Works VII Youth scientific school " Urgent problems of a magnetic resonance and his appendices " November 11-13 2003r., Kazan, p. 200-204.

**FREE INDUCTION DECAY AND ECHO PHENOMENA IN MEDIA
WITH DIPOLE INTERACTION**

O. Kh. Khasanov, G. A. Rusetsky, V. V. Samartsev, N. N. Rubtsova

Inst. of Phys. Solids & Semicond. NASB, 17 P.Brovka str., Minsk 220072, Belarus

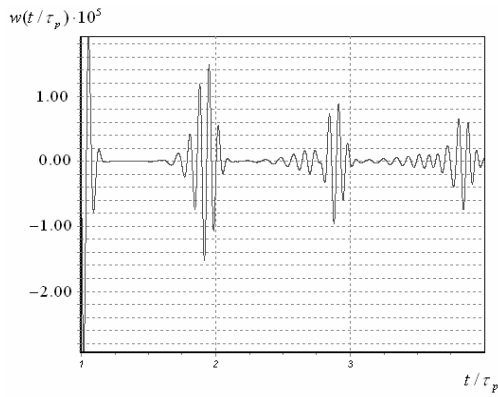
Kazan Physical- Technical Institute KSC RAS, Sibirskii Trakt str, 10/7, Kazan' 420029 Russia

Inst. of Semicond. Phys., Sib. Branch RAS, acad. Lavrentyev prosp., 13, Novosibirsk, 630090, Russia

e-mail: khasanov@iftp.bas-net.by

The dynamics of dense atomic ensemble in coherent radiation fields differs from that would be displayed by the individual constituent oscillators. The classic example of this is the Lorentz-Lorenz shift, which results in a shift of the resonance frequency of a dense material. This shift arises because the electric field at a given oscillator is modified by the reradiated field from all of the other oscillators in the medium. As a result, interaction of the system with the coherent field occurs on the red wing of the spectral line. The very interaction among the oscillators is the key phenomenon in dense resonant media, changing to a considerable extent the behavior of a system of coupled atoms in a field of coherent light in both stationary and in nonstationary regimes.

The main goal of this paper is to study the effect that may be exerted by an interatomic dipole-dipole interaction (DDI) upon optical transient processes and, in particular, upon the character of the free induction (FI) decay and echo phenomena in dense resonant media. Specific features of spontaneous responses in such media are that all of them are phase modulated with the oscillation frequency varying with time and being dependent on the DDI constant, on the detuning of the exciting pulse carrier frequency from the resonance δ , and on the pulse intensity and its spectral width. The law and rate of the FI signal relaxation also depend on the ratio of the above parameters. The decay of the FI signal in time may occur either by the power or by the exponential law, depending on the value of total detuning $\delta + \omega_L$, where ω_L is the Lorentz frequency. The FID peculiarities in media with homogeneous and inhomogeneous broadening as a function of spectral linewidth are discussed. At that, the excitation induced dephasing processes and other relaxation canals are taken into account. The conditions for single pulse photon echo (PE) generation are analysed. It is shown that in media with DDI such an echo can be excited by pulse at the smaller pulse area than it is necessary for its generation when the DDI is negligible. Besides, multiple signals of such an echo-response as shown in Fig. can be generated.



As for primary PE generation, we should note one of remarkable peculiarities connected with possibility of observation of signals under different phase matching conditions. The observation time of these signals is also different. When such relaxation canal as up-conversion process becomes significant, it results in not only the signal amplification but

acceleration of its observation time. The possibility of echo-like responses generation in homogeneously broadened dense media and their registration by phase sensitive methods are discussed. The conditions of experimental realization of above-mentioned results in dense Yb vapors are analyzed.

NUCLEAR RELAXATION IN SYSTEM PrF₃ – LIQUID ³He

K.R. Safiullin, A.N. Yudin, V.V. Naletov, M.S. Tagirov, D.A. Tayurskii, I.N. Kurkin

Physics Department, Kazan State University, 18 Kremlyovskaya St., Kazan 420008, Russia

e-mail: kajum@inbox.ru

Introduction

The suggestion of using dielectric Van Vleck paramagnets for dynamic polarization of nuclei liquid ³He was done in work [1]. However, attempt of use for this purpose fine-dispersed powder LiTmF₄ has come across serious obstacles [2].

Dielectric Van Vleck paramagnetic PrF₃ has two main advantages in comparison with LiTmF₄. First, crystals PrF₃ have cleavage planes and therefore it is possible to expect, that surfaces of a crystal powder will be atomically-smooth. Second, two of three component of γ -tensor of nuclei ¹⁴¹Pr ($\gamma_x/2\pi=3.322$ kHz/Oe, $\gamma_y/2\pi=3.242$ kHz/Oe) have the values close to gyro-magnetic ratio of nuclei liquid ³He ($\gamma/2\pi=3.243$ kHz/Oe). So, it is possible to achieve more coincidence of zeeman levels of energy of nuclei Van Vleck ion and nuclei liquid ³He in case of powder samples.

Samples

As samples, fine-dispersed crystal powders LaF₃ and PrF₃ have been chosen. Characteristic sizes are 45-56 microns and 1 micron. Samples have been prepared by mechanical grinding of crystal LaF₃ in sapphire mortars. Researches of a crystals (from which samples have been prepared) on the maintenance impurity paramagnetic ions by ESR method have shown, that it contains in quantity no more than 0,001% paramagnetic ions Gd³⁺.

The LaF₃ crystal is similar on a structure to PrF₃ crystal, however, it is diamagnetic, consequently has no cross-relaxation effects. Thus, in nuclei ³He relaxation times comparing, taking place in contact with these crystal powders, it is possible to find out existence of a resonance magnetic coupling.

System LaF₃ - ³He

Spin-lattice and spin-spin relaxation times of nuclei ³He have been measured at various resonant frequencies and temperature T = 1.5 K by using spin echo method.

Appeared, that in finer powder, the relaxation of nuclei ³He proceeds more faster. Longitudinal relaxation rate of nuclei liquid ³He increases in 3-4 times in a submicronic

powder (see fig. 1). This is the effect of interaction surface increasing and changing geometry

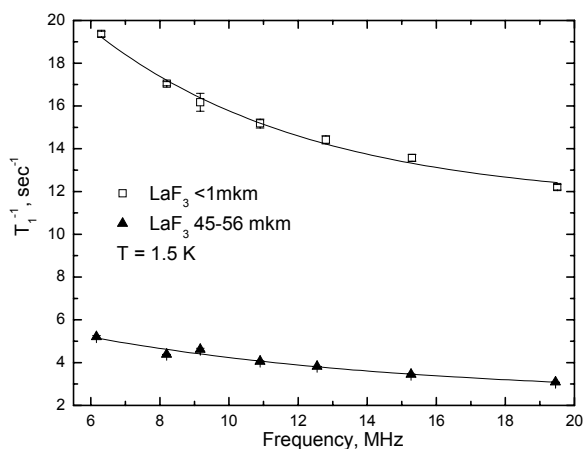


Fig. 1. Longitudinal relaxation rate of nuclei ^3He in contact with powders LaF_3 in dependence on frequency

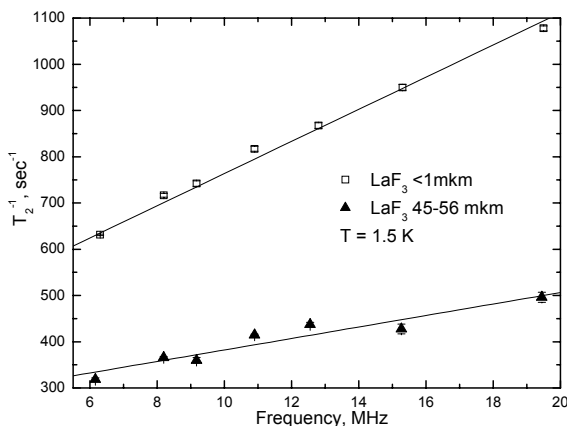


Fig. 2. Transverse relaxation rate of nuclei ^3He in contact with powders LaF_3 in dependence on frequency

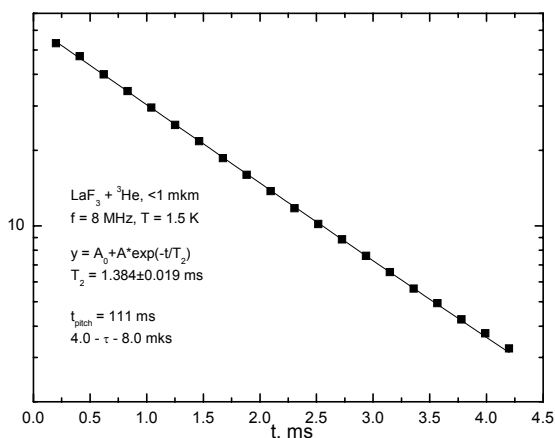


Fig. 3. Transverse magnetization decay of nuclei ^3He in contact with LaF_3 (<1 mkm)

System $\text{PrF}_3 - ^3\text{He}$

In this work nuclei ^{141}Pr , ^{19}F and ^3He relaxation in system $\text{PrF}_3 - ^3\text{He}$ and in "dry" powder PrF_3 was studied. Field dependence of intensity of spin echo signal (see fig. 4) has been measured at frequency of 19,5 MHz. Used durations of RF-pulses are following: first sequence gave the maximal signal of nuclei ^{141}Pr , the second sequence – maximal signal of nuclei ^3He . According to this field dependences, there are contributions to a signal of nuclei ^3He , nuclei ^{19}F , also there is a contribution of nuclei ^1H which are situated in surrounding subjects, in glass ampoule, in coil. As against them, the signal of nuclei ^{141}Pr is present in a wide range of an external constant magnetic field.

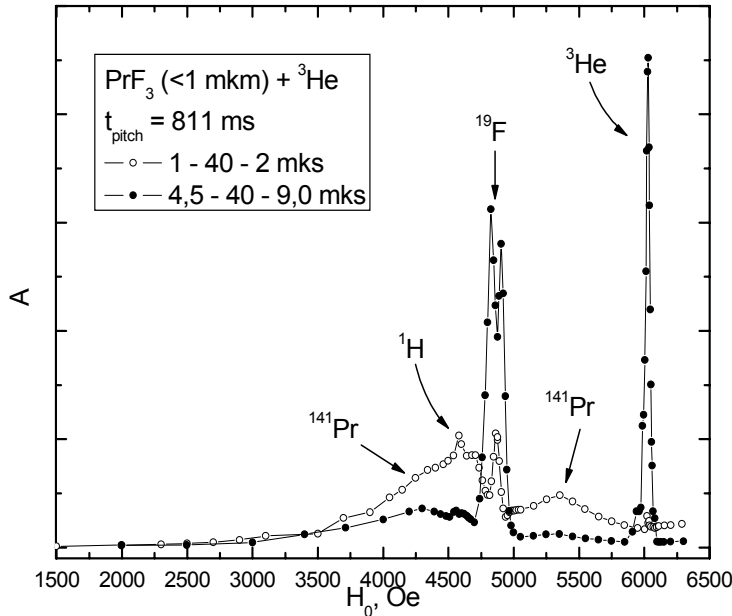


Fig. 4. Field dependence of intensity of spin echo signal of system PrF₃ – liquid ³He.

magnetic field (fig. 5). Contributions to spin echo signal are following: signal of nuclei ¹⁴¹Pr with narrow width and more slowly decreasing than ¹⁴¹Pr signal – signal of nuclei ³He with wide width.

According to experimental data, relaxation of ³He in contact with PrF₃ powder turned out to be unusual. Transverse magnetization decay is described by two exponential function (fig. 6).

In this case, interference of signals of various nuclei is observed in system PrF₃ - ³He. At observing relaxation of ³He, the contribution to a signal is also given by nuclei ¹⁴¹Pr. On fig. 6

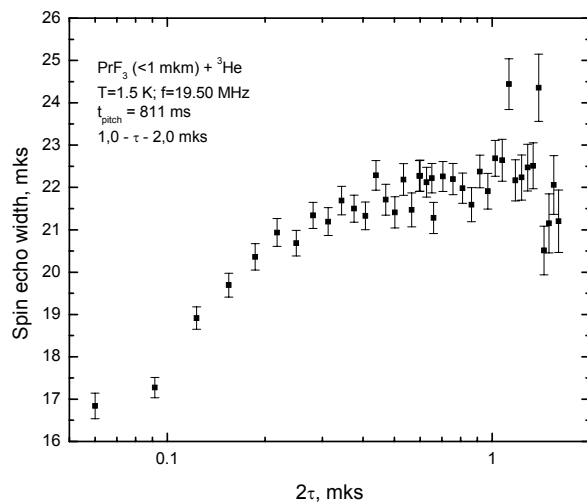


Fig. 5. Spin echo width dependence on delay time in system PrF₃ (<1 mkm) - liquid ³He

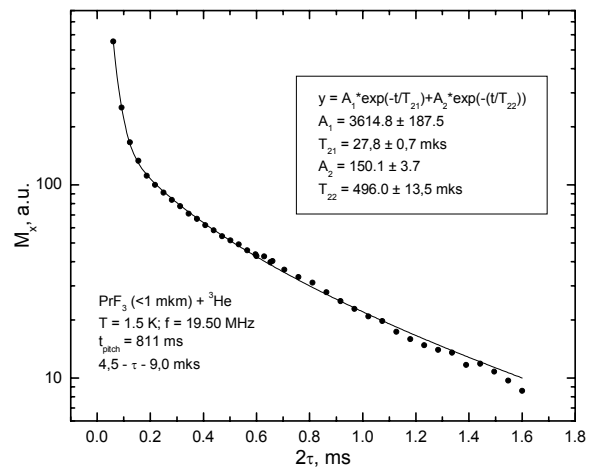


Fig 6. Transverse magnetization decay of nuclei ³He in system PrF₃ (<1 mkm) - liquid ³He

This dependence shows, that cross-relaxation effects should be observed between nuclei ¹⁴¹Pr and nuclei ³He, and between ¹⁴¹Pr and ¹⁹F. So, it is system with three connected spin systems. Also, echo width dependence on delay time between RF-pulses was measured. This dependence has been measured with using pulses that provide for the maximal signal at a ³He resonant

transverse magnetization decay of system is submitted, and duration of pulses and magnetic field are adjusted to a resonance of ^3He . Transverse magnetization decay is the sum of two exponent functions, first of which is formed by signal of nuclei ^{141}Pr , the second corresponds to signal of nuclei ^3He . In fact, transverse relaxation time of nuclei ^{141}Pr in "dry" powder PrF_3 is the same as in contact with ^3He .

Conclusions

Experimental data testify that in the given system there are two types of cross-relaxation effects: intracrystalline between nuclei ^{19}F and ^{141}Pr , and on border of two mediums (solid and liquid) between nuclei ^3He and ^{141}Pr . Experimentally investigated relaxation processes for nuclei ^3He , ^{19}F and ^{141}Pr in system PrF_3 - liquid ^3He .

Acknowledgements

This work is supported by RFBR (grant N 02-04-16800), BRHE (REC-007) and Scientific Program "Universities Of Russia" (grant N 01.01.010).

References

- [1] M. S. Tagirov, D. A. Tayurskii. – *JETP Lett.*, **61**, 652 (1995)
- [2] V. V. Naletov, M. S. Tagirov, D. A. Tayurskii. – *Low Temp. Phys.*, **28**, 431 (2002)

**DIRECT OBSERVATION OF INTERCENTER CHARGE TRANSFER PROCESS
IN SEMI-INSULATING 4H SiC MATERIAL BY PHOTO EPR METHOD**

D.V. Savchenko, S.N. Lukin, E.K. Kalabukhova

Institute of Semiconductor Physics National Academy of Science of Ukraine, 03028, pr. Nauki 45,
Kiev, Ukraine.

e-mail: katia@i.kiev.ua

Abstract

We present direct observation by photo EPR method the temperature induced intercenter charge transfer process occurring in the high purity semi-insulating (HPSI) 4H SiC material. Intercenter charge transfer process between a series of deep donor like defects are shown to be efficient when quasi Fermi level is moving towards the middle of the band gap with increasing the temperature. Decay kinetics of persistent photoconductivity in HPSI 4H SiC after photoexcitation has terminated was studied. The intercenter charge transfer process is shown to represent an important shunt for the carrier recombination process in HPSI 4H SiC material. The possible electronic model for trapping recombination process in HPSI 4H SiC is discussed.

Introduction

It is well known that trapping and recombination (TR) of non-equilibrium charge carriers at defects and impurity levels are among the most important processes in semi-conductor physics and technology. An understanding of these processes is essential for device development with SiC. Therefore the objective of the present project was to establish the role of deep centers in the trapping and recombination process occurring in HPSI SiC.

Experimental Details

Several samples of HPSI 4H SiC samples were investigated by EPR in the temperature range from 77 K to 145 K at the 37 GHz. The photo-EPR experiments were performed using a 250 W high-pressure mercury vapor lamp and a 100 W halogen lamp combined with interference filters for a wavelength range of 380 nm to 1000 nm.

EPR Results

Fig.1 shows the EPR spectrum observed in a series of undoped HPSI 4H SiC samples at

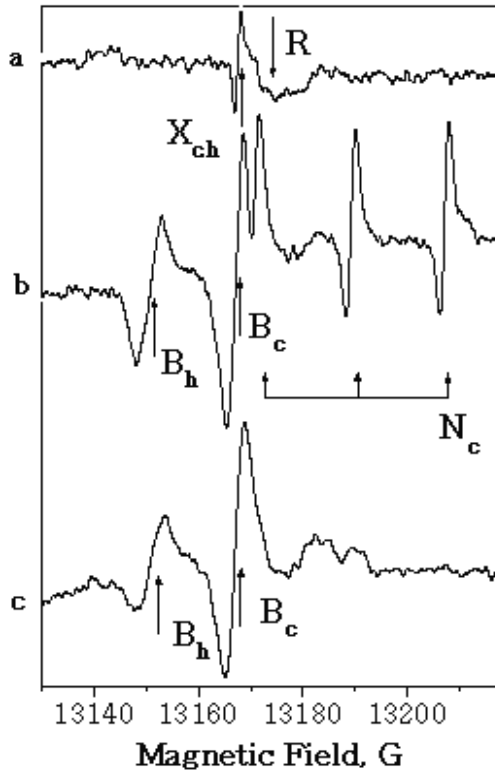


Fig. 1. EPR spectra photoresponse in HPSI 4H SiC sample measured at 37 GHz and 77K.

a. dark; b. illumination with UV light; c. 26 h after the light is switched off. $B_0 \perp c$

37 GHz and 77 K in the dark and under illumination of the sample with band gap light for $B \perp c$. In the dark EPR spectrum consists one single line labeled X due to the intrinsic defect located in the upper half of the band gap approximately at 1.15 ± 0.06 eV below E_c [1]. When the sample is illuminated with above band-gap ultraviolet (UV) light (Fig. 1 b), the EPR lines of boron on the hexagonal I_h^B and cubic site, I_c^B , and nitrogen on cubic site, I_c^N , which is easily recognized by the characteristic three line hyperfine pattern appear and persist in EPR spectrum after the illumination is removed, showing a very small recombination rates of photocreated electrons and holes at $T = 77$ K [2]. Fig. 2 shows the time characteristics of the photo-carriers captured by nitrogen and boron levels. As was seen from Fig. 2, time characteristics of the photo-carriers captured by nitrogen and boron levels consist of the fast and

slow component of decay curves. Due to the similar behavior of the fast component of decay curves for the carrier concentration captured by nitrogen and boron energy levels indicates that the fast component is responsible for the recombination process between nitrogen and boron. The slow component of decay curves for the photo-carriers captured on the nitrogen

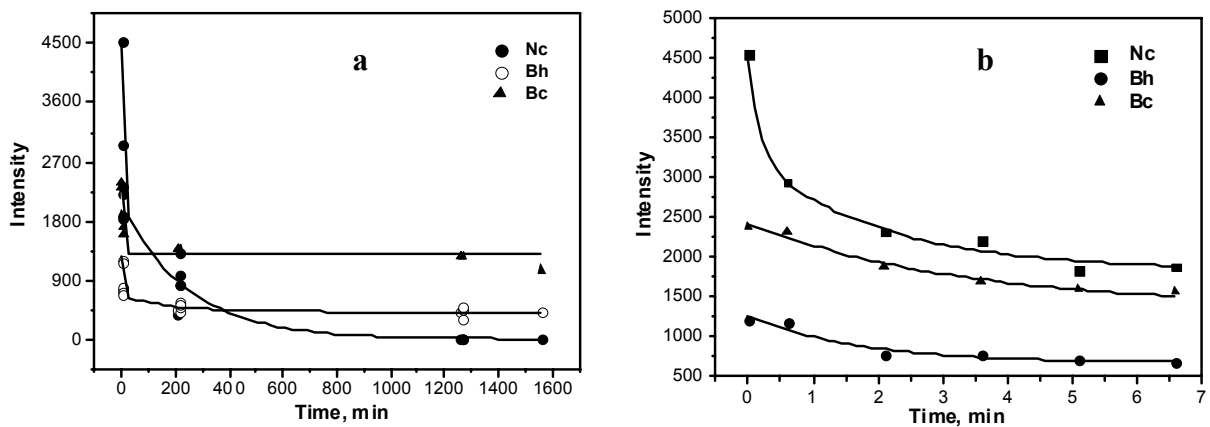


Fig. 2. a. Nitrogen and boron EPR line intensity decay after UV excitation light is switched off b. Fast component of decay curve of the carrier concentration captured by nitrogen and boron energy levels.

and boron levels have the different behavior and could be caused by the existence of trap level in the forbidden band. This conclusion is supported by the appearance of the single EPR line due to intrinsic defect labeled P in the dark after photoexcitation is removed and nitrogen EPR line decays to about 0.3 of its light-on value (Fig. 1 c). Electrons from nitrogen energy level recaptured by trap level labeled P where the lifetime of the trapped electrons is very long and recombination process between electrons captured by trap and holes captured by boron can be neglected which is supported by slow component for boron center. The P center has been previously studied in detail in HPSI 4H SiC and identified as deep donor-like defect located in the upper half of the band gap approximately at 1.15 ± 0.06 eV below E_C [1, 2]. Thus, the intercenter charge transfer process is shown to represent an important shunt for the carrier recombination process in HPSI 4H SiC material.

Intercenter charge transfer process between a series of deep donor like defects was discovered to be efficient when quasi Fermi level is moving towards the middle of the band gap with increasing the temperature. Fig. 3 shows the temperature evolution of EPR spectrum observed in HPSI 4H SiC sample preliminary illuminated by UV light and afterwards keeping

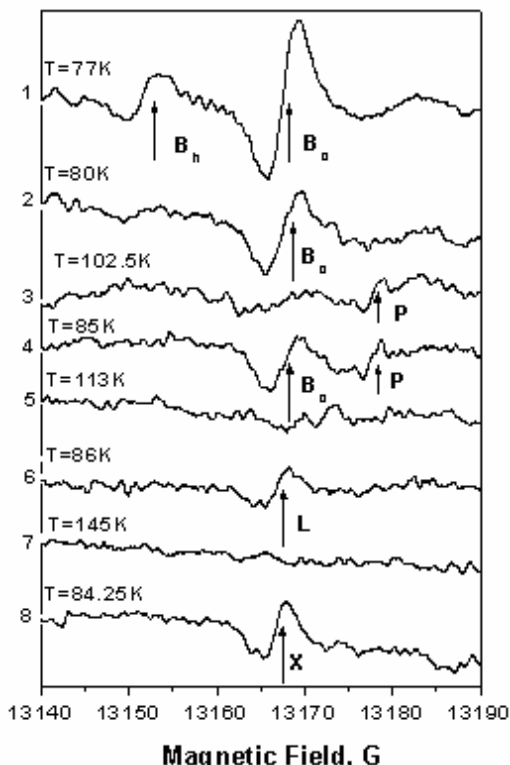


Fig. 3. The EPR spectrum temperature evolution in HPSI 4H SiC samples in the dark preliminary excited by UV light. 1 -26 h after the UV light is switched off.

26 h in the dark when EPR lines of nitrogen practically vanished in EPR spectrum. After the first stage of the heating up to 102 K EPR spectrum of boron disappears and simultaneously EPR line of P defect is appeared in EPR spectrum.

The second stage of the heating up to 113 K leads to ionization of the carriers both from boron and P defect energy levels and as a result their EPR spectra are vanished at 113 K. The free electrons are recaptured by the level at which the Fermi level is locked at given temperature. As was seen from Fig. 3, a new EPR line labeled L with $\Delta H_{pp}(L) = 1.65$ G appeared in EPR spectrum at 86 K.

The g-factor of L-line defect EPR line coincides with that of cubic boron EPR line but their line width differs from each other: $\Delta H_{pp}(L)$

= 1.65 G, $\Delta H_{pp}(B) = 3.37$ G. The subsequent rising of the temperature up to 145 K gave rise to the ionization of free carriers from L defect and when the temperature goes down EPR line of X defect appeared in EPR spectrum which can be easily recognized by its small width line: $\Delta H_{pp}(X) = 1.26$ G.

Summary

The EPR spectrum temperature evolution observed in HPSI 4H SiC sample indicates that at elevated temperature non-equilibrium electrons released from nitrogen energy level are recaptured by the other deep donor-like level due to the moving of the Fermi level down to the midgap with increasing the temperature. The free electrons are captured by the level at which the Fermi level is locked at given temperature. First stage of the heating up to 102 K locks the Fermi level at P defect level, the second stage of the heating up to 113 K locks the Fermi level at L defect level and the third stage of the heating up to 145 K locks the Fermi level at X defect level. As a result EPR spectrum of P, L and X defects appeared in the dark at elevated temperature after photoexcitation of the HPSI 4H SiC sample has terminated.

The Fig. 4 shows the temperature induced intercenter charge transfer process occurring in HPSI 4H SiC material. The electrons released from nitrogen energy level located at $E_C - 0.090$ eV [3] are subsequently recaptured by a series of closely located energy levels due to P, L and X defects with the difference in energy of: $\Delta T = 140$ K – 107 K = 33 K = 2.85 meV

The holes are also released from boron energy level and can be recaptured by boron or other

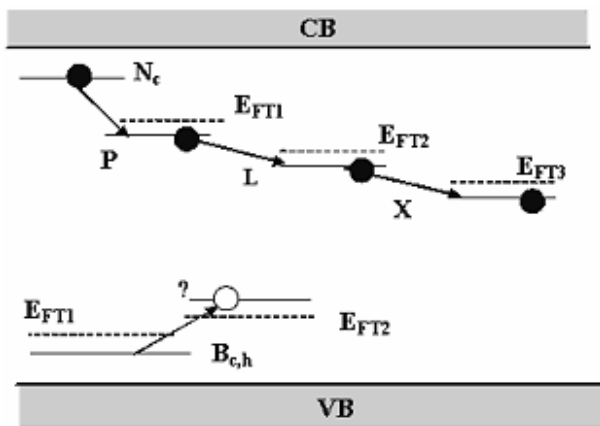


Fig. 4. Temperature induced charge transfer process in 4H SiC HPSI material.

nonparamagnetic energy level when the temperature is going down. As was seen from Fig. 3, after heating up to 107 K the non-equilibrium holes released from boron energy level are recaptured by boron energy level again when the temperature goes down. As a result the EPR signal from cubic boron is restored in EPR spectrum. After second stage of the heating the boron EPR line is not appeared in EPR spectrum

showing that the holes released from boron energy level are recaptured by other nonparamagnetic energy level. The temperature of around 100 K = 8 meV is too low for the ionization of the free holes from boron energy level with ionization energy of $E_i = 0.35$ eV [4] into the valence band.

References

- [1] Kalabukhova E.N., Lukin S.N., Savchenko D.V., Mitchel W.C., Mitchel W.D. Materials Science Forum Vols. 457-460, p. 501 (2004).
- [2] Kalabukhova E.N., Lukin S.N., Saxler A, Mitchel W.C., Smith S. R., Solomon J.S. Ewwaraye A.O., Phys. Rev. B. 64, 235202-(1-5), 2001.
- [3] W. Goetz, A. Schoner, G. Pensl, W. Suttrop, W.J. Choyke, R. Stein and S. Leibenzeder, J., Appl. Phys. 73, 3332, 1993.
- [4] M. Ikeda, H. Matsunami, T. Tanaka, Phys. Rev. B 22, 2842 (1980).

**STUDY OF ELECTRONIC PHASE SEPARATION IN LIGHTLY DOPED
ANTIFERROMAGNETIC $\text{YBa}_2\text{Cu}_3\text{O}_6$ BY $\text{Cu}(1)$ NQR**

A.V. Dooglav, A.V. Savinkov

Magnetic Resonance Laboratory, Kazan State University, 420008 Kazan, Russia

e-mail: Andrey.Savinkov@ksu.ru

1. Introduction

At very low doping of parent $\text{YBa}_2\text{Cu}_3\text{O}_6$ compound with holes antiferromagnetism of CuO_2 planes is rapidly destroyed giving way to conductivity and then superconductivity at hole concentration greater than $p_{\text{sh}}=0.05$ holes per Cu atom in the CuO_2 sheet. The main results on the unusually efficient suppression of antiferromagnetism by doped holes were obtained predominantly in the muon spin rotation (μSR) experiments [1, 2] which revealed the freezing of the doped holes spin degrees of freedom in a form of spin glass at low temperatures. It is however evident that a detailed information on the processes of spin freezing can also be obtained with the help of nuclear quadrupole resonance (NQR) of chain copper, the probe located between two CuO_2 planes and experiencing the hyperfine magnetic field from two adjacent antiferromagnetically coupled $\text{Cu}(2)$ ions which is normally cancelled at $\text{Cu}(1)$ position. Any disorder induced by doped holes in the CuO_2 plane antiferromagnetic network should at least partly lift up this cancellation and inevitably influence spectroscopic and dynamic parameters of $\text{Cu}(1)$ nuclei.

2. Samples and experimental method

2.1. Samples preparing. The samples were prepared by G. Collin in Laboratoire de Leon Brillouin, CE Saclay, CEA-CNRS, 91191 Gif-sur-Yvette, France. Two samples of $\text{YBa}_2\text{Cu}_3\text{O}_6$ were studied in which hole doping was obtained by heterovalent substitution of Y^{3+} ions by Ca^{2+} (2% and 4%). Such substitution gives the doping level of $p_{\text{sh}}=0.01$ and 0.02 holes per $\text{Cu}(2)$ atom, respectively, both levels lying in the range at which antiferromagnetism is only partly suppressed. One more sample of $\text{YBa}_2\text{Cu}_3\text{O}_{6+x}$ with oxygen content $x \sim 0.27$ (without impurities) was prepared in our laboratory.

2.2. Experimental method. $^{63,65}\text{Cu}(1)$ pulse NQR method was used for studying the samples. Longitudinal relaxation rate was measured by standard method of echo recovery after saturating pulse. The transverse relaxation rate was measured by standard technique also.

3. Results

The temperature dependence of Cu(1) longitudinal and transverse nuclear relaxation rates together with Cu(1) NQR spectra led us to the following conclusions:

1. At high temperatures mobile holes occupy the whole CuO₂ plane and influence the relaxation of all Cu(1) nuclei.

2. There are temperature regions, where transverse and longitudinal relaxation rate of Cu(1) nuclei separates into fast and slow relaxing parts. The temperature region for the longitudinal relaxation rates is located in the temperature scale higher than one for the transverse relaxation rate. Thus at $T < T_S$ the separation of the CuO₂ plane into hole-rich and hole-poor phases takes place, the fact which was not noticed earlier in μ SR experiments [1,2]. This separation is seen in both Cu(1) transverse and longitudinal nuclear relaxation rates as well as in NQR spectra in which there are two NQR lines: wide and narrow. The fraction of the hole-rich phase weakly depends on doping (Ca content) and is equal to about 2/3 of the plane. T_S is also weakly doping-dependent and equals to about 18 K and 22 K for $p_{sh}=0.01$ and 0.02 calcium samples, respectively. T_S for YBa₂Cu₃O_{6.27} equals about 33 K.

3. The spin freezing at $T=T_f$ is felt in the experiments through the peaks in both longitudinal and transverse relaxation rates of Cu(1) nuclei belonging to hole-rich phase. The temperatures at which the peaks are observed are higher for longitudinal relaxation than for transverse one, either due to different fluctuation frequency scales influencing these two relaxation processes or different fluctuating magnetic field orientation in respect to the quantization axis.

Acknowledgements

This study is supported by Russian Foundation for Basic Research, under Project 03-02-16550, and by the Russian Ministry of Industry and Science, under Project 98014-4. A.V.S. acknowledges the support of CRDF under Grant REC-007.

References

- [1] Ch. Niedermayer et al. - Phys. Rev. Lett. **80**, 3834 (1998).
- [2] C.E.Stronach et al. - Physica C **311**, 19 (1999).

**ELECTRON EXCHANGE SPIN RELAXATION OF RADICALS
IN LOW AND ZERO MAGNETIC FIELDS**

S. Shakirov¹⁾, P. Purtov²⁾, Yu. Grishin²⁾, E. Bagryanskaya¹⁾

¹⁾International Tomography Center SB RAS, Novosibirsk, 630090, Russia,

²⁾Institute of Chemical Kinetics and Combustion SB RAS, Novosibirsk, 630090, Russia,

e-mail: shakirov@tomo.nsc.ru, purtov@ns.kinetics.nsc.ru

Recently we have shown that the rate of spin relaxation induced by anisotropic HFI, isotropic HFI and spin-rotational interaction in low magnetic fields is significantly different in comparison with high magnetic field, and thus the use of high-field expressions for relaxation times is incorrect [1]. The consideration was done for a radical with one and two magnetic nucleus with spin $I=1/2$. In this work we extend this research to electron spin relaxation caused by electron spin exchange. The theoretical predictions have been compared with experimental EPR spectra of nitroxide radicals in low magnetic fields.

The calculation of spin relaxation of radicals in solutions shows that the probabilities of relaxational transitions are different in low and high magnetic fields. The use of high-field expressions with the only the adjustment of ω_e to the exact splitting between the energy terms is not correct. We have presented the analytical results for a radical with one magnetic

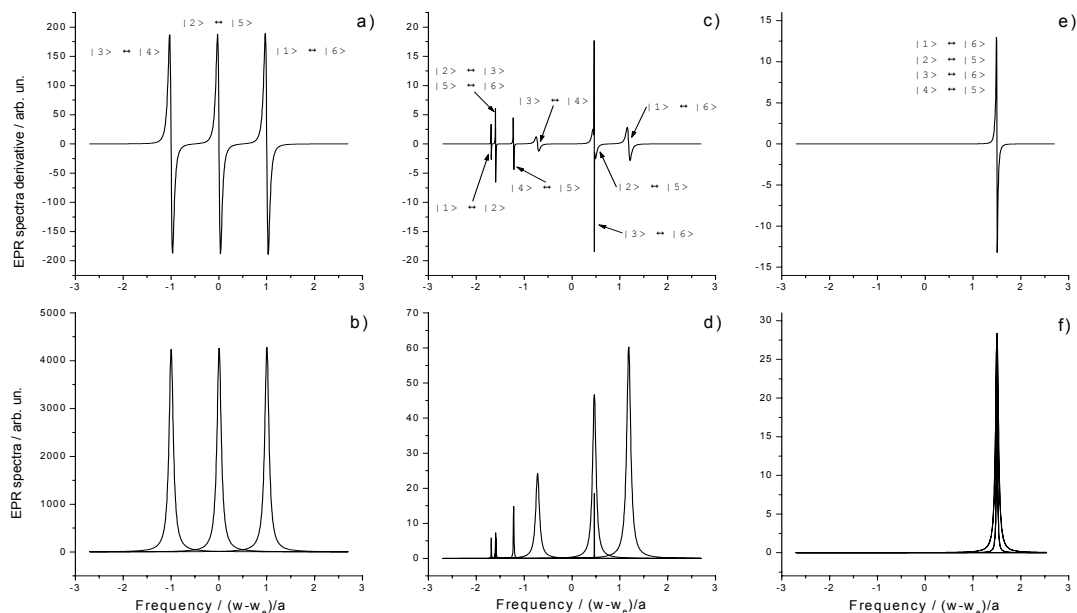


Fig. 1. Calculated ESR spectra and ESR spectra derivative for radical with one magnetic nuclei $I=1$ at $H_0 \gg a$ (a, b), $H_0 = 2a$ (c, d), $H_0 = 0$ (e, f).

nucleus $I=1/2$ and $I=1$. Analysis of spin relaxation caused by electron spin exchange has been analysed at two different cases of slow and fast electron exchange rate. The results of this work are important for experimental study of ion-radical reactions in low magnetic fields.

Acknowledgement

The financial support of the Russian Foundation for Basic Research (Grant N 02-03-32073), and Russian Scientific Schools (SC-2298,2003,3) is gratefully acknowledged.

References

[1] M. Fedin, P. Purtov, E. Bagryanskaya, J. Chem.Phys., **118**, 192 (2003).

INVESTIGATION OF MAGNETIC NANOSTRUCTURES OBTAINED IN PMMA BY ION BEAM SYNTHESIS IN MAGNETIC FIELD

A.I. Shipov, V.Yu. Petukhov, N.R. Khabibullina

Kazan Physical Technical Institute, Sibirskii Trakt 10/7, Kazan, 420029, Russia

e-mail: ashipov@mail.ru

Introduction

The investigation of magnetic nanostructures has become a very active field of current research, which is driven for the most part by their practical applicability as the high-density data recording and storage medium. Composite materials containing single-domain nanoparticles evenly distributed in the substrate are considered to be one of the best because of their unique magnetic properties. Ion beam synthesis (IBS) based on the high-dose ion implantation offers a number of advantages in comparison to traditional methods of nano-sized particle synthesis [1]. However, there's still a need to master certain techniques that allow to control magnetic properties of nanostructured thin films. The goal of this research is to study the influence of external magnetic field on the process of IBS and to investigate magnetic properties of nanostructured ferromagnetic films obtained in polymethylmethacrylate (PMMA).

Experiments

Thin metal-polymer films were produced by high-dose implantation of single-charged Fe^+ ions into PMMA. The samples were tightly fixed onto the self-made attachable sample holder, which allowed performing ion implantation in the presence of applied magnetic fields. Uniform magnetostatic field was generated by an electromagnet with a permalloy core. By varying both the field in the range of 0...127 Oe and its orientation to the film surface, a series of samples with various ion doses has been obtained. Commercial PMMA with the thickness of 1 mm and the starting decomposition temperature of $\sim 72^\circ\text{C}$ was used as a substrate for all samples. IBS was performed with the ILU-3 implanter. The ion energy was 40 keV, the doses and ion current density varying in the range of $\Phi=10^{16}\dots 6*10^{17}$ ions/cm² and 1...6 $\mu\text{A}/\text{cm}^2$, respectively.

The magnetic properties have been investigated both by ferromagnetic resonance (FMR) and magneto-optical Kerr effect (MOKE).

FMR spectra of all the samples were recorded at room temperature with the use of the radiospectrometer “Varian E-12” operating at the frequency $\omega/2\pi=9.3\text{GHz}$. Measurements were carried out for two orientations of the sample, the normal direction of the films being either parallel or perpendicular to the magnetic field.

Hysteresis parameters, such as coercitivity and saturation magnetization, versus the implantation dose were recorded with the MOKE magnetometer at room temperature with in-plane orientation.

Results

The FMR spectra of PMMA implanted with Fe^+ ions at doses above 10^{17}cm^{-2} reveal the formation of a ferromagnetic phase [2]. The dependence of FMR spectra on the orientation has been measured for all samples. Measurements were carried out for two orientations of the sample, normal direction (\mathbf{n}) of the films being either parallel or perpendicular to DC magnetic field (\mathbf{H}). The values of the effective magnetization were calculated from the orientation dependence.

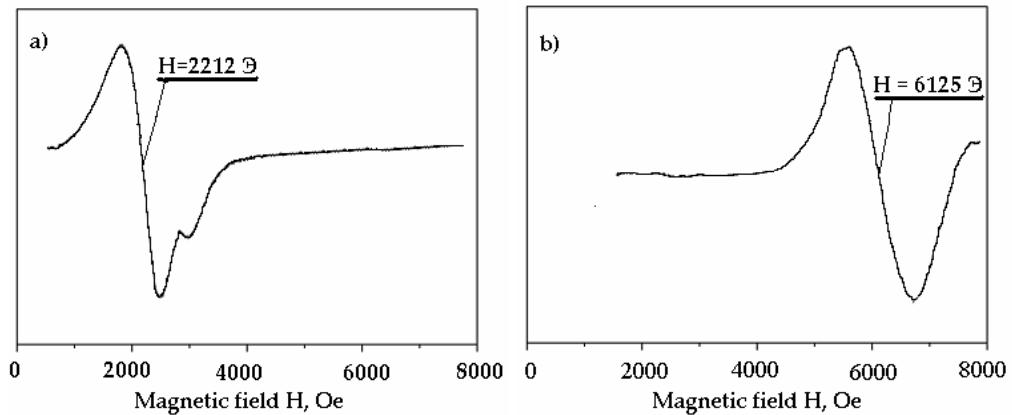


Fig.1. FMR spectra of Fe^+ -implanted PMMA with a dose of $3 \cdot 10^{17}\text{cm}^{-2}$ for two orientations: a) $\mathbf{n} \perp \mathbf{H}$, b) $\mathbf{n} \parallel \mathbf{H}$

To calculate the magnetic parameters in a case of uniaxial anisotropy, the Kittel’s equation is used [3]

$$(\omega/\gamma)^2 = (H_0 \cos(\theta - \theta_H) - H_{\text{eff}} \cos 2\theta)(H_0 \cos(\theta - \theta_H) - H_{\text{eff}} \cos^2 \theta) \quad (1)$$

where θ and θ_H – the angles between the direction of the magnetization and the applied magnetic field to the normal direction of the films, respectively. H_{eff} is an effective anisotropy field, which is given as

$$H_{\text{eff}} = 4\pi\Delta D M_s + H_i. \quad (2)$$

Here M_s is a saturation magnetization, H_i – is the intrinsic anisotropy field, ΔD for oblate ellipsoids is given by Osborn as [4].

$$\Delta D = \frac{2 + \mu^2}{2(1 - \mu^2)} - \frac{3}{2} \frac{\mu}{(1 - \mu^2)^{3/2}} \arcsin \sqrt{1 - \mu^2} , \quad (3)$$

where μ - parameter of ellipticity (ratio of short and long semiaxis). H_{eff} and the gyromagnetic ratio γ were calculated by substituting the experimental data H_0 for the perpendicular and parallel orientations of the samples into Eq.(1). The value of H_i was estimated from the anisotropy of the resonance line at a sample rotation around the normal to the film ($\mathbf{n} \perp \mathbf{H}$).

For the obtained samples no changes in the in-plane angular dependence were observed in FMR spectra. The absence of this anisotropy in the plane parallel to the sample surface is the evidence of a negligible contribution of the intrinsic field H_i (including crystalline magnetic and magnetically induced uniaxial anisotropies) to the effective anisotropy field. In this case, H_{eff} is determined mainly by the demagnetization factors. Therefore

$$M_{\text{eff}} = \Delta D M_s \quad (4)$$

where M_{eff} is an effective saturation magnetization calculated from the FMR data using Eqs.(1) and (2). Assuming that the saturation magnetization is equal to the value for α -Fe ($M_s = 1700\text{G}$) we can calculate ΔD from Eq.(4) and then determine μ using the Osborn's equation (Eq.(3)).

The specific saturation magnetization, relative saturation remanence $m_r = M_r / M_\infty$ and coercivity H_c were taken from the hysteresis loops shown in Fig.2. The saturation magnetization rises with the increase of Fe content in the substrate.

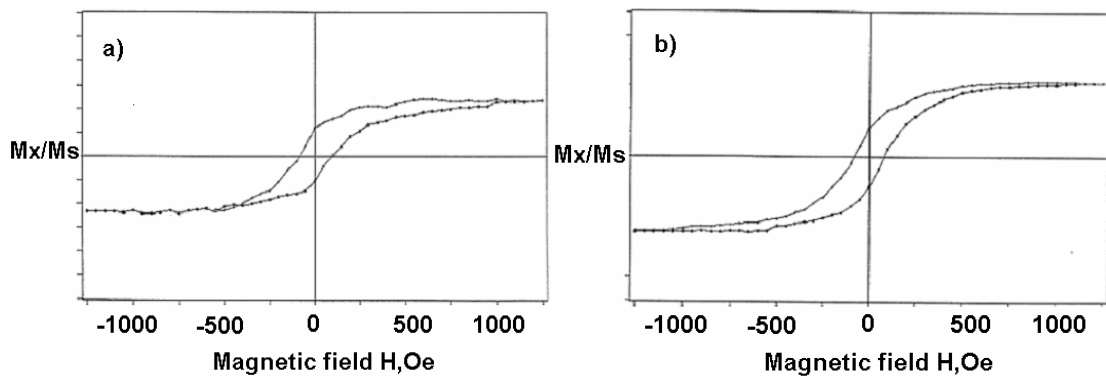


Fig.2 Hysteresis loops for Fe^+ -implanted PMMA samples with doses of a) $D = 1,2 \times 10^{17}$ ион/см², b) $D = 2,5 \times 10^{17}$ ион/см²

Discussion

The FMR spectra of PMMA implanted with Fe^+ ions did not show obvious influence of the magnetic field applied to the nanostructured metal-polymer films during the implantation. The resonance absorption lines of the films had a large width of about 500-1000 Oe, in contrast with that for samples obtained in crystalline substrate. It can be explained by a large dispersion of ferromagnetic nanoparticles in size and shape in amorphous polymers.

Similar FMR studies and rf susceptibility measurements of Si implanted with Fe^+ ions at the same conditions show distinct changes in magnetic parameters of the formed nanostructured films [5]. We assume that this difference is due to the influence of crystalline structure and lack of microcavities which serve as centers of nanoparticles' nucleation and growth in PMMA.

This comparative analysis suggests that for IBS of nanostructured magnetic films in polymers with enhanced and controlled properties substrates with better crystallinity are much more preferable.

References

- [1] Petukhov V.Yu. Ion beam synthesis of thin films in non-metals. – Doctorate Dissertation in Physics and Math, Kazan, 1998. – p. 311.
- [2] Petukhov V.Yu., Zhikharev V.A., et al // Solid State Communications. 1996. V.97. № 5. P.361.
- [3] Kittel C. // Phys. Rev. 1948. V.65. P.155.
- [4] Osborn J.A. Demagnetizing Factors of the General Ellipsoid. - Phys.Rev.- 1945.- V.67, N 11-12.- P.351-357.
- [5] Lutfullin I.A. IBS of magnetic nanostructures.– Diploma thesis. KSU, Kazan, 2002, p.41.

EPR INVESTIGATION OF THE ACTIVE SITE OF [Fe]HYDROGENASE

A. Silakov¹⁾, E. Reijerse¹⁾, S. Albracht²⁾, W. Lubitz¹⁾

¹⁾Max-Planck Institute for Bioinorganic Chemistry, Muelheim a.d. Ruhr, 45470. Germany

²⁾Swammerdam Institute for Life Sciences, Biochemistry, University of Amsterdam., Netherlands

e-mail: silakov@mpi-muelheim.mpg.de

Hydrogenases are enzymes found in microorganisms, which catalyze the simple redox reaction: $\text{H}_2 \rightarrow 2\text{H}^+ + 2\text{e}^-$. The potential use of these microorganisms for H_2 production as fuel makes hydrogen metabolism a fascinating and very relevant field of research [1].

The active center in [Fe]hydrogenase (the so-called H-cluster) contains a six-iron cluster consisting of a classical cubane connected to a binuclear iron cluster coordinated by CO and CN ligands [2]. The oxidized state of the cluster shows an axial EPR spectrum corresponding to an effective spin one half. The enzyme is inhibited under CO atmosphere. In this case a rhombic EPR spectrum is observed. Upon light excitation at temperatures between 20 and 70K the external CO ligand can be (reversibly) removed [3] and the original axial EPR spectrum is restored. Since from theoretical investigation of model complexes the CO ligand geometry is assumed to change during the reaction cycle [4, 5] it is quite relevant to investigate this process in more detail.

We present the first wavelength dependent studies on the photo-dissociation of the external CO ligand. It turns out that a species which most probably has lost its bridging CO ligand acts as intermediate in this process.

Another important question concerns the redox states of the iron atoms in the bi-nuclear subcluster during the catalytic cycle. The spin distribution over the H-cluster was studied using ENDOR and HYSCORE experiments on ⁵⁷Fe enriched hydrogenase at X- and Q-band frequencies. In this context we present the first Q-band ⁵⁷Fe HYSCORE study on an Iron-Sulfur cluster. In total, at least four different ⁵⁷Fe couplings could be distinguished pointing to a strong delocalization of the unpaired electron over the H-cluster.

References

- [1] Fraser A Armstrong, *Current Opinion in Chemical Biology* 8(2004) 133–140
- [2] Y. Nicolet, C. Cavazza, J.C. Fontecilla-Camps, *J. Inorg. Biochem.* 91(2002) 1-8Z. Chen, B. J. Lemon, S.Huang, D.J. Swartz, J.W. Peters, K.A. Bagley. *Biochemistry*, 41 (2002), 2036-2043

POSTER SESSION PS37

- [4] M. Bruschi, P. Fantucci, and L. De Gioia. *Inorganic Chemistry*, vol.42, 15 (2003), 4773-4781
Zhi-Pan Liu and P.Hu. *J.Am. Chem. Soc.* 124(2002) 5175-5182

MULTIFREQUENCY EPR STUDY OF MINERAL-ORGANIC NANO-ASSOCIATED SYSTEMS AND THEIR SYNTHETIC ANALOGOUS

S.N. Lukin¹⁾, A.A. Sitnikov¹⁾, A.B. Brik²⁾

¹⁾Institute of Semiconductor Physics National Academy of Science of Ukraine, 03028, pr. Nauki 45, Kiev, Ukraine.

²⁾Institute of Geochemistry, Mineralogy and Ore Formation of National Academy of Sciences of Ukraine, 03680, 34 pr. Palladina, Kiev, Ukraine.

e-mail: sit@nest.ntu-kpi.kiev.ua

Abstract

The properties of high-mineralized biological tissues (cow and rat bones) as Mineral-Organic Nano-Associated Systems and their synthetic analogue (hydroxyapatite) were studied. Information about their structure, anisotropy and mechanisms of interaction between components was obtained by using paramagnetic markers CO_2^- . The correlation between EPR parameters of biological and synthetic apatite was established. The advantages and disadvantages of EPR measurements at 9 and 37 GHz for Mineral-Organic Nano-Associated system are discussed.

Introduction

The synthetic apatite is used for various kinds of implants manufacturing, which are applied for bone and teeth treatment. The information about structure and properties of biogenic and synthetic apatite is important for bone tissue disease mechanism determination and for respective counter-measure and treatment methods development. [1, 2]. Moreover, information about bone internal structure and other mineralized tissues can open a new possibilities for new devices creation, which diagnose bone state in live organisms, as well as for technical devices creation, using in their work the principles of internal structure and functioning of biological tissues. Biominerals should be considered as mineral-organic nano-associated (MONA) systems [1, 2]. The organic and barrier layers that are between mineral and organic subsystem are the base units in MONA systems. All these subsystems have sizes within the limits of nanometers and bond with joint MONA matter. Since the bones and another mineralized biological tissues involve nanoscale solid-state particles (hydroxyapatite), then it open the wide possibilities for solid state physics methods application, including electron paramagnetic resonance (EPR).

Experimental Details

It were carried out the investigations by EPR method of synthetic hydroxyapatite powders (HAP) and bone plates from rat and bull. The samples of HAP were obtained by technology described in [3, 4] and annealed by 1000°C. The plates were extracted and dried. All samples were irradiated on cobalt unit (dose≈15 Mrad). The coordinate axis determination for these plates was in that way [1]: horizontal axis (*h*), perpendicular (*p*) and vertical (*v*). The directions of these axes coincide with corresponding directions by natural bone positions in animal organism. EPR spectra were registered by room temperature on 9 GHz and 37 GHz with etalon which constitutes Cr³⁺ ions in MgO powder.

EPR Results

On Fig. 1a there is an EPR spectra of HAP measured on 9 GHz. The EPR spectra there are two unsolved lines: I₁₂ and I₃. The comparing of EPR spectra general form with [1, 3] allows to conclude that this spectrum is appear to be a spectrum from polycrystalline sample with axial symmetry g-factor ($g_{\perp}=2,0027$ and $I_2 g_{\parallel}=1,9973$), electron spin $S=1/2$, nuclear spin $I=0$ and belongs to CO₂⁻.

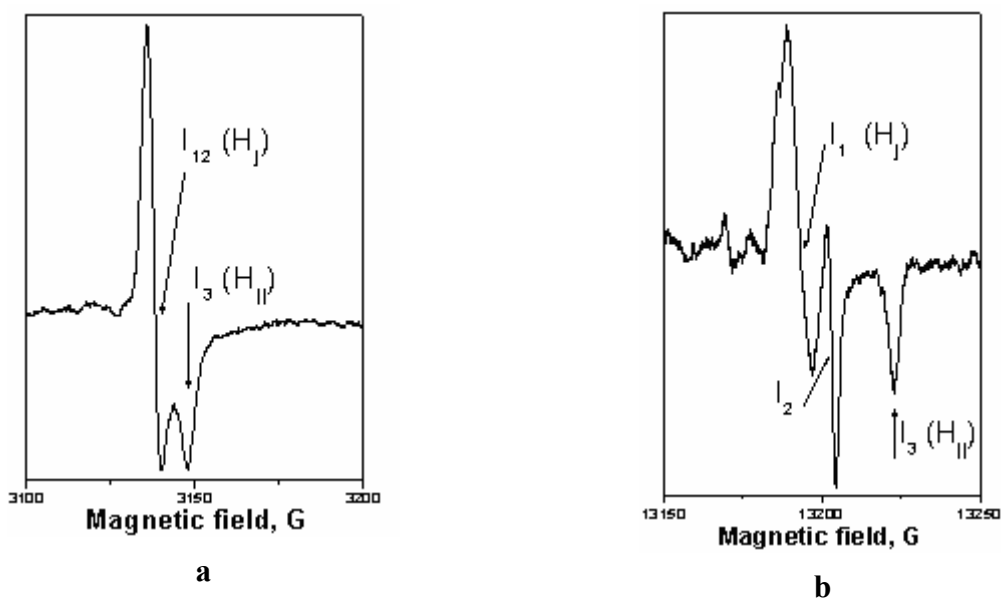


Fig. 1. The HAP EPR spectra. **a** - measured on 9 GHz, **b** - measured on 37 GHz.

The EPR spectra of the same sample measured on 37 GHz is shown on Fig. 1b. The EPR spectra consists of three lines: I₁, I₂ and I₃. I₁ and I₃ spectra with axial-symmetric g-factor belongs to CO₂⁻ radical. The single line I₂ with isotropic g-factor ($g=2,0008$) also belongs to CO₂⁻. Thus, the EPR spectra of polycrystalline synthetic HAP sample belongs to CO₂⁻

The measurements on 37 GHz allow to solve I₁₂ spectrum and evolve two EPR lines I₁

and I_2 which belong to CO_2^- radical with isotropic g-factor and CO_2^- with axial symmetry g-factor. This fact demonstrates the obvious advantage of investigations on higher microwave (MW) frequency which allow to detect, separate and identically interpret EPR spectra that appear to be a several EPR signals superposition. There are differences in EPR signal behavior which are concerned with CO_2^- with isotropic g-factor and CO_2^- with axial symmetry g-factor depending on MW power level.

Fig. 2a shows the HAP EPR spectra measured on 37 GHz by different MW power attenuation levels. As it seen from Fig. 2a the MW power change results in EPR spectra components intensity change. Each of three EPR spectrum components: I_1 , I_2 , and I_3 has different intensity dependences from MW power level. Fig. 2b shows the EPR spectra intensity I_1 , I_2 , and I_3 dependences from MW power attenuation value. The EPR spectrum intensity of CO_2^- radical with axial-symmetry g-factor, which has low-field component I_1 and high-field component I_3 , is proportional to MW power level in interval of 42-18 dB. By lower attenuation (<18 dB) there is a saturation of EPR signal form CO_2^- radical with axial-symmetry g-factor.

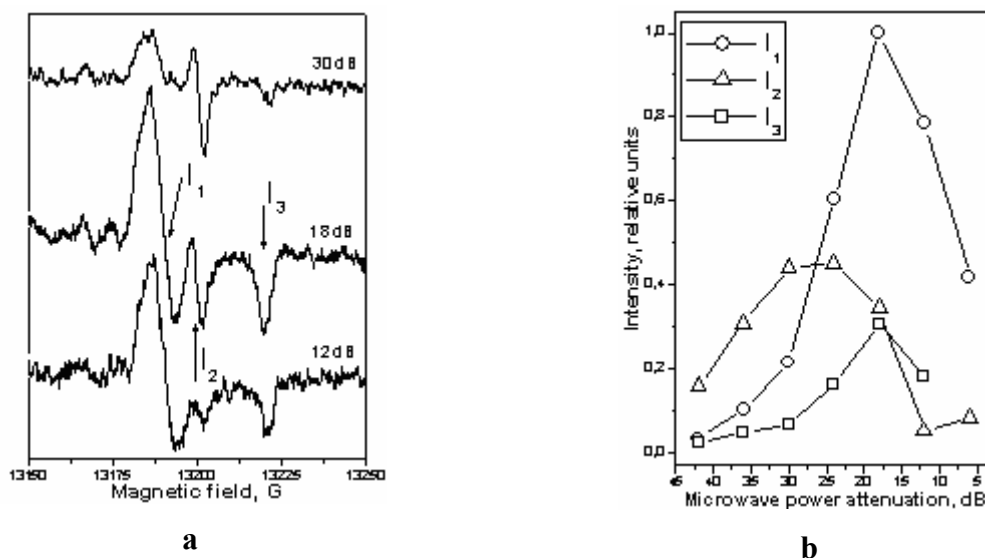


Fig. 2. **a** - The HAP EPR spectra measured on 37 GHz by different MW power attenuation levels. **b** - Intensity dependence of calcium HAP I_1 , I_2 , and I_3 EPR spectra measured on 37 GHz from attenuation MW power value. The intensity unit is an I_1 spectra intensity.

The EPR spectra concerned with CO_2^- with isotropic g-factor is saturated by MW power in order of 24 dB. Thus, by varying of MW power level it is possible to simplify the general form of composite EPR signal, to evolve necessary components from general EPR spectrum, to determine the carbonate radical type by its EPR signal behavior and to obtain an information about spin- spin-lattice relaxation time.

With the purpose of texturing and anisotropy of bone tissue there were investigated EPR spectra of bull and rat bone. Fig. 3a shows EPR spectra of rat bone plates by different orientations in magnetic field H measured on 37 GHz. These EPR spectra represents the EPR signals of biogenic apatite concerned with carbonate radicals CO_2^- . The main contribution in these spectra contributes the CO_2^- radical with axial-symmetry g-factor: $g_{\perp}=2,0025$ and $g_{\parallel}=1,9973$. The typical bone EPR spectrum peaks I_{\perp} and I_{\parallel} have $g_1=2,003$ and $g_2=1,997$.

It is well known that the EPR spectrum of teeth enamel and bone is represented by two types of carbonate radicals CO_2^- [5]. One of these has chaotic orientation in biomineral structure, another one is orientated by organic matrix and responsible for native bone tissue EPR signal anisotropy. The CO_2^- radical with axial-symmetry g-factor oxygen-oxygen bond is corresponded to g_{\parallel} direction. The CO_2^- radicals in apatite structure are localized so, that the bond oxygen-oxygen direction coincides with the direction of nanocrystal apatite main axis c .

Thus, by signal I_{\parallel} intensity we can predetermine the orientation of apatite crystals in bone. From Fig. 3 b we can conclude that in bone the nanocrystals are orientated mainly along the vertical axis v (in rotation plane v - p).

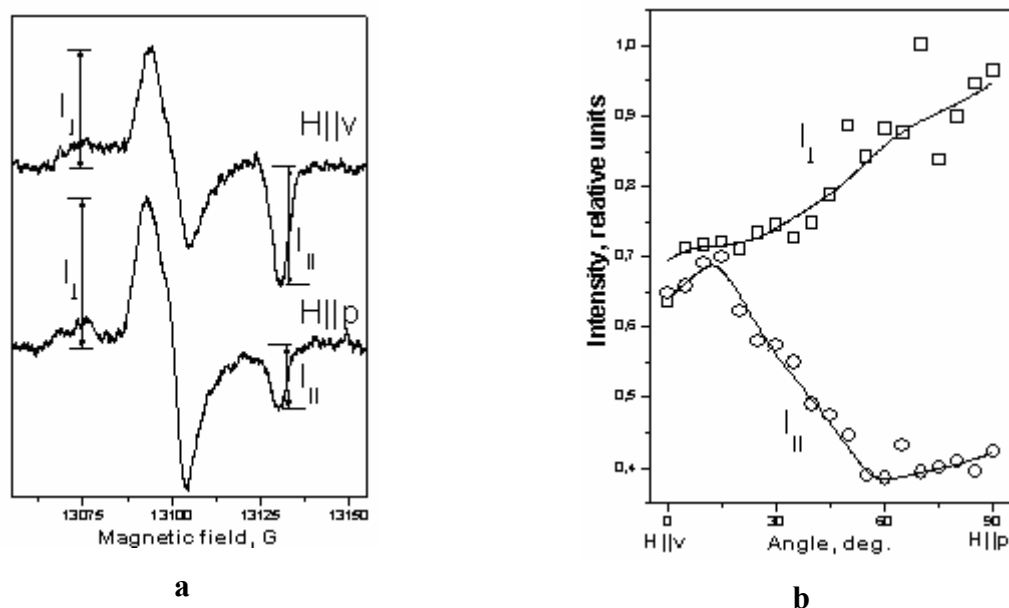


Fig. 3. **a** - Rat bone EPR spectrum by different plate orientations in magnetic field (rotation axis is h); **b** - Rat bone EPR signal intensities I_{\perp} and I_{\parallel} peaks dependence by magnetic field p axial rotation. Intensity unit is maximum I_1 spectra intensity level.

Summary

The joint studying of synthetic and biogenic apatite methods development in centimeter and millimeter ranges as well as comparison of EPR method possibilities in these ranges are

POSTER SESSION PS38

actual for solving of many medico-biologic problems. Also it is actual for new generation of devices and apparatus development which allow to determine the teeth tissue structure and properties in live organisms.

[1] Brik A., Haskel E., Scherbina O. et al. Applied radiation and isotopes. 52 (2000)

[2] Brik A., Brik V., Mineralogical journal. 20, №5 (1998).

[3] Schramm D., Rossi A., Applied radiation and isotopes. 52 (2000).

[4] Brik A., Ulyanchich N., Kenner G. et al. Mineralogical journal. – 23, №1 (2001).

[5] Callens F., Vanhaelewyn G., Matthys P., Spectrochimica acta part A. 58 (2002).

THE COMPUTER ANALYSIS OF ESR SPECTRA OF EQUILIBRIUM SYSTEMS

A. Sklar, S. Bolotin, V. Panyushkin

Chemistry Department, Kuban State University, Krasnodar, 350040, Russia

e-mail: epr_kb@chem.kubsu.ru

Program for determine of the complexes parameters in the aqueous solution (formation constants, hyperfine coupling (HFC) constants, g-factors, relaxation parameters) by using method of analysis of spectrum lineshape was created. The main program units are the module for calculating the molar fractions of the system components by the standard procedure for solving the set of material balance equations [1]; the module for calculating the lineshape of the ESR spectrum; and the module for optimization of the parameters by the scanning and coordinate descent methods.

The experimental ESR spectrum is usually described as a convolution of the Gaussian and Lorentz lines. The theoretical spectrum was constructed by a superposition of the Lorentz curves, and this method gave a satisfactory agreement in all the cases. The correction for nonuniform broadening of the experimental signal was made by introducing the unresolved HFS. The effect of anisotropy of the HFC of an unpaired electron with the metal nucleus on the line width was calculated by the Wilson-Kivelson equation [2].

Copper(II) – L-histidine – D-ornitin and copper(II) – L(LD)-threonine equilibrium systems were studied in the aqueous solution in the wide pH range. The data for linewidths, the g factor, the HFC constant, and stability constant of the each complexes were varied, until the sum of the squares of differences between the calculated and measured intensities (SSQD) reached its minimum.

Simultaneous calculation of many independent parameters is a complicated task. Therefore, we solved the problem by several steps. To enhance an accuracy of the parameters under estimation, we processed simultaneously up to four spectra recorded at different pH and the component ratios.

At the first step, four experimental spectra recorded at the same ratio $C_M:C_L$ and close pH values were optimized and the parameters of at most three compounds prevailing in the equilibrium system were calculated. The scanning method, which allows one to avoid falling into the local minimum of the SSQD function, was used as the optimization procedure at this step.

At the next step, the obtained values were refined by processing the spectra recorded at different pH and compositions of solutions, which can contain greater number of species. This calculation procedure imposes no restrictions on the number of complexes, whose parameters can be estimated simultaneously. The minimization process was stopped when the further variation of the parameters did not decrease the SSQD function and the theoretical and experimental spectra coincided visually. The reliability of the results was provided by the great number of the experimental points and by the low value of SSQD function.

References

- [1] Beck M., Nagypal I.: Chemistry of complex equilibria. Budapest: Akademiai Kiado 1989.
- [2] Wilson R., Kivelson D.: J. Chem. Phys., **44**, 154 (1966).

EPR IN CHARGE-TRANSFER SALTS WITH METAL-COMPLEX ANIONS

D.V Starichenko¹⁾, Yu.N. Shvachko¹⁾, N.D. Kushch²⁾, E.B. Yagubski²⁾

¹⁾Inst. Metal Physics RAS, Yekaterinburg, 620219, Russia

¹⁾Institute of Problems of Chemical Physics RAS, Chernogolovka, 142432, Russia

e-mail: starichenko@imp.uran.ru, lkushch@icp.ac.ru

Combination of conductivity and magnetic activity in counter ion sub-lattices draw new interest to quasi-two dimensional charge-transfer salts based on bis-[ethylenedithiolo (tetrathiofulvalene)]–BEDT-TTF and its analogs. Linkage between spin state of local moment in anion complex and delocalized charge carriers in cation layer would lead to new polyfunctional materials. It is important at the first step to understand structural aspects of the influence of simple tetrahedral anions on conducting properties. EPR is a useful tool to analyze these interactions [1].

In this work we study 2 salts with diamagnetic tetrahedral metal-complex anions (BEDT-TTF)₂Dy(NO₃)₄ (1) and (BEDO-TTF)₂ReO₄·H₂O (2). BEDO is full BEDT analog, where S atoms in outer ring are replaced with O. Ground state of both compounds depends on metal-complex packing stabilized at higher temperatures. Compound (1) is a semiconductor

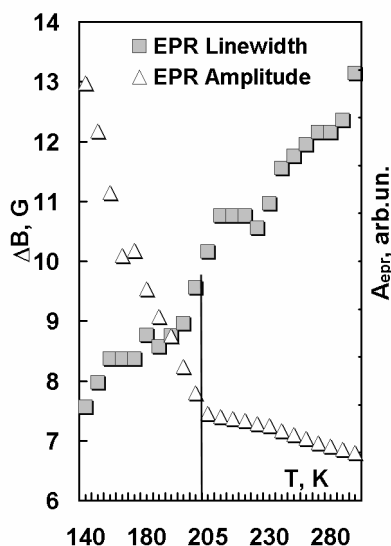


Fig. 1. ΔB(T), A(T) for (ET)₂Dy(NO₃)₄

revealing irreversible transport properties with metallic segment at heating while (2) shows metallic behavior down to helium temperatures and superconductivity at 2,5 K [2, 3].

Both salts demonstrate irreversible behavior of EPR parameters in the vicinity of 200 K. Linewidth for (1) drops from 11 to 8,2 G at cooling around T₀=197 K, within ΔT=20K (see Fig. 1). For (2) ΔB increases from 32 to 37,5 G at T₀=203 K, within ΔT=25 K. Spin susceptibility behavior demonstrate transformation from Pauli-like to Curie type for (1) and weak temperature dependence for (2). Meanwhile, absolute values, ~10⁻⁴

emu/mol, at 300 K are noticeable higher than Pauli susceptibility for non-interacting gas with S=1/2. SQUID measurements are in good agreement with EPR data.

Taking into account X-ray structural data resolved at 300 K and 77 K [3] we conclude that metastable tetrahedron orientations induce disorder through O...H bonds between oxygen

of metal-complex and ethylene groups of cation layer. For (1) at cooling we observe localization effect and narrowing of EPR line. At heating no more metastable orientations exist and “metal” segment is observed. Thus for (1) metal-insulator transition is detected at 197 K. This is consistent with low temperature increase of g-factor from 2,004 to 2,009. For (2) tetrahedron re-arrangement is less effective because of absence of short S-S contacts for outer rings. Mainly, lattice shrink modifies the conduction band, which is observed as Me-Me' transition in the same temperatures. Respectively, integrated EPR intensity is less sensitive than the linewidth. Here cooling rate is critical for low temperature state because at faster cooling residual anion disorder may induce AFM clusters.

This work was supported by Netherlands-Russian program (grant NWO 047.008.020).

References

- [1] K. Itoh, M. Kinoshita, Molecular magnetism, Gordon and Breach Sci. Publ., 2000, 347 p.
- [2] L.I. Buravov *et al.* // J. Phys. I. France 2, 529 (1992).
- [3] S.S. Khasanov *et al.*// Eur. Phys. J. B 1, 419-428 (1998).

**NEW PROGRAM WITH INTERACTIVE FRIENDLY INTERFACE FOR EPR
SPECTRA SIMULATION OF COPPER-CONTAINING PROTEINS**

Y. Tkachov, V. Timofeev

Engelhardt Institute Molecular Biology RAS, Moscow, 119991, Russia

e-mail: tim@eimb.ru

Last time interest is growing among biochemists to different enzymes, containing transition metal atom in active center, copper, for example. Typical sample is a copper-containing oxidases, which catalyze direct electron transfer from substrate to oxygen without a mediator. Active center of such enzymes contain cluster consisting of several paramagnetic copper atoms, so the EPR method is applicable to them. For such investigations it is often necessary to simulate EPR spectra, but deficiency and inaccessibility of most computer programs for this simulation, their direction to people qualified in magnetic resonance spectroscopy strongly limits using of EPR simulation in biochemist's environment. Besides that, many of these programs are written under 16-bit platforms like DOS or MS Windows 3.1, and this makes impossible usage of full computation power of modern machines. Program now presented uses friendly user interface of 32-bit operating systems of Microsoft Windows family, which may be easily understood by enzymologists and does not require special knowledge and long training. Current version carries out spectra simulation of paramagnetic copper(II) species in powder (at liquid nitrogen temperature, 77K) or dynamic (solution at room temperature) computational models. It use main values of diagonalized \mathbf{A} and \mathbf{g} magnetic tensors as initial parameters. Simulations, performed with this program give satisfactory coincidence with experimental results. So further development of this program and it's distribution among enzymologists may promote wider EPR method applications in biochemistry.

**ION-MOLECULAR CHARGE TRANSFER REACTION IN LINEARLY
CONDENSED AROMATIC SYSTEM STUDIED BY MARY AND OD ESR
TECHNIQUES**

V.N. Verkhovlyuk¹⁾, D.V. Stass¹⁾, N.N. Lukzen²⁾, Yu.N. Molin¹⁾

¹⁾Institute of Chemical Kinetics and Combustion, Novosibirsk, 630090, Russia,

²⁾International Tomography Center, Novosibirsk, 630090, Russia

e-mail: v_ver@ngs.ru

The processes of degenerate electron exchange (charge transfer reaction) play an important role in the study of primary radical ionic reactions in solutions under ionizing irradiation. In some cases these processes may proceed with different rates for the radical cation and the radical anion of the same compound. In this work, spin chemistry techniques (MARY spectroscopy and OD ESR) were used to study the peculiarities of the charge transfer reaction of biphenyl and other linearly condensed aromatic systems (*para*-terphenyl, quaterphenyl). These systems were chosen because their neutral molecules and radical cations and anions all have different structures, and so the charge transfer reactions of the radical cation and the radical anion could be expected to proceed with different rates.

As the MARY experiments for hexane solutions of biphenyl at various concentrations have shown, increasing the acceptor concentration up to 0.1 M makes the widths of the EPR spectra of the partners considerably different, while the parameters of the EPR spectra of the biphenyl radical ions are similar. Such a behavior of the EPR spectrum widths of the partners can be due to the fact that only one of the partners is involved in charge transfer reaction (or at least, the partners are in different charge exchange modes). Simulation of the OD ESR spectra of biphenyl in hexane also suggests that the spectrum widths of the partners at high concentration are considerably different. Similar results were obtained for other linearly condensed systems.

Calculated MARY spectra for the pairs *biphenyl*⁺/*biphenyl*⁻ in the case of degenerate electron exchange are also discussed, which allows for estimation of the charge exchange rate of each partner. An attempt was made to register individually the spectrum of the biphenyl radical cation, with a negative charge acceptor (C₆F₆⁻) as the counterion, which shows that it is the radical cation of biphenyl that is in the fast charge exchange mode. This result is indirectly supported by quantum chemical calculations available in literature showing that the radical cation and the neutral molecule of biphenyl have similar (non-planar) structure but the radical anion is planar.

The work was supported by RFBR (grant 03-03-32331) and Minvuz (project E02-5.0-49).

IMPLEMENTATION SCHEMES IN NMR OF UNIVERSAL SET OF QUANTUM GATES BY USING VIRTUAL SPIN REPRESENTATION

N.M. Yakovleva

E.K. Zavoisky Physical-Technical Institute, Russian Academy of Science, 420029, Sibirsky trakt 10/7, Kazan, Russia

e-mail: yana@dionis.kfti.knc.ru

In the standard model of quantum computer several spins $1/2$, coupled by exchange interaction, are used to encode the qubits according to the rule «one qubit - one real spin $1/2$ ». To enlarge the possibilities of the quantum computations it is desirable to encode qubits on the arbitrary quantum systems with the large number of discrete energy levels, in particular, on the states of large spins. It is possible to realize this idea using virtual spin representation [1, 2] and new principle of qubit encoding «one qubit – one virtual spin $1/2$ ».

We shall consider a quadrupole nucleus with spin $7/2$ in an axially symmetric crystalline electric field and in a constant magnetic field parallel to the symmetric axis as a basis for quantum computer. The Hamiltonian of such a system is given by

$$H = -\hbar\omega_z I_z + \hbar\omega_q [I_z^2 - I(I+1)/3], \quad (1)$$

where ω_z and ω_q are Zeeman and quadrupole frequencies. We assume that $\omega_z > \omega_q$, so the nucleus have eight non-equidistant energy levels $\hbar\varepsilon_m$ and eigenfunctions $|\Psi_m\rangle$ ($m = -7/2, -5/2, \dots, 7/2$), which are eigenfunctions of z -component of the nuclear spin.

The evolution operator of the spin state under the influence of the selective pulse of the resonance magnetic field, which is oriented along the y -axis and exciting resonance transitions only between levels $\hbar\varepsilon_m$ and $\hbar\varepsilon_n$ ($\hbar\varepsilon_m > \hbar\varepsilon_n$), has the form

$$Y_{mn}(\varphi, f) = E + (P_{nn} + P_{mm})(\cos(\varphi/2) - 1) + (P_{nm}e^{-if} - P_{mn}e^{if})\sin(\varphi/2), \quad (2)$$

where P_{mn} is a projective operator with the properties $P_{mn}P_{rs} = \delta_{nr}P_{ms}$ and $P_{mn}\Psi_k = \delta_{nk}\Psi_m$; $E = \sum_m P_{mm}$, $\varphi = \gamma H_1 t_i |\langle \Psi_m | I_y | \Psi_n \rangle|$, H_1 , f and t_i – amplitude, phase of the magnetic field and pulse duration.

When magnetic field is polarized along the x -axis or when the phase in (2) is shifted $f \rightarrow f + \pi/2$ the evolution operator assume the form

$$X_{mn}(\varphi, f) = E + (P_{nn} + P_{mm})(\cos(\varphi/2) - 1) - i(P_{nm}e^{-if} + P_{mn}e^{if})\sin(\varphi/2). \quad (3)$$

The essence of the virtual spin representation is to associate each eigenstate $|\Psi_m\rangle$ of the real physical system with the direct product $|\chi_\alpha\rangle \otimes |\xi_\beta\rangle \otimes |\zeta_\gamma\rangle$ ($\alpha, \beta, \gamma = -1/2, 1/2$) of the states of three virtual spins 1/2

$$\begin{aligned} |\Psi_0\rangle &= |\chi_0\rangle \otimes |\xi_0\rangle \otimes |\zeta_0\rangle, & |\Psi_1\rangle &= |\chi_0\rangle \otimes |\xi_0\rangle \otimes |\zeta_1\rangle, \\ |\Psi_2\rangle &= |\chi_0\rangle \otimes |\xi_1\rangle \otimes |\zeta_0\rangle, & |\Psi_3\rangle &= |\chi_0\rangle \otimes |\xi_1\rangle \otimes |\zeta_1\rangle, \\ |\Psi_4\rangle &= |\chi_1\rangle \otimes |\xi_0\rangle \otimes |\zeta_0\rangle, & |\Psi_5\rangle &= |\chi_1\rangle \otimes |\xi_0\rangle \otimes |\zeta_1\rangle, \\ |\Psi_6\rangle &= |\chi_1\rangle \otimes |\xi_1\rangle \otimes |\zeta_0\rangle, & |\Psi_7\rangle &= |\chi_1\rangle \otimes |\xi_1\rangle \otimes |\zeta_1\rangle, \end{aligned}$$

where indices 0,1, ..., 7 are used instead of indices -7/2, -5/2, ..., 7/2 for real spin 7/2 and 0,1 instead of -1/2,1/2 for virtual spins 1/2.

It is well known [3-5], that there are universal sets of one- and two-qubit quantum gates, which are sufficient for constructing a quantum algorithm of any complexity. One possible universal set of quantum gates consists of only two gates - rotation of the single qubit and two-qubit controlled-NOT gate.

The rotation of the single qubit by the angle φ around the y -axis

$$\begin{aligned} Y_a(\varphi) &= Y_{04}(\varphi,0)Y_{15}(\varphi,0)Y_{26}(\varphi,0)Y_{37}(\varphi,0), \\ Y_b(\varphi) &= Y_{02}(\varphi,0)Y_{13}(\varphi,0)Y_{46}(\varphi,0)Y_{57}(\varphi,0), \\ Y_c(\varphi) &= Y_{01}(\varphi,0)Y_{23}(\varphi,0)Y_{45}(\varphi,0)Y_{67}(\varphi,0). \end{aligned} \quad (4)$$

The order of the operators in the sequence is important and the sequence should be read from right to left. The similar implementation schemes can be obtained for the rotation of the single qubit by the angle φ around the x -axis

$$\begin{aligned} X_a(\varphi) &= X_{04}(\varphi,0)X_{15}(\varphi,0)X_{26}(\varphi,0)X_{37}(\varphi,0), \\ X_b(\varphi) &= X_{02}(\varphi,0)X_{13}(\varphi,0)X_{46}(\varphi,0)X_{57}(\varphi,0), \\ X_c(\varphi) &= X_{01}(\varphi,0)X_{23}(\varphi,0)X_{45}(\varphi,0)X_{67}(\varphi,0). \end{aligned} \quad (5)$$

Note, that the most easily the transitions between the states with $|m-n|=1$, which form the operator $Y_c(\varphi)$, are excited. At enough intensity of the alternating field are allowed all transitions. The transitions with $|m-n|=2$ were used for preparation of so-called pseudo pure states [6], which are necessary for the beginning of the quantum computations.

In particular, one-qubit gates, NOT and pseudo Hadamard operator, can be obtained from (5) at $\varphi = \pi$ and from (4) at $\varphi = \pi/2$, respectively.

One-qubit Hadamard operator are

$$\begin{aligned} H_a &= Y_a(\pi/2)X_{45}(2\pi,0)X_{67}(2\pi,0), \\ H_b &= Y_b(\pi/2)X_{23}(2\pi,0)X_{67}(2\pi,0), \\ H_c &= Y_c(\pi/2)X_{13}(2\pi,0)X_{57}(2\pi,0). \end{aligned}$$

Two-qubit controlled-NOT gate, that inverts the state of qubit b , if the qubit a is in the state $|1\rangle$ and leaves the qubit b unchanged if the qubit a is in the state $|0\rangle$

$$\begin{aligned} CNOT_{a \rightarrow b} &= Y_{56}(2\pi,0)Y_{46}(-\pi,0)Y_{57}(\pi,0), \quad CNOT_{a \rightarrow c} = Y_{56}(2\pi,0)Y_{45}(-\pi,0)Y_{67}(\pi,0), \\ CNOT_{b \rightarrow a} &= Y_{36}(2\pi,0)Y_{26}(-\pi,0)Y_{37}(\pi,0), \quad CNOT_{b \rightarrow c} = Y_{36}(2\pi,0)Y_{23}(-\pi,0)Y_{67}(\pi,0), \\ CNOT_{c \rightarrow a} &= Y_{35}(2\pi,0)Y_{15}(-\pi,0)Y_{37}(\pi,0), \quad CNOT_{c \rightarrow b} = Y_{35}(2\pi,0)Y_{13}(-\pi,0)Y_{57}(\pi,0), \quad (6) \end{aligned}$$

Real transition operators have either imaginary, or negative non-diagonal matrix elements, while the real positive elements are required for gates realization. There are two ways to solve this problem: (i) take into account these differences during the whole sequence of the operators, constituting the algorithm (in this case the result of the computations will be presented in some modified form), (ii) to use more complicated pulse sequence to bring into correspondence the form of the influence of the experimental operators with the requirements of the theory of algorithms as was suggested in (6).

Two-qubit SWAP gate that interchanges the states of the two

$$\begin{aligned} SWAP_{a \leftrightarrow b} &= Y_{34}(-\pi,0)Y_{24}(-\pi,0)Y_{35}(\pi,0), \\ SWAP_{a \leftrightarrow c} &= Y_{34}(-\pi,0)Y_{14}(-\pi,0)Y_{36}(\pi,0), \\ SWAP_{b \leftrightarrow c} &= Y_{25}(-\pi,0)Y_{12}(-\pi,0)Y_{56}(\pi,0). \end{aligned}$$

Three-qubit Toffoli gate or the controlled-controlled-NOT gate that inverts the state of the qubit c , if the first two qubits a and b are in the state $|11\rangle$

$$\begin{aligned} CCNOT_{(a,b) \rightarrow c} &= e^{-i\pi/8}\Pi_6 Y_{67}(\pi,0), \\ CCNOT_{(a,c) \rightarrow b} &= e^{-i\pi/8}\Pi_5 Y_{57}(\pi,0), \\ CCNOT_{(b,c) \rightarrow a} &= e^{-i\pi/8}\Pi_3 Y_{37}(\pi,0). \end{aligned}$$

Simpler implementation schemes of the controlled-controlled-NOT gate can be achieved, if one agrees with the presence of imaginary non-diagonal matrix elements

$$CCNOT_{(a,b) \rightarrow c}^* = Y_{67}(\pi,0), \quad CCNOT_{(a,c) \rightarrow b}^* = Y_{57}(\pi,0), \quad CCNOT_{(b,c) \rightarrow a}^* = Y_{37}(\pi,0).$$

Three-qubit Fredkin gate or controlled-SWAP interchanges the states of the qubits b and c , if qubit a is in the state $|1\rangle$

$$CSWAP_{a \rightarrow (b \leftrightarrow c)} = e^{-i\pi/8} \Pi_5 Y_{56}(\pi, 0),$$

$$CSWAP_{b \rightarrow (a \leftrightarrow c)} = e^{-i\pi/8} \Pi_3 Y_{36}(\pi, 0),$$

$$CSWAP_{c \rightarrow (a \leftrightarrow b)} = e^{-i\pi/8} \Pi_3 Y_{35}(\pi, 0).$$

Three-qubit it gate Π_i that changes the sign of the state $|\Psi_i\rangle$

$$\Pi_i = Y_{01}(\eta_1\pi, 0)Y_{12}(\eta_2\pi, 0)Y_{23}(\eta_3\pi, 0)Y_{34}(\eta_4\pi, 0)Y_{45}(\eta_5\pi, 0)Y_{56}(\eta_6\pi, 0)Y_{67}(\eta_7\pi, 0) \times \\ \times Y_{67}(\pi, \pi/8)Y_{56}(\pi, \pi/8)Y_{45}(\pi, \pi/8)Y_{34}(\pi, \pi/8)Y_{23}(\pi, \pi/8)Y_{12}(\pi, \pi/8)Y_{01}(\pi, \pi/8),$$

where $\eta_j = 1$, when $j = i$ and $\eta_j = -1$, when $j \neq i$.

This work was supported by NIOKR RT (grant 06-6.1-158) and RFFI (grant 03-01-00789).

References

- [1] Kessel A.R., Ermakov V. L. «Multiqubit spin» *JETP Lett.* **70** (1999) 61-65; «Virtual qubits: multilevels instead of multiparticles» *JETP* **117** (2000) 452-459; « Physical Implementation of Three-Qubit Gates on a Separate Quantum Particle» *JETP Lett.* **71** (2000) 307-309.
- [2] Kessel A.R., Yakovleva N.M. «Implementation schemes in NMR of quantum processors and the Deutsch-Jozsa algorithm by using virtual spin representation» *Phys. Rev. A* **66** (2002) 062322.
- [3] Barenco A., Bennett C.H., Cleve R., DiVincenzo D.P., Margolus N., Shor P., Sleator T., Smolin J., Weinfuter H. «Elementary Gates for Quantum computation» *Phys. Rev A* **52** (1995) 3457-3467.
- [4] D. P. DiVincenzo «Two-bit gates are universal for quantum computation» *Phys. Rev. A* **51** (1995) 1015-1022.
- [5] D. Deutsch, A. Barenco, A. Ekert « Universality in Quantum Computation» *Proc. R. Soc. Lond. A* **449** (1995) 669.
- [6] A.K. Khitrin, H. Sun, B.M. Fung «Method of multifrequency excitation for creating pseudopure states for NMR quantum computer» *Phys. Rev. A* **63** (2001) 020301(R).

NUCLEAR SPIN-LATTICE RELAXATION IN CARBON-BASED CHARS

A.N. Yudin¹⁾, G.V. Mamin^{1,2)}, M.S. Tagirov¹⁾, D.A. Tayurskii¹⁾, H. Suzuki²⁾,
B.M. Odintsov³⁾, R.B. Clarkson³⁾

¹⁾Physics Department, Kazan State University, 18 Kremlyovskaya St., Kazan 420008, Russia

¹⁾Physics Department, Kanazawa University, Kanazawa, 920-1192, Japan

¹⁾Illinois Research EPR Center, University of Illinois, Urbana, Illinois 61801, USA

e-mail: Alexey.Yudin@ksu.ru

1. Introduction

The idea to use dynamic polarization method to obtain hyperpolarized noble gases (³He and ¹²⁹Xe) was published in [1]. Carbon-based chars [2] can be used in this method. They have well-developed surface and a lot of paramagnetic centres (PC) allocated on the surface [3]. The EPR-measurements showed that EPR-line of paramagnetic centres is narrow because of exchange interaction and is very sensitive to presence of different gases. Magnetic coupling between paramagnetic centres and ³He nuclei was detected by changes of EPR-line in presence of ⁴He and ³He. Calculations show that NMR signal enhancement up to 430 can be obtained by dynamic polarization. Nevertheless attempts of polarizing ³He in such systems were not successful [4].

2. Samples and method

2.1. Samples preparing. Chars used in the investigations were produced by a thermal treatment of fructose in vacuum. After desintegration the powder consisted of fine flakes. The powder was separated by particle size and powder with size 150-250 mkm was used in further experiments.

The powder was placed to quartz ampoule and pumped down. Then the ampoule was filled with ³He (0.9 atm.) and sealed.

2.2. Experimental method. Longitudinal relaxation time was measured by standard method of echo recovery after saturating pulse. NMR-signals of three nuclei types were studied:

- The ¹³C nuclei that are distributed in the char (natural abundance 1.108%)
- The protons situated on the surface of char
- The ³He situated outside the char

3. Results and discussion

Since the relaxation times were rather short we can assume that the major process was relaxation through the paramagnetic centres of char.

The longitudinal relaxation rate of ^{13}C nuclei rises with temperature increase. It can be explained by increase of amplitude of local magnetic fields created by paramagnetic centres. But large local magnetic fields impeded the magnetization transfer so above 10 K relaxation rate did not depend on temperature.

The relaxation time of protons was very short because they were situated near the paramagnetic centres on the surface. The atoms of ^3He were situated outside the char but over fast diffusion could relax through paramagnetic centres almost without obstacles. So there is some similarity between relaxations of these two types of nuclei.

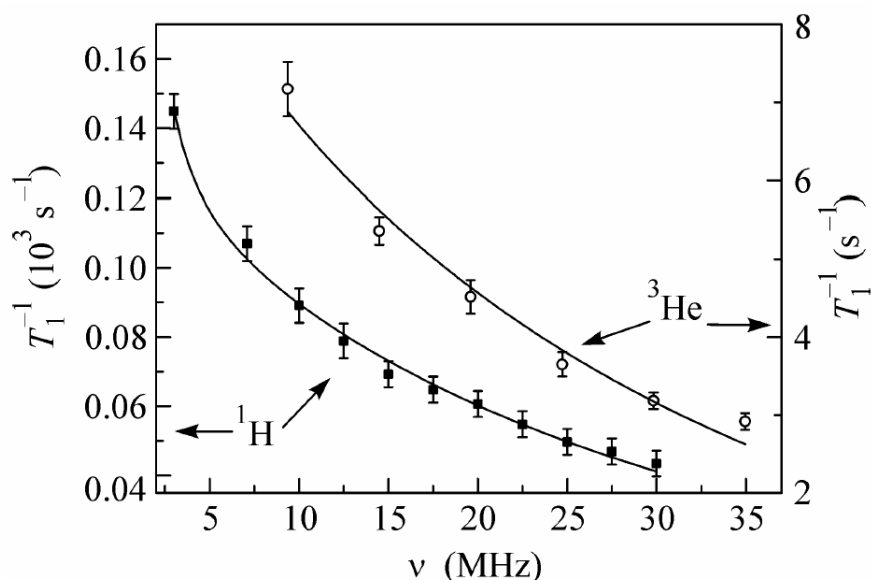


Fig. 1. Frequency dependence of longitudinal relaxation rates for ^3He nuclei and protons.

Frequency dependences of longitudinal relaxation rates for ^3He nuclei and protons (Fig. 1) could be fitted with exponential decay. That can be explained as suppressing of exchange interaction inside paramagnetic clusters of char.

It is reasonable to assume that both the isolated PCs and the clusters of exchange-coupled PCs exist at the surface of char particles. In the model suggested, the NSLR rate of protons and ^3He spins is given by

$$T_1^{-1} = T_1^{-1}{}_{is} + T_1^{-1}{}_{clus} \quad (1)$$

NSLR through isolated PCs accounts for the second-type scalar relaxation, so $T_1^{-1}{}_{is} \sim \nu^{-2}$. Assuming that the exchange interaction between the paramagnetic centers is caused by a partial and rather weak overlap of electron shells, $T_1^{-1}{}_{clus} \sim \exp(-K\nu)$. Since the parameter K

includes only the properties of electron shells and should be independent of the types of relaxing nuclei, its values obtained by approximating the frequency dependences are the same for the ^3He and ^1H NSLRs.

The NSLR model suggested above is in agreement with the experimentally measured temperature dependence of the proton relaxation rate in different magnetic fields (Fig. 2). The increase in the slope of temperature curve and the decrease in the relaxation rate in a higher magnetic field correspond to the increase in the relative contribution of the first term in Eq. (1) as a result of the field-induced suppression of exchange interaction in clusters.

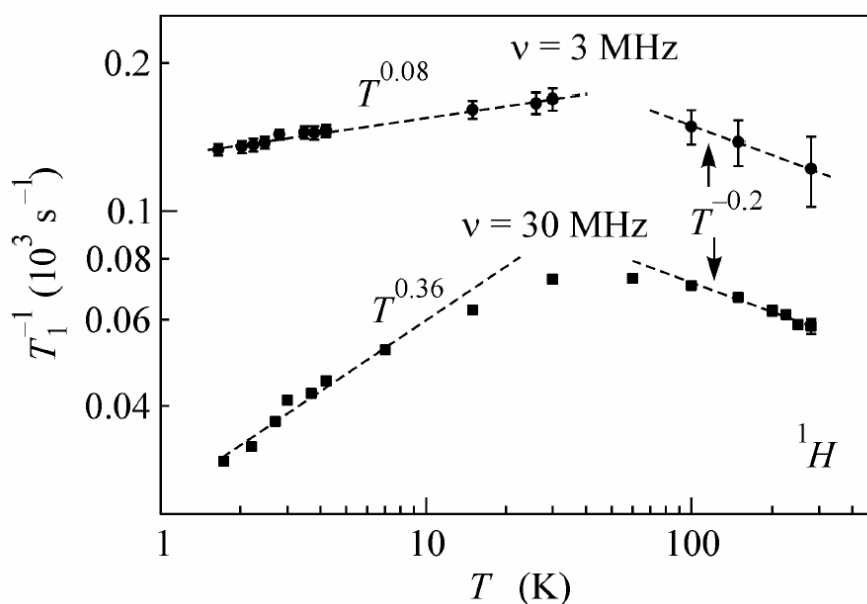


Fig 2. Temperature dependence of longitudinal relaxation rates of protons.

4. Future works

Hypothesis about suppressing of exchange interaction of paramagnetic centres can be verified by EPR-measurements in different magnetic fields. We suppose to provide them in the nearest future.

The main barrier in dynamic polarization with the char is magnetization leakage through protons that have the shortest relaxation time. So it is necessary to develop method of producing chars without protons impurities.

Acknowledgements

This work is supported by RFBR (grant N 02-04-16800), Ministry of Education of Russian Federation (grant A03-2.9-516), BRHE (REC-007) and program “Universities of Russia” (grant N 01.01.010).

References

- [1] M.S.Tagirov, D.A.Tayurskii, JETP Letters, **61**, 652 (1995).
- [2] R.B.Clarcson et al, Phys.Med.Biol., **43**, 1907 (1998).
- [3] G.V.Mamin, et al, Physica B. **329**, 1237 (2002).
- [4] L.W.Engel and K.DeConde, Phys. Rev. B. **33**, 2035 (1986).
- [5] G.V.Mamin, et al, JETP Letters, **79**, 641 (2004)

ANISOTROPIC EXCHANGE IN α' - NaV_2O_5 : AN ESR STUDY

D.V. Zakharov¹⁾, M. V. Eremin¹⁾, H.-A. Krug von Nidda²⁾

¹⁾Kazan State University, Kazan, 420008 Russia

²⁾Experimental Physics V, EKM, University of Augsburg, 86135 Augsburg, Germany

e-mail: Dmitri.Zakharov@ksu.ru

Since the phase transition into a spin-gapped (SG) phase in α' - NaV_2O_5 was reported [1], a lot of experimental efforts have been devoted to understand the nature of this transition. Although it was initially identified as a spin-Peierls transition, a room-temperature structural study questioned this interpretation: it concluded that all V ions are in a uniform oxidation state of $\text{V}^{4.5+}$ and form a quarter-filled trellis lattice composed of two-leg ladders. After that, NMR measurements revealed charge ordering of V^{4+} and V^{5+} states below $T_C \cong 34\text{ K}$. Different models for the CO phase, which account for SG formation, have been proposed. At present the “zig-zag” type of CO is considered as the most probable CO pattern [2], however recently Clay [3] has argued in favour of a formation of local dimers in α' - NaV_2O_5 .

It has also been pointed out that the $\sim 1\text{eV}$ features of the observed optical conductivity [4] cannot be interpreted without assuming the system to be charge disproportionated even above T_C . Nishimoto and Ohta [5] have argued that a rapid charge oscillation should exist in the system above T_C to be reconciled with the picture of the uniform valence of V ions. They have summarized optical conductivity data and concluded that the coherent fluctuations start to develop in a temperature range of $T \square 50\text{--}150\text{ K}$ [6]. It should be noted also that the uniform susceptibility has significant deviations from the Bonner-Fisher law already at T below 250 K [7].

Here we report the values of anisotropic exchange interaction parameters which we have extracted from the angular and temperature dependence of the ESR linewidth (ΔH) in α' - NaV_2O_5 [8]. Their values shed a new light on the charge and orbital ordering picture in this compound.

There are three characteristic features of ΔH in α' - NaV_2O_5 : the $\pi/2$ -periodic modulations in the bc -plane* at $T_C < T < 60\text{ K}$, the π -periodic angular dependence of ΔH at high temperatures with $\Delta H_c / \Delta H_{a,b} \approx 2$, and a peculiarity of the temperature dependence of ΔH is observed at $T_C < T < 60\text{ K}$, where $\Delta H \square a$ exceeds $\Delta H \square c$.

* We have used crystallographic coordinates. Thus $\{x, y, z\}$ are equal to $\{a, b, c\}$.

There is only one possible source [9, 10] of a $\pi/2$ -periodic angular dependence – symmetric anisotropic exchange (SAE) with the spectral density functions not equal to each other. It means nonzero nondiagonal components of the anisotropic exchange tensor J_{bc} and corresponds to exchange via $|yz\rangle$ and $|x^2 - y^2\rangle$ orbitals. Thus, it is most likely the interladder exchange (Fig. 1).

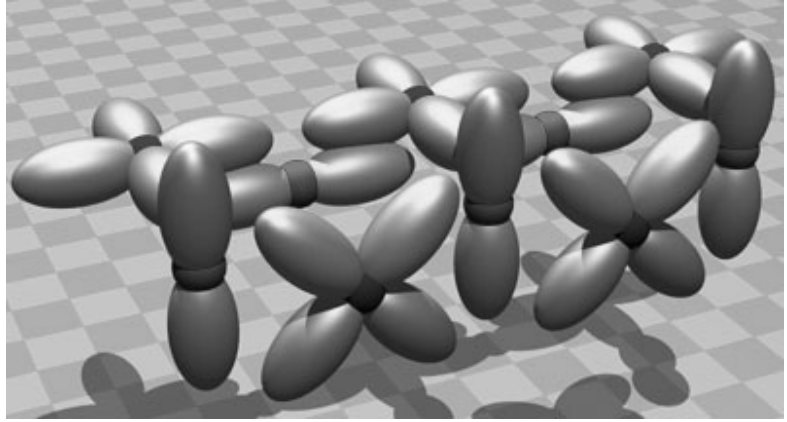


Fig. 1. The model of interladder exchange in NaV_2O_5 via $|yz\rangle$ and $|x^2 - y^2\rangle$ orbitals.

The next point is that in the temperature range $T \square T_c$ according [10] $\Delta H_c / \Delta H_{a,b} \approx 2$. This is a strong evidence for SAE, since the Dzyaloshinskii-Moriya (DM) interaction exhibits only a small component $\vec{d} \square a$ at $T \square T_c$. Therefore, there is only a single nonzero component of the anisotropic exchange tensor – J_{cc} which originates from intraladder exchange via $|x^2 - y^2\rangle$ -orbitals (Fig. 2). It is essential to note that at $T < J \approx 560$ K in the presence of an exchange anisotropy the linewidth is not simply proportional to J_{ij}^2 / J but has an additional temperature dependent factor which is linear (T/J) at temperatures far below the exchange constant and far above any phase transition [10]. Thus J_{cc} is nearly temperature independent at $T > 200$ K.

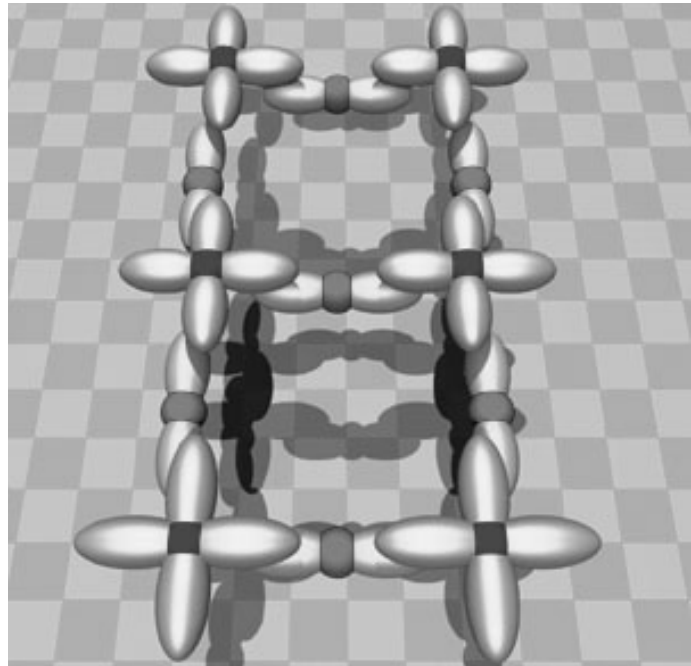


Fig. 2. The model of high-temperature intraladder exchange in NaV_2O_5 via $|x^2 - y^2\rangle$ orbitals.

The interesting peculiarity in the temperature dependence of ΔH is observed at $T_C < T < 60$ K, where $\Delta H \square a$ exceeds $\Delta H \square c$. Most likely it is a hint of charge fluctuations,

which start to develop in α' - NaV_2O_5 far above T_C , since this effect is absent in the samples with inhibited phase transition (e.g., $\text{Na}_{0.987}\text{Li}_{0.013}\text{V}_2\text{O}_5$ [11]). This feature has several possible explanations, each of them is related to a certain picture of charge and orbital order in the compound.

This effect can be produced by a strong DM interaction with $\vec{d} \parallel a$.

The large component $\vec{d} \parallel a$ arises by a chain-like CO [10], however the existence of this CO-pattern is questionable [12], in particular due to the Coulomb repulsion. The most plausible CO patterns are a “zig-zag” distribution and “dimers” [5]. In the case of a “dimers”-CO pattern the largest component of the DM vector is $\vec{d} \parallel b$ which is not in accord with the ESR data. In the case of a “zig-zag” pattern the component $\vec{d} \parallel b$ arises too, but it is alternated along the ladder, and according to Oshikawa and Affleck [13] does not give an appreciable contribution to the ESR linewidth. Thus, the ESR data can be explained in terms of

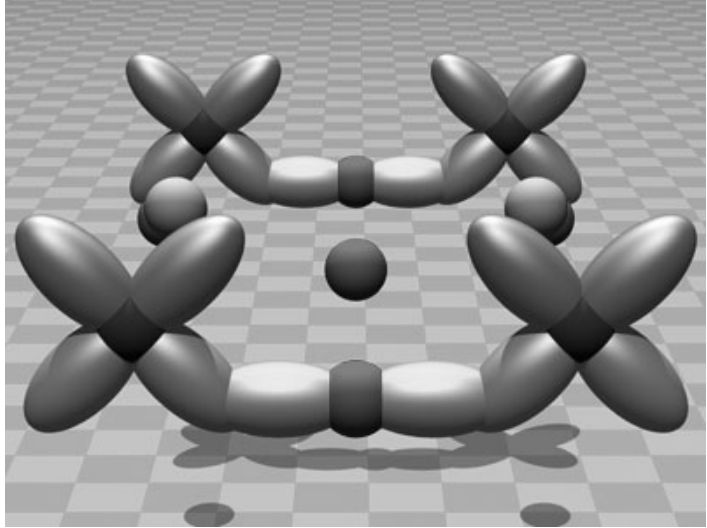


Fig. 3. The model of low-temperature intraladder exchange in NaV_2O_5 via $|xz\rangle$ orbitals.

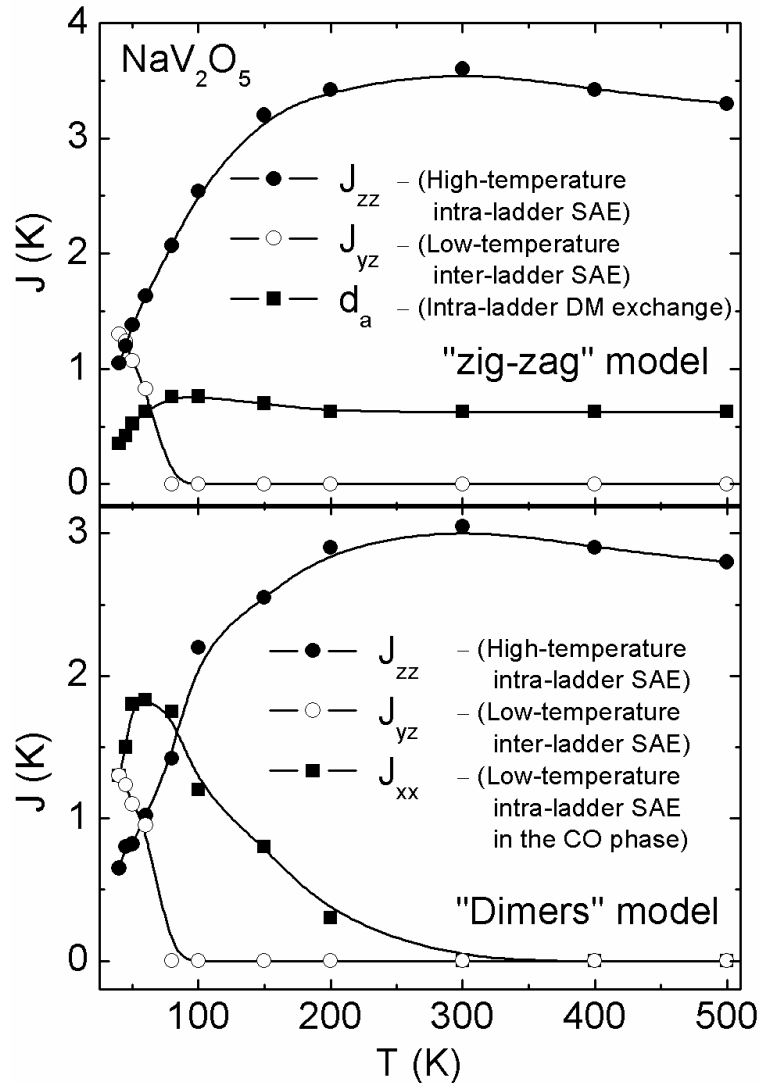


Fig. 4. The temperature dependence of the superexchange parameters in NaV_2O_5 .

a “zig-zag”-CO pattern with a strong SAE and a weak DM interaction with d_a . d_a must be temperature independent at $T > 250$ K and in a temperature range $T_C < T < 250$ K it is submitted to the influence of a few factors. The decrease of d_a on approaching T_C is caused by the increase of the distance between interacting electrons, the increase of d_a is determined by the lifting of the electron density over the oxygen plane.

One more explanation of the crossing of $\Delta H \square a$ and $\Delta H \square c$ at $T_C < T < 60$ K is possible in terms of the influence of SAE only. It means that the J_{aa} -element of the anisotropic exchange tensor exceeds the J_{cc} in this temperature range. This indicates the preferred exchange via $|xz\rangle$ -orbitals and, hence, excludes the chain-CO pattern. In this case the “zig-zag”-CO pattern is improbable too because of weak overlap of the $|xz\rangle$ -orbitals of diagonal V-ions. But the picture of superexchange over $|xz\rangle$ -orbitals in the CO phase agrees nicely with a model of “local dimers” with double occupancy of the rungs.

In conclusion, from the ESR data we have deduced the superexchange parameters for the two most probable charge-ordering patterns in α' - NaV_2O_5 : “zig-zag” and “dimers”. The temperature dependences of all exchange parameters are shown in the Fig. 4.

The work was supported by the RFFI (Grant № 03-02-17430) and CRDF (BRHE REC-007).

References

- [1] M. Isobe and Y. Ueda, J. Phys. Soc. Jpn. **65**, 1178 (1996).
- [2] H. Seo and H. Fukuyama, J. Phys. Soc. Jpn. **67**, 2602 (1998).
- [3] R. T. Clay, S. Mazumdar, cond-mat/0305479 (2003).
- [4] A. Damascelli *et al.*, Phys. Rev. B **61**, 2535 (2000).
- [5] S. Nishimoto and Y. Ohta, J. Phys. Soc. Jpn. **67**, 3679 (1998).
- [6] S. Nishimoto and Y. Ohta, J. Phys. Soc. Jpn. **67**, 4010 (1998).
- [7] J. Hemberger *et al.*, Europhys. Lett. **42**, 661 (1998).
- [8] M. Lohmann *et al.*, Phys. Rev Lett. **85**, 8, 1742 (2000).
- [9] J. Deisenhofer *et al.*, Phys. Rev. B **65**, 104440 (2002).
- [10] M. Oshikawa and I. Affleck, Phys. Rev. B **65**, 134410 (2002).
- [11] M. Lohmann *et al.*, Phys. Rev. B **61**, 9523 (2000).
- [12] C. Gros and R. Valenti, Phys. Rev. Lett. **82**, 5, 976 (1999).

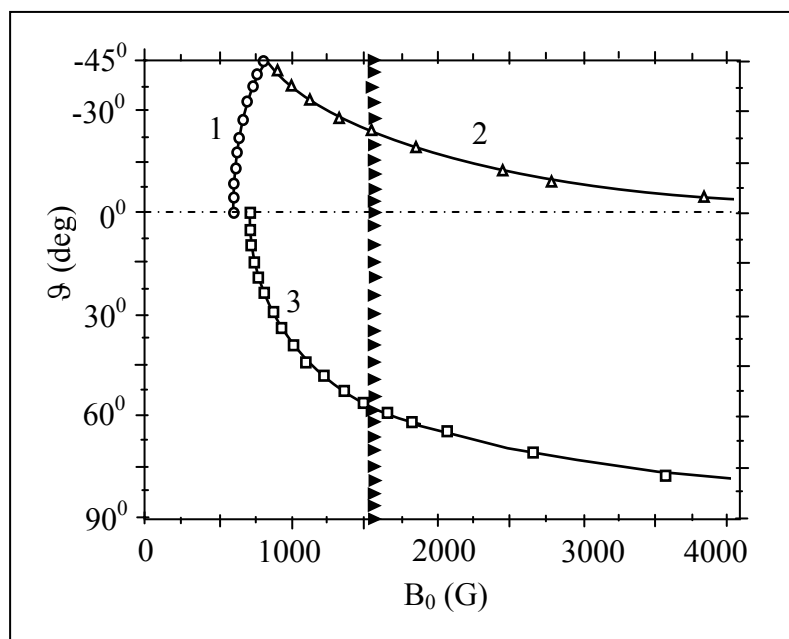
EPR OF Ni²⁺ IMPURITY JAHN-TELLER CENTERS IN SrF₂ CRYSTAL

E.R. Zhiteytsev, V.A. Ulanov, M.M. Zaripov

Department of radiospectroscopy of insulators, Zavoisky Physical-Technical Institute, Kazan, Russia

e-mail: evg@kfti.kcn.ru

In the SrF₂ fluorite type crystals activated by Ni impurity ions the EPR spectra of rhombic paramagnetic centers were observed at the temperature 4.2K and frequency 9.3 GHz. The angular dependencies of the resonance magnetic fields in these EPR spectra are shown in Fig.1. In this figure positive angles correspond to rotations of the magnetic field vector B₀ in a [110] plane of the SrF₂:Ni crystal while the negative angles to [001] rotation plane. In the first case the direction of the radiofrequency magnetic field B_{rf} acting on the the SrF₂:Ni sample remains to be perpendicular to the [110] plane all the time of rotation. In the second case B_{rf} is perpendicular to the [001] plane. Experimental points and theoretical curves labeled by the figures 1 and 2 represent the doubly degenerated EPR lines. The points and curves labeled by the figure 3 correspond to the non-degenerated EPR lines. The resonance positions of the EPR line arisen due to the paramagnetic centers of another type are denoted by the black triangles. An orientation B₀ || <001> associates with the angle ϑ = 0⁰. The angle ϑ = 90⁰ corresponds to the orientation B₀ || <110> and ϑ = -45⁰ to B₀ || <001>. Centers of two groups of the EPR lines observed at ϑ = 0⁰ with the various orientations of the vector B_{rf} (namely, B_{rf} || <001> and B_{rf} || <110>) correspond to two values of an effective g-factor, g(1) = 11.05 and g(3) = 9.55.



As it can be seen in Fig.1 the probabilities of the EPR transitions strongly depend on an orientation of the vector B_{rf}. This implies that the EPR lines observed in our experiment arise due to the resonance transitions between two electronic spin levels characterised by integer M'_s and M''_s with ΔM_s = M'_s - M''_s > 1.

POSTER SESSION PS46

Reasons of unusual features of the observed EPR spectra are the following. Substituting for basic cation of SrF_2 an impurity Ni^{2+} ion finds itself in a cubical crystal field. The ground electronic state of $\text{Ni}^{2+}(3d^8)$ in a cubical co-ordination is the 3T_1 orbital state. This is the situation well known as Jahn-Teller one. Usually Jahn-Teller effect leads to a static deformation of the cubical nuclear configuration of an impurity center. It was found that in the case of cubical complexes with a triply degenerated ground orbital state the Jahn-Teller static deformation can be very large. The result is a multiwell ground adiabatic potential sheet of such a center. There are some possible schemes of vibronical interactions of an orbital triplet $({}^{2S+1})T$ with the crystal lattice vibrations ($T \otimes (a_{1g} + e_g)$, $T \otimes (a_{1g} + t_{2g})$ or $T \otimes (a_{1g} + e_g + t_{2g})$). Sometimes the Jahn-Teller pseudo-effect is possible. Experimental results obtained in this work were described by the model of dynamical Jahn-Teller effect on the ground ${}^3T_{2g}$ orbital state of the Ni^{2+} impurity center.

The work is supported by the Russian Foundation of Basic Research (grant 04-02-16616) and by BRHE REC-007.

EPR STUDY OF MIXED CRYSTALS $\text{BaF}_2(1-x)+\text{LaF}_3(x)$ DOPED WITH Ce^{3+} IONSL.K. Aminov, R.Yu. Abdulsabirov, S.L. Korableva, I.N. Kurkin, S.P. Kurzin, A.G. Ziganshin

Kazan State University, 420008, Kremlevskaya 18, Kazan, Russia

e-mail: zairat@inbox.ru

The direct observation by EPR methods of rare earth ions clusterization in paramagnetic mixed crystals $(\text{MeF}_2)_{1-x}(\text{REF}_3)_x$ is practically impossible due to strong broadening of resonance lines at concentrations higher than $x \approx 0.1\%$. In this respect the binary solutions $(\text{MeF}_2)_{1-x-y}(\text{RF}_3)_x(\text{REF}_3)_y$ with diamagnetic R (La, Lu, Y) and small concentrations y of the paramagnetic rare earth component seem to be more convenient. Observing optically detectable EPR spectra in a number of such compounds, Kazanskii [1] has concluded that the process of clusters formation is determined by the summary concentration $x + y$ of trifluorides, and EPR spectra of RE^{3+} ions at concentrations $x + y \geq 0.001$ reflect the tetragonal symmetry of R ions positions in R_6F_{37} clusters. For more complete clarification of EPR potentialities it seems useful to investigate usual EPR spectra of different mixed crystals $(\text{MeF}_2)_{1-x-y}(\text{RF}_3)_x(\text{REF}_3)_y$ in as wide as possible range of concentrations x,y.

Recently we have investigated mixed crystals $\text{BaF}_2(1-x)+\text{LaF}_3(x)$ doped with 0.1% Yb^{3+} ions by EPR methods [2]. It was established that even at small $x = 0.001$ extra EPR lines arise due to formation of trigonal clusters involving two rare earth ions and two compensating fluorine ions (of $\text{La}^{3+} - \text{F}^- - \text{Yb}^{3+} - \text{F}^-$ type). Analysis of these lines was complicated by hyperfine structure of the original (for $x = 0$) EPR spectra due to ^{171}Yb and ^{173}Yb isotopes, however no tetragonal spectra which could be assigned to Yb^{3+} ions within clusters La_6F_{37} was observed.

In the present work we have again studied the same mixed crystals $\text{BaF}_2(1-x)+\text{LaF}_3(x)$, however, Ce^{3+} ion has been used as a paramagnetic probe. This ion has no magnetic isotopes and consequently hyperfine structure of the EPR spectra.

Samples with $x = 0, 0.001, 0.002, 0.005, 0.01, 0.02$ doped with 0.1 at. % of Ce^{3+} were investigated. EPR spectra were measured at frequency of ~ 9.5 GHz and temperature of ~ 15 K. For “pure” BaF_2 ($x = 0$) only one EPR center with tetragonal symmetry ($g_{\parallel} = 2.601, g_{\perp} = 1.555$; cf. [3]) is observed (Fig.1).

At $x = 0.001$ intensity of tetragonal center decreases and extra EPR lines are observed rather clearly. Further increase of concentration x brings to essential decrease of original

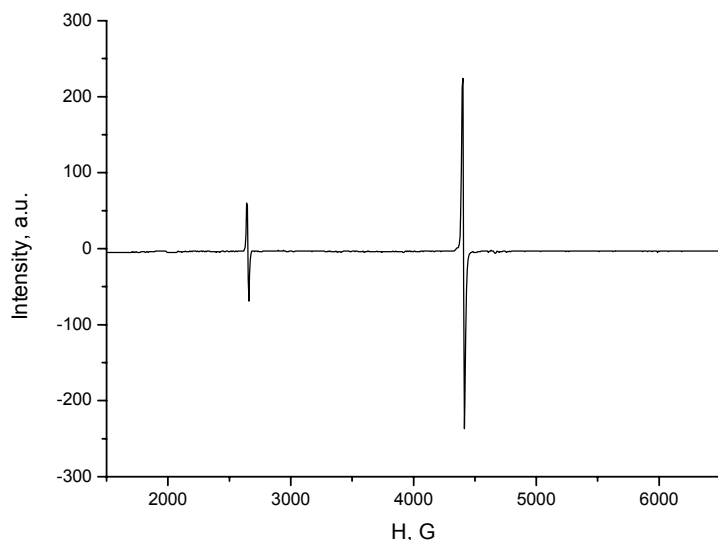


Fig.1. EPR spectrum of $\text{BaF}_2+0.1\%\text{Ce}^{3+}$ ($x=0$) at $\text{H}\parallel\text{C}_4$. The single line at $H=2603\text{G}$ and the double line at $H=4355\text{G}$ are due to the main tetragonal centers of Ce^{3+} ions.

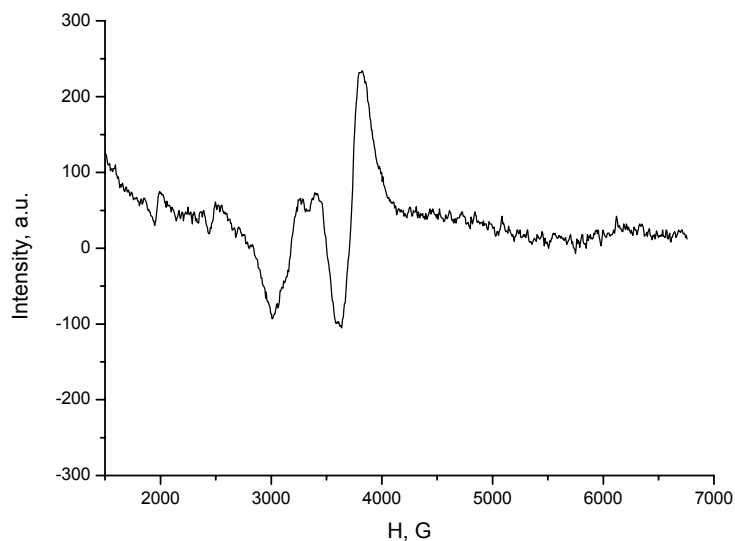


Fig.2. EPR spectrum of the sample $\text{Ba}_{1-x}\text{La}_x\text{F}_{2+x} + 0.1\%\text{Ce}^{3+}$ for $x=0.02$. Applied magnetic field is oriented approximately along trigonal axis. At precise orientation $\text{H}\parallel\text{C}_3$ one “triple” EPR line would be observed.

tetragonal spectrum (\sim by two orders of magnitude at $x = 0.02$) and not so notable change of extra lines intensity.

The preliminary analysis of angular dependence shows that additional lines also belong to centers with the tetragonal symmetry and g -values: $g_{\parallel}=0.75$; $g_{\perp}=2.4$.

EPR spectrum for the sample $\text{BaF}_2(1-x)+\text{LaF}_3(x) + 0.1\%\text{Ce}^{3+}$ with $x=0.02$ and the magnetic field orientation close to $\text{H}\parallel\text{C}_3$ is shown in the Fig.2.

These centers are possibly connected to clusters of La_6F_{37} type [1], which is corroborated by the closeness of the corresponding g factors to those in $\text{KY}_3\text{F}_{10}:\text{Ce}^{3+}$ system ($g_{\parallel}=0.77$, $g_{\perp}=2.46$; see [4]).

We conclude that cubo-octahedral complexes of R_6F_{36} type in mixed crystals $\text{BaF}_2(1-x)+\text{LaF}_3(x)$ can be registered by direct EPR measurements.

References:

[1] S.A.Kazanskii, JETP, **89**, 1258-1268 (1985); S.A.Kazanskii et al., Fiz. tv. tela, **44**, 1356-1366 (2002)

POSTER SESSION PS47

- [2] L.K.Aminov et al., Abstracts Special. Coll. AMPERE 2003: NMR and EPR of Broad-Line Solids (Bernardin, Portoroz, Slovenia, Sept. 8-12, 2003), p. 114
- [3] A.A.Antipin et al., Fiz. tv. tela, **6**, 2014 (1964)
- [4] V.A.Ivanshin et al., Fiz. tv. tela, **28**, 2580-2582 (1986)

CONTENTS

Program	3
---------	---

TUTORIAL

<u>G. Eska</u>	6
----------------	---

ac Josephson effect in superfluid ^3He

<u>K. Kumagai</u> , Y. Furukawa, S. Kawakami, Y. Hatanaka, F. Borsa	7
---	---

NMR studies of molecular nanomagnets

<u>F.S. Dzheparov</u>	9
-----------------------	---

Spin dynamics in disordered media

POSTER SESSION

<u>D.I. Abubakirov</u> , M.S. Tagirov, D.A. Tayurskii, H.Suzuki	11
---	----

Magnetic susceptibility of Van Vleck paramagnet thulium ethylsulfate at high magnetic fields

<u>M.M. Barlukova</u> , N.P. Gritsan, V.A. Bagryansky, <u>V.F. Starichenko</u> , I.A. Grigor'ev,	15
--	----

Yu.N. Molin

OD ESR detection of the radical ions of cyclic nitrones in liquid solutions

<u>M.M. Barlukova</u> , I.V. Beregovaya, V.P. Vysotsky, L.N. Shchegoleva,	17
---	----

V.A. Bagryansky, Yu.N. Molin

Study of 1,2,3-trifluorobenzene radical anion by OD ESR spectroscopy

<u>A.V. Belskaya</u> , D.A. Fayzullin, V.D. Fedotov	19
---	----

Side chain dynamics of solid globular proteins. Comparative study by ^1H -NMR relaxation and FTIR spectroscopy

<u>A.N. Bukharaev</u> , Yu.I. Talanov	20
Irreversibility Line of the Bi-2212 Thin Films as Revealed by Nonresonant Microwave Absorption	
<u>V.Yu. Buzko</u> , I.V. Sukhno, S.V. Dubrovin, I.V. Kornienko	24
The influence of diamagnetic salts on the state of paramagnetic aqua-ion Gd(3+) by EPR-spectroscopy data	
<u>P.V. Chaplieva</u> , I.V. Borovykh, O.E. Trubetskaya, I.I. Proskuryakov, O.A. Trubetskoj	26
Investigation of Mn²⁺ Ions Interaction with Humic Substances	
<u>A.V. Donets</u> , V.I. Chizhik	28
Temperature dependence of the ion coordination in water solution and the problem of thermoregulation of warm-blooded animals	
<u>R.R. Garipov</u> , V.G. Shtyrilin, A.L. Kon'kin, Yu.I. Zyavkina, A.V. Aganov, N.G. Zabiurov, A.V. Zakharov	32
EPR Spectroscopy, Structures and Dynamics of Copper(II) Complexes with N,O,P,S-Containing Ligands	
<u>E.V. Gazeeva</u> , R.V. Saburova	34
Phonon echo of interacting tunneling states in glass	
M.L. Falin, <u>K.I. Gerasimov</u> , V.A. Latypov, A.M. Leushin	38
Magnetic Resonance and Optical Spectroscopy of Tetragonal Yb³⁺ Center in CaF₂	
<u>R.R.Gubaidullin</u> , S.B.Orlinskii, R.M.Rakhmatullin	40
Study of SiO₂ glasses doped with Er³⁺ ions and co-doped with N and F	
<u>E.N. Irinyakov</u>	44
The Program for Calculation the Electronic Structure of the Impurity Centers in Crystals	

<u>A.I. Ismailova</u> , L.N. Muranova, V.V Andrianov, Kh.L. Gainutdinov, O.I. Gnezdilov, A.G. Nasyrova, R.R. Nigmatullina, A.A. Obynochny, F.F. Rahmatullina, A.L. Zefirov	46
The determination of NO in heart and liver of rats by method of EPR-spectroscopy after myocardial infarction	
<u>I. Karyagina</u> , J. Pushkar, D. Stehlik	47
TR EPR Study of the Electron Transfer Properties in Photosystem I with Anthraquinone as Secondary Acceptor	
<u>S.V. Kharlamov</u> , A.A. Nafikova, A.S. Mihajlov, V.S. Reznik, Sh.K. Latypov, A.V. Aganov	48
Pulsed field gradient NMR spectroscopy in investigation of association of macromolecules in liquids	
D.Ya. Osokin, <u>R.R. Khusnutdinov</u>	51
Two-frequency excitation. New applications	
<u>D. Komarov</u> , I. Slepneva, V. Glupov, V. Khramtsov	53
Detection of free radicals formation in haemolymph of insects by EPR spectroscopy	
<u>L.V. Korobchenko</u> , R.T. Galeev, E.R. Zhiteytsev	55
Frequency dependence of the EPR spectrum of pentanuclear cluster [Cu₃Dy₂(ClCH₂COO)₁₂(H₂O)₈] 2H₂O	
<u>A.V. Kozlov</u> , Sh.K. Latypov, A.A. Nafikova, A.V. Aganov, A.S. Mihajlov, V.S. Reznik	57
Investigation of 3D structure of bioactive compounds based on Pyrimidine derivates using Dynamic NMR spectroscopy	
<u>V.I. Krinichnyi</u> , S.V. Tokarev, H-K. Roth, M. Schroedner, B. Wessling	59
Multifrequency EPR study of metal-like domains in polyaniline	

M.L. Falin, B.N. Kazakov, <u>V.A. Latypov</u> , A.M. Leushin, A. Hofstaetter	60
Magnetic Resonance and Optical Spectroscopy of Trigonal Yb³⁺ Center in CsCaF₃ Single Crystal	
<u>A.E. Mambetov</u> , K.M. Salikhov	62
Calculations of rate constants of the bimolecular spin exchange between paramagnetic particles in a case of a diffusion passage of the interaction region	
<u>A.V. Minkin</u> , S.L. Tsarevskii	63
Distribution of magnetic field in anisotropic superconductors with nonregular vortex lattice	
<u>L.N. Muranova</u> , A.I. Ismailova, V.V. Andrianov, Kh.L. Gainutdinov, O.I. Gnezdilov, A.A. Obynochny, A.L. Zefirov	66
The measurements of NO in rat tissues by method of EPR-spectroscopy at temperature 77 °K	
<u>A.R. Mursalimov</u> , K.M. Salikhov	67
Numerical calculations of the electron spin polarization for sequential radical pairs in micelles	
I.A. Nikolaev, L.U. Grunin, <u>E.A. Nikolskaya</u> , L.V. Shvaleva, T.V. Smotrina, U.B. Grunin	68
Surface NMR: sensors development and investigation of elastomers	
<u>V. Novikov</u> , V. Timofeev	70
New programs with the WYSIWYG interface for simulation of EPR spectra nitroxide spin-label	
<u>N.Yu. Panarina</u> , N.R. Khabibullina, V.Yu. Petukhov	71
Observation of noise-like magnetic resonance spectra of thin films produced by Fe⁺ implantation into PMMA	

<u>E.A. Prokofeva</u> , A.V. Kovalenko	75
Research of dimensional-independent components of a spectrum of a magneto-dimensional resonance	
O. Kh. Khasanov, <u>G. A. Rusetsky</u> , V. V. Samartsev, N. N. Rubtsova	78
Free induction decay and echo phenomena in media with dipole-dipole interaction	
<u>K.R. Safiullin</u> , A.N. Yudin, V.V. Naletov, M.S. Tagirov, D.A. Tayurskii, I.N. Kurkin	80
Nuclear relaxation in system PrF₃ – liquid ³He	
<u>D.V. Savchenko</u> , S.N. Lukin, E.K. Kalabukhova	84
Direct Observation of Intercenter Charge Transfer Process in semi-insulating 4H SiC Material by Photo EPR method	
A.V. Dooglav, <u>A.V. Savinkov</u>	89
Study of electronic phase separation in lightly doped antiferromagnetic YBa₂Cu₃O₆ by Cu(1) NQR	
<u>S. Shakirov</u> , P. Purtov, Yu. Grishin, E. Bagryanskaya	91
Electron exchange spin relaxation of radicals in low and zero magnetic fields	
<u>A.I. Shipov</u> , V.Yu. Petukhov, N.R. Khabibullina	93
Investigation of magnetic nanostructures obtained in PMMA by ion beam synthesis in magnetic field	
<u>A. Silakov</u> , E. Reijerse, S. Albracht, W. Lubitz	97
EPR Investigation of the Active Site of [Fe]hydrogenase	
S.N. Lukin, <u>A.A. Sitnikov</u> , A.B. Brik	99
Multifrequency EPR study of Mineral-Organic Nano-Associated Systems and their synthetic analogous	

<u>A. Sklar</u> , S. Bolotin, V. Panyushkin	104
The computer analysis of ESR spectra of equilibrium systems	
<u>D.V. Starichenko</u> , Yu.N. Shvachko, N.D. Kushch, E.B. Yagubski	106
EPR in charge-transfer salts with metal-complex anions	
<u>Y. Tkachov</u> , V. Timofeev	108
New program with interactive friendly interface for EPR spectra simulation of copper-containing proteins	
<u>V.N. Verkhovlyuk</u> , D.V. Stass, N.N. Lukzen, Yu.N. Molin	109
Ion-molecular Charge Transfer Reaction in Linearly Condensed Aromatic System Studied by MARY and OD ESR Techniques	
<u>N.M. Yakovleva</u>	110
Implementation schemes in NMR of universal set of quantum gates by using virtual spin representation	
<u>A.N. Yudin</u> , G.V. Mamin, M.S. Tagirov, D.A. Tayurskii, H. Suzuki, B.M. Odintsov, R.B. Clarkson	114
Nuclear spin-lattice relaxation in carbon-based chars	
<u>D.V. Zakharov</u> , M. V. Eremin, H.-A. Krug von Nidda	118
Anisotropic exchange IN NaV₂O₅: an ESR study	
<u>E.R. Zhiteytsev</u> , V.A. Ulanov, M.M. Zaripov	122
EPR of Ni²⁺ impurity Jahn-Teller centers in SrF₂ crystal	
L.K. Aminov, R.Yu. Abdulsabirov, S.L. Korableva, I.N. Kurkin, S.P. Kurzin, <u>A.G. Ziganshin</u>	124
EPR study of mixed crystals BaF₂(1-x)+LaF₃(x) doped with Ce³⁺ ions	